Supporting Information

Multiple complexes of long-aliphatic N-acyltransferases led to synthesis of novel 2,6-diacylated/2-acyl-substituted glycopeptide antibiotics effectively killing VRE.

Syue-Yi Lyu,[†,‡] Yu-Chen Liu,[†] Chin-Yuan Chang,[†] Chuen-Jiuan Huang,[‖] Ya-Huang Chiu,[§] Chun-Man Huang,[†,‡] Ning-Shian Hsu,[†] Kuan-Hung Lin,[†] Chang-Jer Wu,[§] Ming-Daw Tsai[‖] & Tsung-Lin Li[*,†,⊥]

[†]Genomics Research Center, Academia Sinica, Taipei 115, Taiwan.

[‡]Department of Microbiology and Immunology, National Yang-Ming University, Taipei 112, Taiwan.

[§]Department of Food Science, National Taiwan Ocean University, Keelung 200, Taiwan.

[‖]Institute of Biological Chemistry, Academia Sinica, Taipei 115, Taiwan.

[⊥]Biotechnology Center, National Chung Hsing Univerisity, Taichung 402, Taiwan.

This PDF file includes:

Supporting Methods
Supporting Results (Figures S1-22, Tables S1-7)
Supporting References

Supporting Methods

Cloning and protein purification. The *orf11** and *dbv8* genes were amplified and subcloned into the expression vector pET-28a(+). These clones were transformed into *E. coli* BL21(DE3) for protein over-expression. The typical procedure is described as follows: One liter of LB medium containing 50 mg/L kanamycin was inoculated with 10 mL of an overnight culture grown in LB medium (containing 50 mg/L kanamycin), induced with 1 mL 1.0 M IPTG (to give 1.0 mM; exact concentrations varied from one to the other) at an OD600 of 0.7, and grown for further 8 hours at 16°C. Cells were harvested by centrifugation at 6000 rpm for 20 min at 4°C, resuspended in 30 mL binding buffer (50 mM Tris at pH 8.0, 500 mM NaCl, 10 mM imidazole, 10% glycerol) and disrupted by microfluidizer. The cell lysate was centrifuged at 18000 rpm for 30 minutes to remove cell debris. The supernatant was applied to a Ni^{2+}-NTA agarose resin column (2 mL, Novagen) pre-equilibrated with binding buffer. The column was washed sequentially with 20 mL of binding buffer and 10 mL washing buffer (50 mM Tris at pH 8.0, 500 mM NaCl, 50 mM imidazole, 10% glycerol). The bound protein was then eluted with 10 mL of elution buffer (50 mM Tris at pH 8.0, 500 mM NaCl, 250 mM imidazole, 10% glycerol). Gel filtration was performed using an Äkta FPLC system equipped with an S-200 Superdex column (Amersham Bioscience) under an isocratic condition (50 mM Tris at pH 8.0, 500 mM NaCl). The buffer was exchanged using Millipore centrifugal filters and HEPES buffer (50 mM, pH 8.0). Protein purity was determined by SDS-PAGE and Western blotting, and electrospray mass spectrometry (ESI-MS). Protein concentrations were estimated by the Bradford assay.

Site-directed mutagenesis. Site-directed mutagenesis was carried out using QuickChange (Stratagene). The wild-type Orf11* was used as the template for single mutation. For multiple mutations, the single or double mutant was used as the template. All mutations were confirmed by DNA sequencing. Mutant proteins were purified with the same protocol as wild-type Orf11*.

Primer list (primers used in this study)

Mutants	Primer
Orf11*-E145L	F: 5-CCTGACGCAGTTGGGG**GCG**CTGGTGGCCATTCATC-3
	R: 5-GATGAATGGCCACCAG**CGC**CCCCAACTGCGTCAGG-3
Orf11*-W163S	F: 5-CGGCATGAACATGCAG**TCG**TGGACCACCTACCACC-3
	R: 5-GGTGGTAGGTGGTCCA**CGA**CTGCATGTTCATGCCG-3
Orf11*-W164S	F: 5-CATGAACATGCAGTGG**TCG**ACCACCTACCACCTGC-3
	R: 5-GCAGGTGGTAGGTGGT**CGA**CCACTGCATGTTCATG-3
Orf11*-H196A	F: 5-GCCGCACCTCGGCCTG**GCC**GTTCCCGAGTGGGGCG-3
	R: 5-CGCCCCACTCGGGAAC**GGC**CAGGCCGAGGTGCGGC-3
Orf11*-S236A	F: 5-GGTGGCCTGGGGAAGC**GCG**TGGATGCTCGATCCGC-3
	R: 5-GCGGATCGAGCATCCA**CGC**GCTTCCCCAGGCCACC-3
Orf11*-W237A	F: 5-GGCCTGGGGAAGCTCG**GCG**ATGCTCGATCCGCAAC-3
	R: 5-GTTGCGGATCGAGCAT**CGC**CGAGCTTCCCCAGGCC-3

Enzymatic activity assay. The Orf11*/Dbv8 enzymatic activity was determined by using LC-MS. The assay mixture containing Orf11*/Dbv8 (10 μg) and given substrates (1 mM acyl-CoAs/acyl-NACs, 1 mM Tei-pseudoaglycone or vancomycin) in a buffer solution (50 mM Tris pH 8.0, 100 mM NaCl, 1 mM DTT) in a total volume of 150 μl was incubated for 2 h at 25 °C. Each reaction mixture was centrifuged at 16,000g for 5 min (Heraeus Biofuge Pico) and filtered through an ultracentrifugal filter unit (5 kDa cut-off membrane, Millipore) in due course. The filtrate was directly subjected to HPLC-ESI-LTQ (Agilent 1200 Series interfaced with an ESI source coupled to a Thermo-Finnigan LTQ-XL ion trap spectrometer) on a gradient of 0–60% acetonitrile in 0.1% TFA in water over 30 min. Online LC-MS spectra were monitored and recorded using Xcalibur (Thermo Fisher Scientific, Inc.).

Analytical ultracentrifuge analysis. The sedimentation velocity experiments were performed with a Beckman-Coulter XL-I analytical ultracentrifuge. Samples and buffers were loaded into 12-mm standard double-sector Epon charcoal-filled centerpieces and mounted in an An-60 Ti rotor. We introduced 400 μl of 1 mg/ml sample into the cell. Sedimentation velocity experiments were performed at a rotor speed of 42,000 r.p.m. at 20 °C. The signals of samples were monitored at 280 nm and collected every 3 min for 6 h. The experimental raw data were processed by using

the SedFit software. The density and viscosity of buffers were calculated by using the Sednterp software (http://www.jphilo.mailway.com/default.htm).

Crystallization and data collection. The purified proteins were crystallized using the hanging drop vapor-diffusion method. For apo-Orf11*, pyramidal crystals were obtained in a solution containing: 0.1 M Tris pH 7.5, 2.5 M NaCl. For Orf11*/decanoyl-CoA, hexagonal crystals were obtained in a solution containing: 0.1 mM MES pH 6.5, 0.2 M ammonium sulphate, 30% (V/V) PEG 5000 MME and 1 mM decanoyl-CoA. For Dbv8/decanoyl-CoA, crystals were obtained in a solution containing: 0.1 M sodium cacodylate pH 6.5, 0.2 M sodium acetate, 30% (V/V) PEG 8000 and 2 mM decanoyl-CoA. For Orf11*/octanoyl-CoA, crystals were obtained in a solution containing: 0.1 mM MES pH 6.5, 0.2 M ammonium sulphate, 28% (V/V) PEG 5000 MME and 4 mM octanoyl-CoA. The crystals of the Orf11*H196A/decanoyl-CoA/Tei pseudoaglycone (pre-acylation), Orf11*H196A/decanoyl-CoA-Tei pseudoaglycone (intermediate) and Orf11*H196A/CoA/10C-teicoplanin (post-acylation) complexes were obtained by soaking the Orf11*H196A/decanoyl-CoA binary complex crystals with Tei-pseudoaglycone (40 mM) for 1, 4 and 20 hr, respectively. Then the protein crystals were transferred to a cryoprotectant solution containing glycerol (20%, v/v) and flash-cooled in liquid nitrogen prior to data collection. X-ray diffraction data sets were collected on an ADSC Quantum-315 or Quantum-210 CCD detectors at beamlines 13B1 and 13C1 of the National Synchrotron Radiation Research Center (Taiwan) and beamlines 12B2 and 44XU of Spring-8 (Japan). Data were indexed and scaled with the HKL2000 package.[1] The redundancy independent merging R factor ($R_{\text{r.i.m}}$) and the precision indicating merging R factor ($R_{\text{p.i.m.}}$) were calculated using the program *RMERGE*. The contents of asymmetric units were estimated from the Matthews coefficient.[2] The data suggest that a value of 2.40 Å^3 Da^{-1} with 48.7% solvent corresponds to one molecules per asymmetric unit in the $P2_12_12_1$ crystal (Dbv8/decanoyl-CoA), a value of 3.44 Å^3 Da^{-1} with 64.2% solvent content indicates one molecules per asymmetric unit in the $P6_5$ crystal (Orf11*/octanoyl-CoA, Orf11*/decanoyl-CoA) and a value of 5.88 Å^3 Da^{-1} with 79% solvent content indicates one molecules per asymmetric unit in the $P6_2$ crystal (Orf11*).

Structure determination and refinement. The initial phase was determined by the single wavelength anomalous dispersion method. The anomalous diffraction data were collected by selenium labeled Orf11*. The single wavelength anomalous dispersion (SAD) method was used to obtain phase information, and CRANK[3] was used to find the phase solution. Other native structures were solved by the molecular
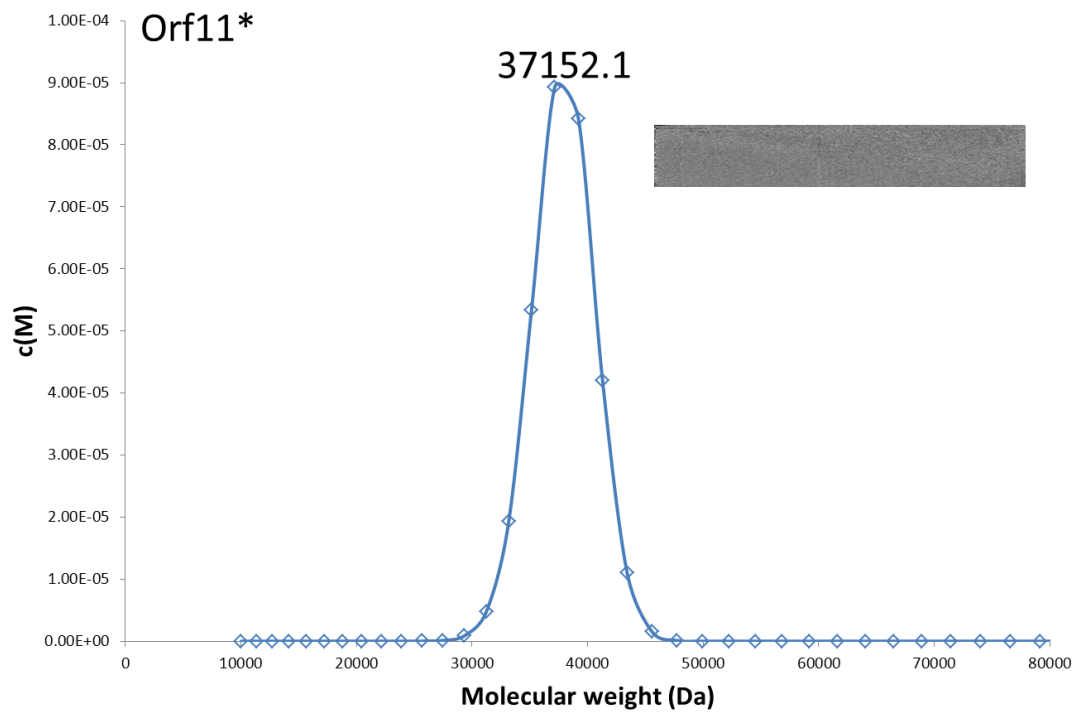
replacement method using the Se-Orf11* as the search model. The CRANK pipeline started with substructure detection and ended with model building, including procedures of substructure detection by AFRO/CRUNCH2,[4] substructure refinement by BP3,[5] Hand determination and density modification by SOLOMEN,[6] and model building by BUCCANEER.[7,8] Phase extension yielded electron density maps into which a polypeptide model was built with the program COOT.[9,10] The model was further refined with REFMAC.[11] Figures were generated using PyMOL (http://www.pymol.org). Detailed refinement statistics are given in Table S1.

Enzymatic synthesis of new Tei analogs. Teicoplanin was purchased from Sigma/Aldrich Chemical Co. (St. Louis, MO, USA). Acyl-NAC was chemically synthesized. In brief, the reaction mixture containing Orf11* (50 μg) and corresponding substrates (2 mM acyl-CoAs/acyl-NACs and 1 mM teicoplanin) in a buffer solution (50 mM Tris pH 9.0, 100 mM NaCl, 20% DMSO) was incubated for 6 h at 25 °C. The reaction mixtures were quenched by adding 10% HCl (6N) and purified by HPLC (Agilent 1200 Series). The collected peak fractions were lyophilized and confirmed by LC-MS.

MIC determination for new analogs. All MIC assays were performed following the National Committee for Clinical Laboratory Standards recommendations.[12] In brief, broth microdilution MICs were determined in brain heart infusion (BHI) broth. Test strains were grown overnight on BHI agar at 37°C. They were subcultured into BHI broth and grown for 4 to 6 h until a turbidity of 0.5 McFarland unit reached. Final inocula were adjusted to 5×10^5 CFU/ml. Aliquots (0.1 ml) of these suspensions were introduced into 96-well plates containing twofold dilutions (0.1 ml, the final compound concentrations ranged from 64 mg/L to 0.0625 mg/L) of testing compound solutions. The plates were incubated in air at 37°C for 18-24 h. The MICs were considered to be the lowest compound concentrations at which there was no visible growth in the wells.

Supporting Results

a.

b.

c.

Orf11*+decanoyl-CoA

2.89

d.

Orf11*+decanoyl-CoA

37152.1

e.

Orf11*+decanoyl-CoA+Tei pseudoaglycone

45564.4

c(M) vs Molecular weight (Da)

f.

Orf11*+decanoyl-CoA+Tei pseudoaglycone

2.91

c(s) vs Sedimentation coefficient (S)
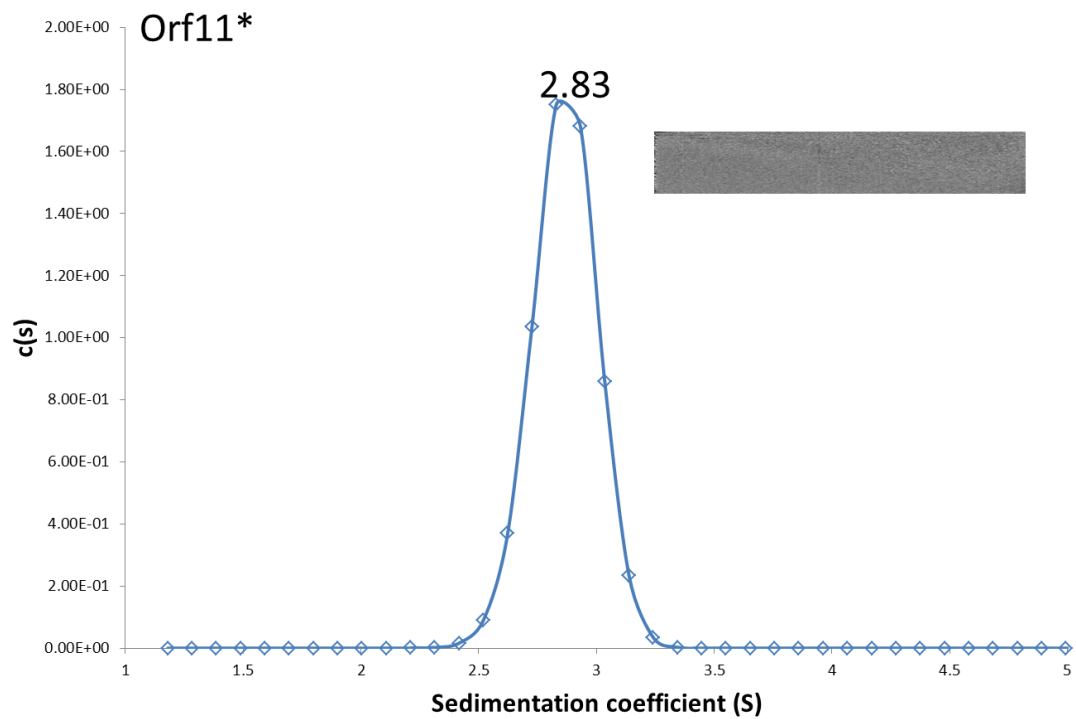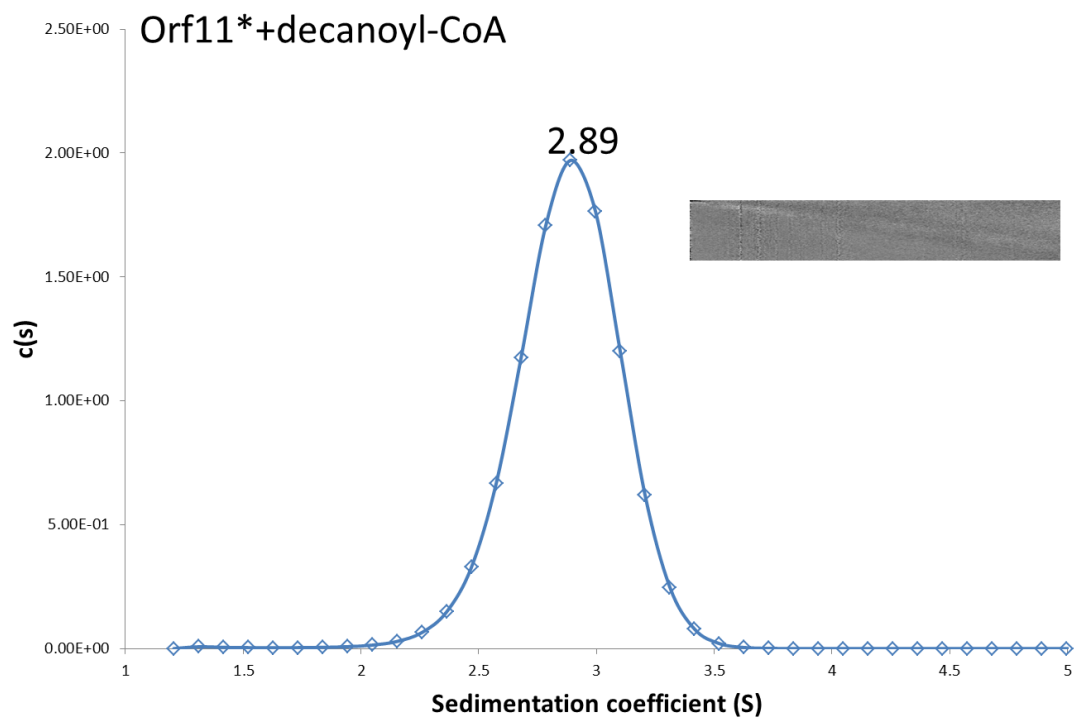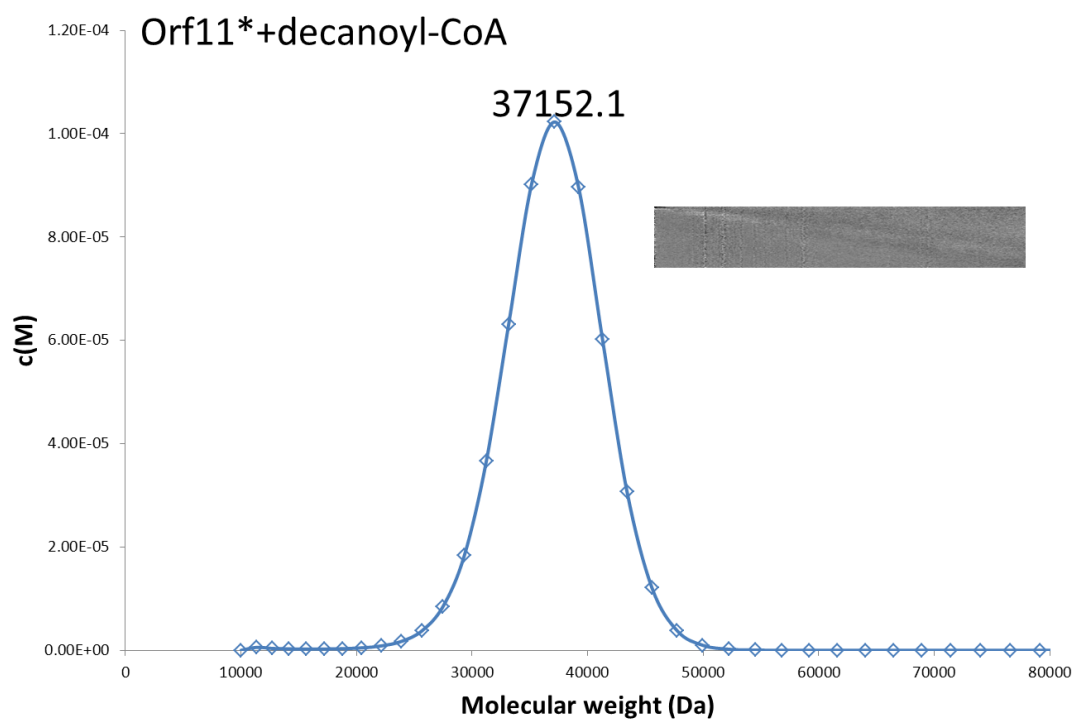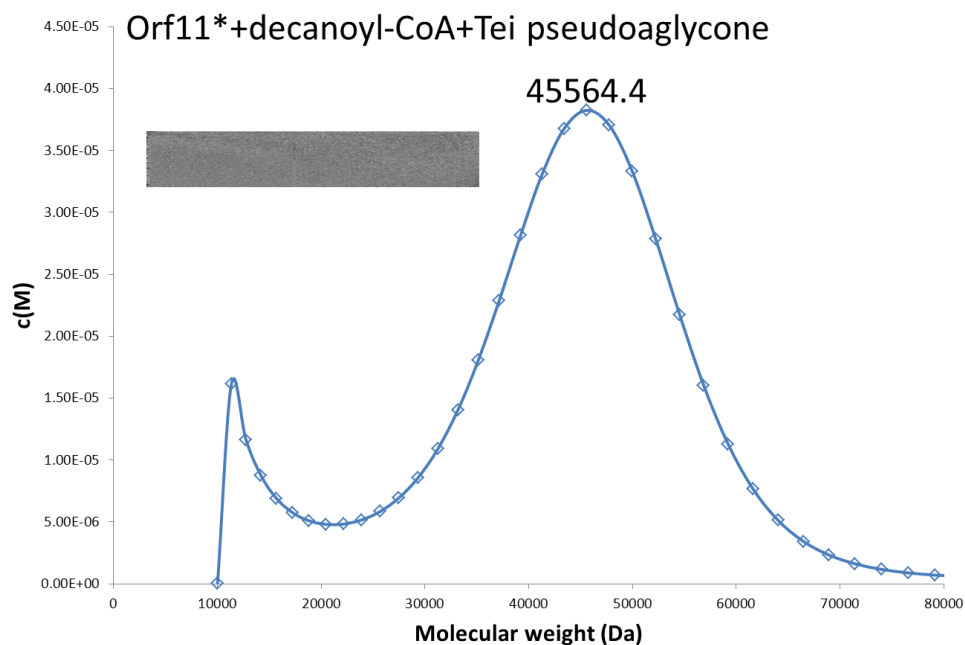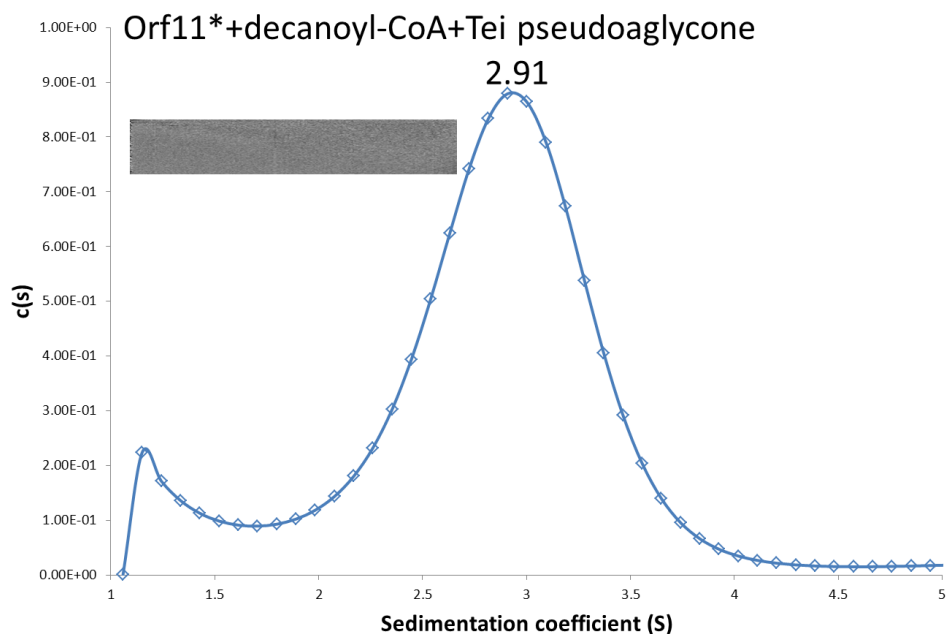
Figure S1. Analytical ultracentrifugation analysis of Orf11*, Orf11*/decanoyl-CoA and Orf11*/decanoyl-CoA/Tei pseudoaglycone. The AUC data were analyzed using SedFit (http://www.analyticalultracentrifugation.com/default.htm). The calculated *c(M)* and *c(S)* distributions are shown in panels (a) (c) (e) and panels (b) (d) (f), respectively. The insert grayscale bars indicate the residuals bitmap in each fit.

a. Orf11*
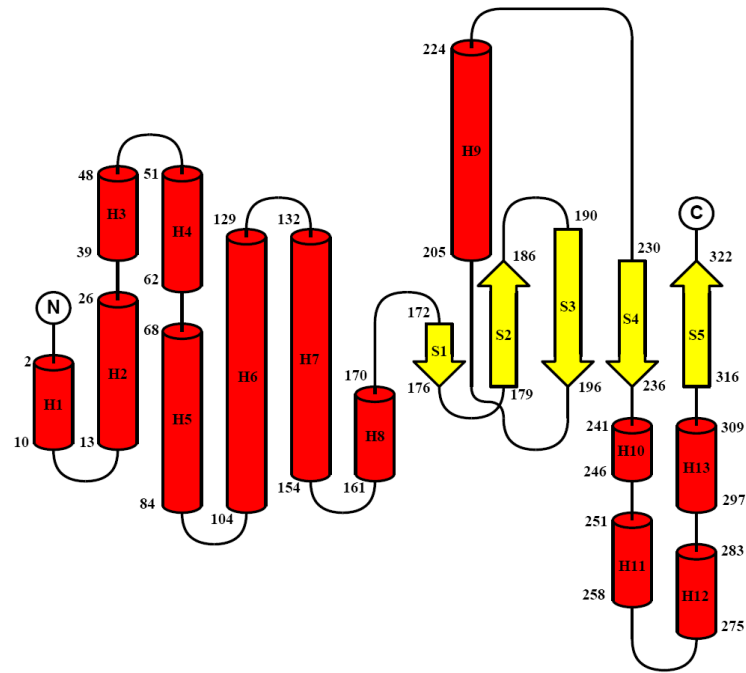
b. Dbv8
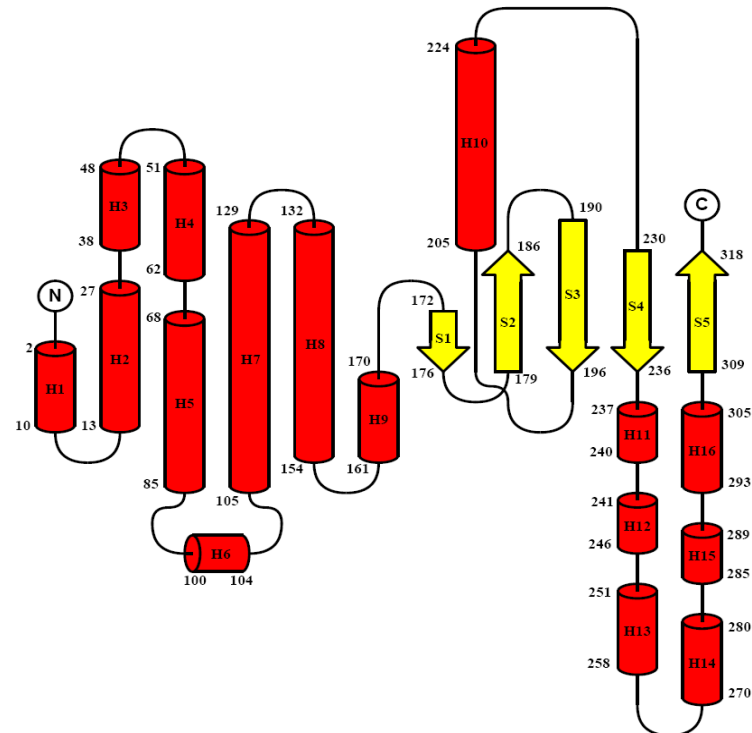
Figure S2. Schematic topologies of Orf11* and Dbv8. The topology diagrams were generated using TopDraw. The secondary structures of α-helix and β-sheet are colored red and yellow, respectively. Orf11*/Dbv8 is composed of two domains, an N-terminal all-helix domain (residues 1-170) and a C-terminal GNAT domain (residues 171-323/residues 171-319 for Orf11*/Dbv8).

Orf11*

No:	Chain	Z	rmsd	lali	nres	%id	PDB	Description
1:	2ge3-B	5.0	3.7	93	163	11	PDB	MOLECULE: PROBABLE ACETYLTRANSFERASE;
2:	2ob0-B	4.8	3.7	95	152	5	PDB	MOLECULE: HUMAN MAK3 HOMOLOG;
3:	2ge3-D	4.7	3.9	95	164	11	PDB	MOLECULE: PROBABLE ACETYLTRANSFERASE;
4:	2ge3-C	4.7	4.0	95	164	11	PDB	MOLECULE: PROBABLE ACETYLTRANSFERASE;
5:	1vhs-B	4.7	4.0	91	158	10	PDB	MOLECULE: SIMILAR TO PHOSPHINOTHRICIN ACETYLTRANSFERASE;
6:	2jdd-A	4.7	2.8	86	145	14	PDB	MOLECULE: GLYPHOSATE N-ACETYLTRANSFERASE;
7:	2ge3-A	4.7	4.1	92	164	10	PDB	MOLECULE: PROBABLE ACETYLTRANSFERASE;
8:	2bsw-A	4.6	3.1	86	145	15	PDB	MOLECULE: GLYPHOSATE N-ACETYLTRANSFERASE;
9:	2i79-C	4.6	4.0	94	171	9	PDB	MOLECULE: ACETYLTRANSFERASE, GNAT FAMILY;
10:	2i79-E	4.6	4.1	94	168	9	PDB	MOLECULE: ACETYLTRANSFERASE, GNAT FAMILY;
11:	2jdc-A	4.6	2.8	86	145	14	PDB	MOLECULE: GLYPHOSATE N-ACETYLTRANSFERASE;
12:	2psw-A	4.6	3.7	95	155	5	PDB	MOLECULE: N-ACETYLTRANSFERASE 13;
13:	3g8w-A	4.6	4.1	96	162	4	PDB	MOLECULE: LACTOCOCCAL PROPHAGE PS3 PROTEIN 05;
14:	1vhs-A	4.5	3.8	92	165	10	PDB	MOLECULE: SIMILAR TO PHOSPHINOTHRICIN ACETYLTRANSFERASE;
15:	2i79-A	4.5	4.1	94	171	9	PDB	MOLECULE: ACETYLTRANSFERASE, GNAT FAMILY;

N-termial all-helix domain

No:	Chain	Z	rmsd	lali	nres	%id	PDB	Description
1:	3ctd-A	3.6	3.2	80	150	6	PDB	MOLECULE: PUTATIVE ATPASE, AAA FAMILY;
2:	3u61-C	3.6	4.5	94	319	3	PDB	MOLECULE: DNA POLYMERASE ACCESSORY PROTEIN 44;
3:	1sxj-E	3.6	3.9	90	317	4	PDB	MOLECULE: ACTIVATOR 1 95 KDA SUBUNIT;
4:	3pvs-C	3.5	3.4	85	420	6	PDB	MOLECULE: REPLICATION-ASSOCIATED RECOMBINATION PROTEIN A;
5:	3ctd-B	3.5	3.1	79	158	6	PDB	MOLECULE: PUTATIVE ATPASE, AAA FAMILY;
6:	3bge-B	3.5	3.1	81	163	5	PDB	MOLECULE: PREDICTED ATPASE;
7:	3u60-D	3.5	3.2	83	319	2	PDB	MOLECULE: DNA POLYMERASE ACCESSORY PROTEIN 44;
8:	1sxj-D	3.5	5.1	94	328	4	PDB	MOLECULE: ACTIVATOR 1 95 KDA SUBUNIT;
9:	3u61-E	3.5	3.6	90	294	4	PDB	MOLECULE: DNA POLYMERASE ACCESSORY PROTEIN 44;
10:	3u61-D	3.5	3.3	84	320	4	PDB	MOLECULE: DNA POLYMERASE ACCESSORY PROTEIN 44;
11:	3u5z-D	3.5	4.9	92	320	2	PDB	MOLECULE: DNA POLYMERASE ACCESSORY PROTEIN 44;
12:	3u60-B	3.4	3.4	78	319	3	PDB	MOLECULE: DNA POLYMERASE ACCESSORY PROTEIN 44;
13:	3u61-B	3.4	9.1	84	305	4	PDB	MOLECULE: DNA POLYMERASE ACCESSORY PROTEIN 44;
14:	3bge-A	3.3	3.3	80	163	5	PDB	MOLECULE: PREDICTED ATPASE;
15:	3pvs-B	3.3	4.0	85	417	5	PDB	MOLECULE: REPLICATION-ASSOCIATED RECOMBINATION PROTEIN A;

Figure S3. Structural alignments for Orf11* and its N-terminal domain. Structural alignment was performed using the DALI server. The overall structure of Orf11* belongs to the protein family of acetyltransferases. The N-terminal all-helix domain belongs to the protein family of AAA ATPases. Z score: the statistical significance of the similarity between protein-of-interest and other neighborhood proteins. RMSD: the root-mean-square deviation of C-alpha atoms in the least-squares superimposition of the structurally equivalent C-alpha atoms. Lali: the number of structurally equivalent residues. Nres: the total number of amino acids in the hit protein. % id: the percentage of identical amino acids over structurally equivalent residues.
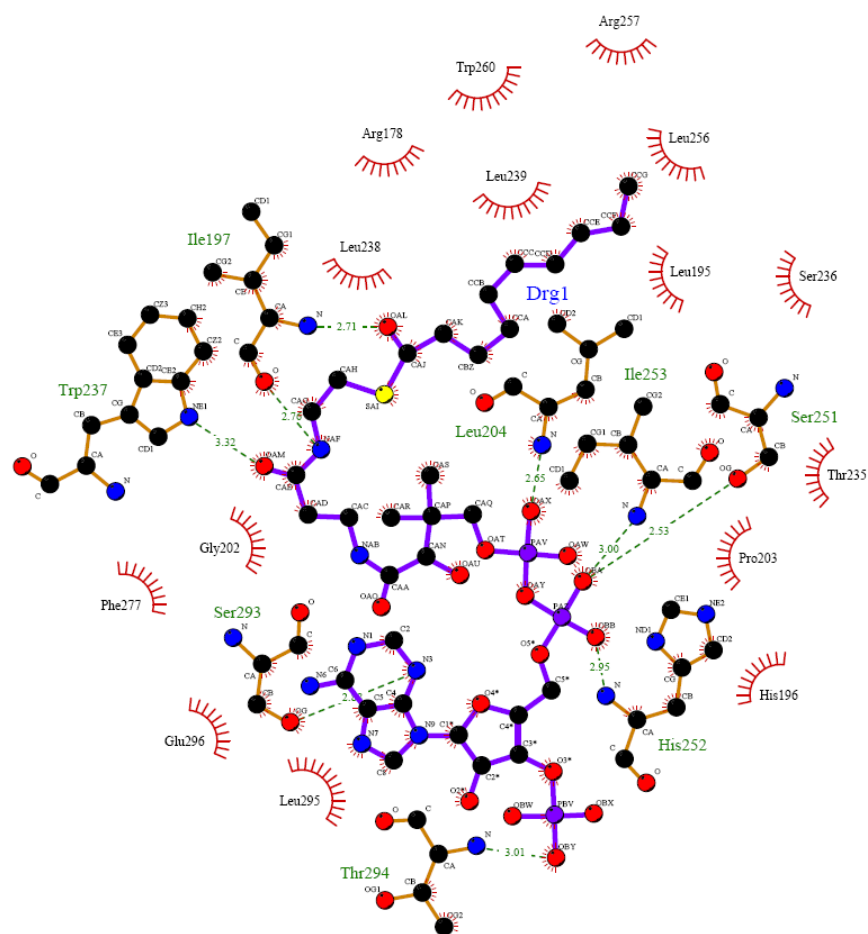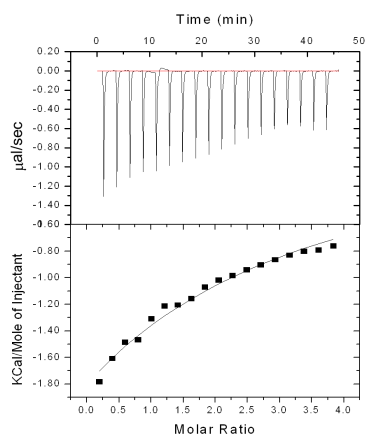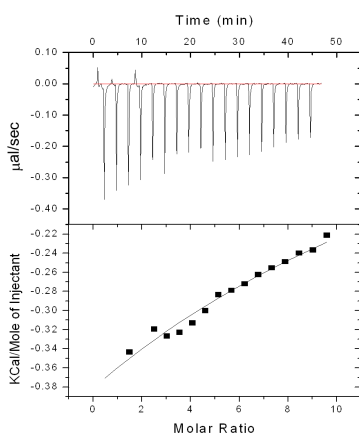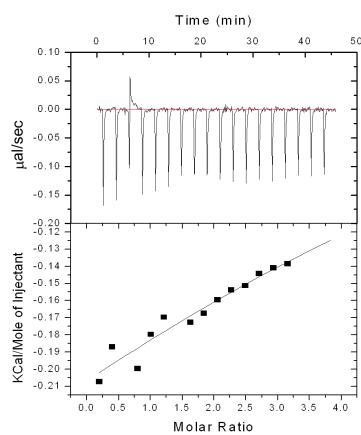
Figure S4. Ligplot diagram of the interaction between decanoyl-CoA and Orf11*.
This plot was generated using the Ligplot software.

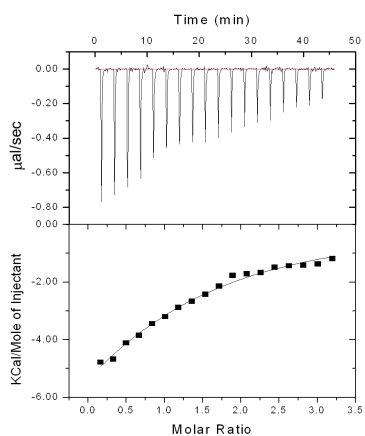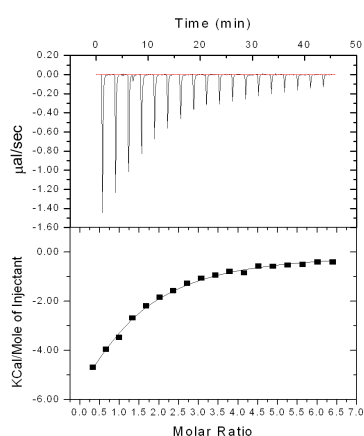**Tei pseudoaglycone**
K_d=ND

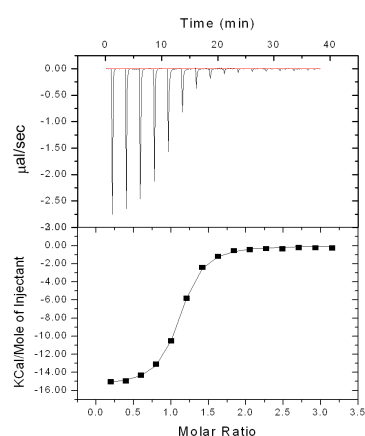**CoA**
K_d=ND

acetyl-CoA
K_d=ND

butyryl-CoA
K_d=111±23 μM

hexanoyl-CoA
K_d= 85.6±9 μM

octanoyl-CoA
K_d= 1±0.1 μM
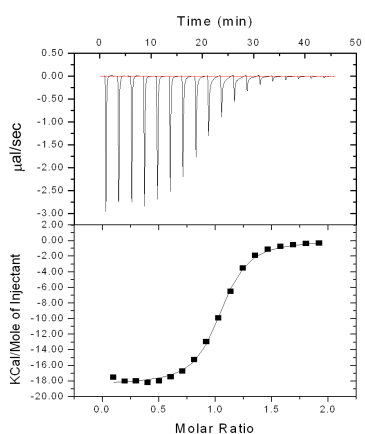
decanoyl-CoA
K_d= 1±0.1 μM

lauroyl-CoA
K_d=4.1± 0.8 μM

myristoyl-CoA
K_d= 5.9 ± 1.2 μM

palmitoyl-CoA

$K_d= 0.4 \pm 0.08 \, \mu M$
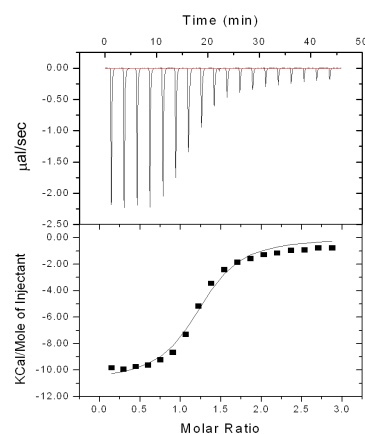
stearoyl-CoA

$K_d= 4.3 \pm 0.8 \, \mu M$
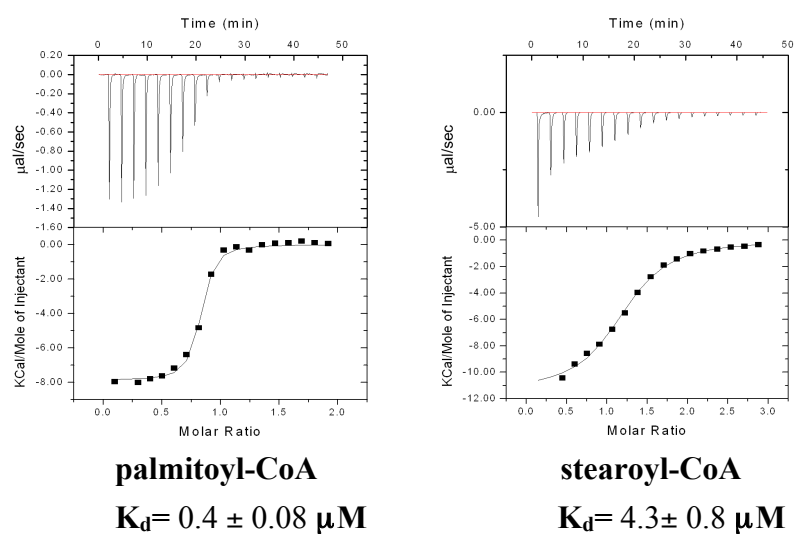
Figure S5. Isothermal titration calorimetry (ITC) analysis of Orf11*. ITC thermograms of Orf11* versus CoA, acetyl-CoA, butyryl-CoA, hexanoyl-CoA, octanoyl-CoA, decanoyl-CoA, lauroyl-CoA, myristoyl-CoA, palmitoyl-CoA, stearoyl-CoA or Tei pseudoaglycone. Each exothermic heat pulse corresponds to an injection of 2 μl of ligands (1 mM~5 mM) into a protein solution (0.1 mM); integrated heat areas constitute a differential binding curve that was fitted with a standard single-site binding model (Origin 7.0, MicroCal iTC$_{200}$).
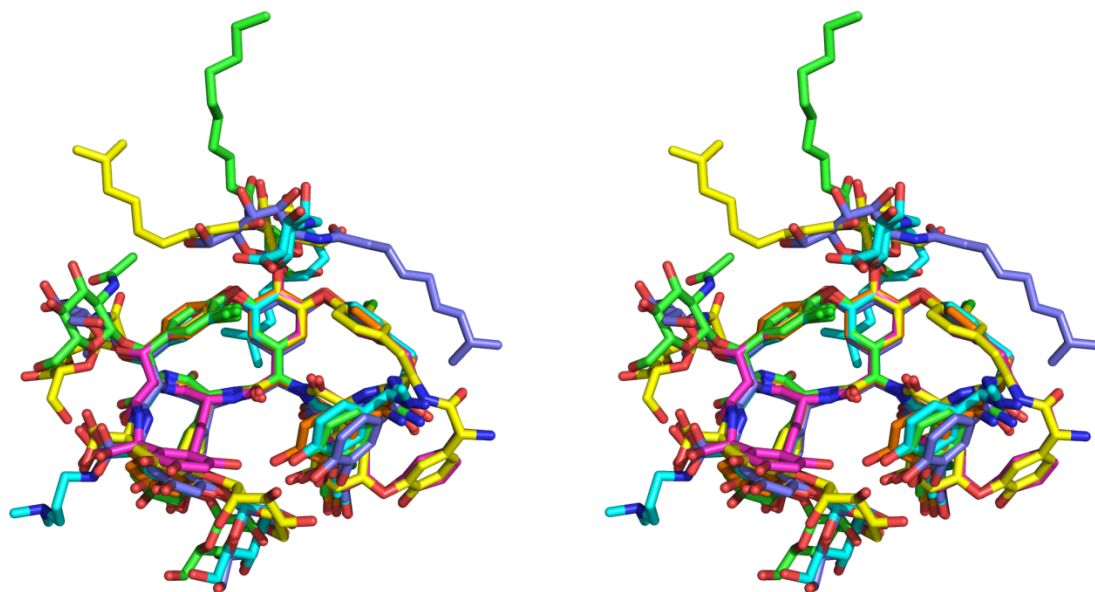
Figure S6. Stereoview for superposition of the teicoplanin class glycopeptides. Teicoplanin **13** (green, PDB code 4MFQ, this study), dalbavancin (cyan, PDB code 3RUL, in couple with ubiquitin), teicoplanin **1** (yellow, PDB code 2XAD, in the Orf2* complex), desulfo-A47934 (magenta, PDB code 4EEC, in the StaL complex), teicoplanin aglycone (orange, PDB ID code 3MGB, in the Teg12 complex) and teicoplanin **1** (purple, PDB code 4K3T, in the Dbv29 complex) are superposed using residues 4–7 of the scaffold.

a.
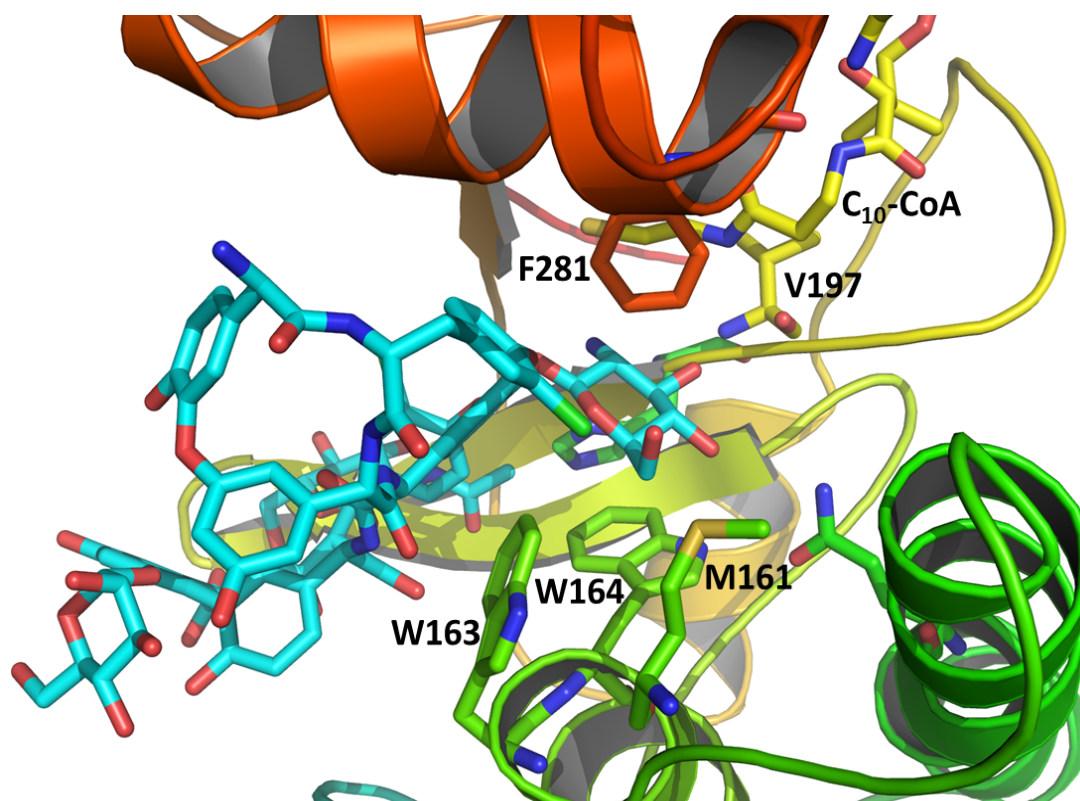
b.
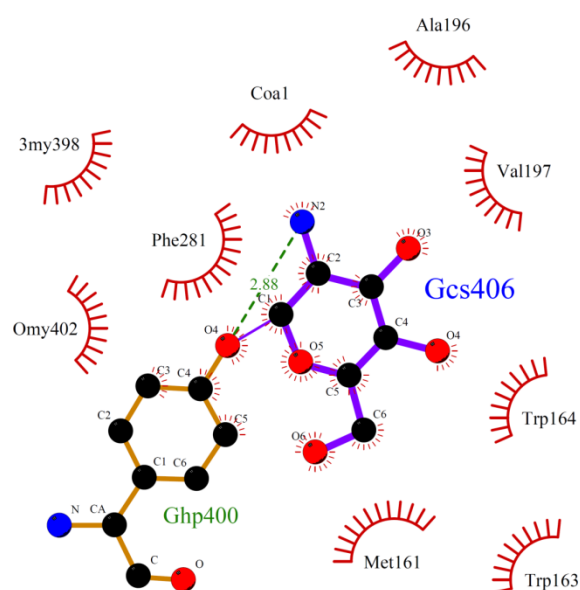
Figure S7. The binding site of r4-glucosamine of Tei pseudoaglycone in Orf11*.
(a) The binding site of r4-glucosamine of Tei pseudoaglycone in the structure of Orf11* H196A/decanoyl-CoA/Tei pseudoaglycone complex. (b) The Ligplot diagram shows the binding site of the r4-glucosamine in the complex.
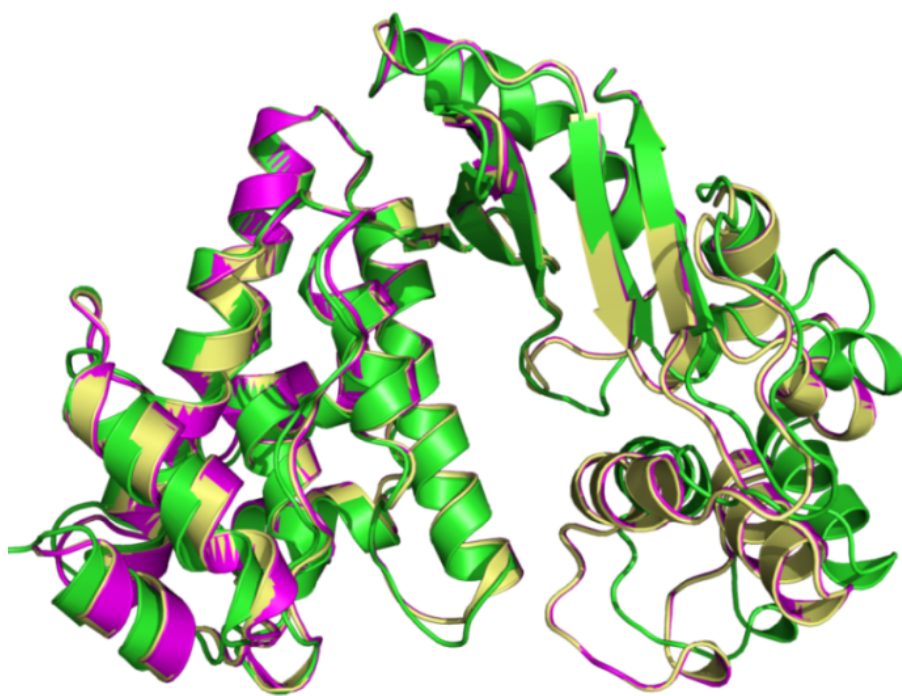
Figure S8. Superimposition of unary, binary and ternary structures. Unary structure: native Orf11* (colored green). Binary structure: Orf11* in complex with decanoyl-CoA (colored gold). Ternary structures: Orf11* in complex with decanoyl-CoA and Tei pseudoaglycone (colored magenta).
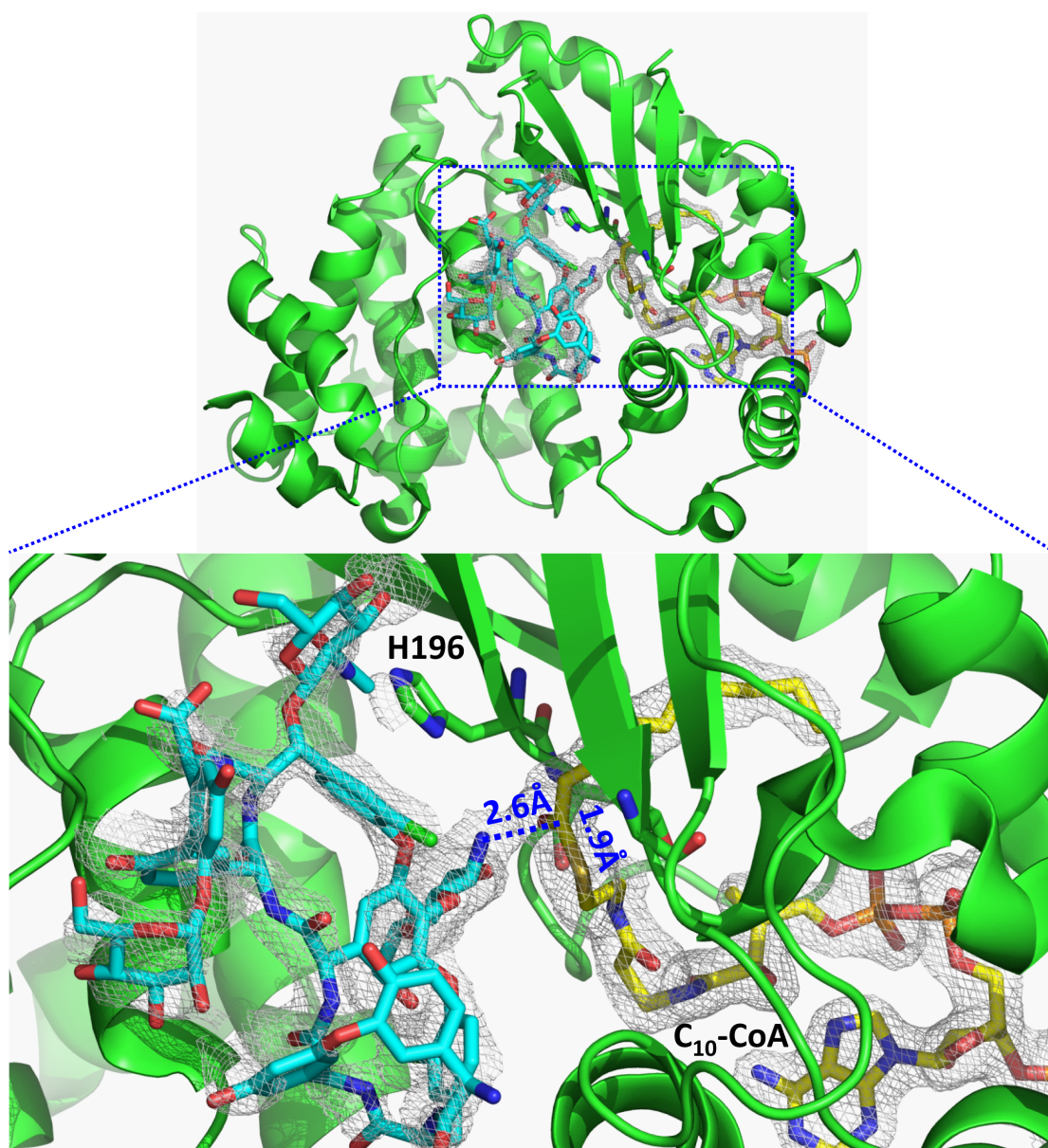
Figure S9. The active site of Orf11*H196A/decanoyl-CoA/Tei pseudoaglycone complex structure. The H196A is modeled back to His196 based on the corresponding geometry at the active site of the binary wild-type structure. The difference electron density maps (F_o-F_c) are contoured at 2.0 σ.
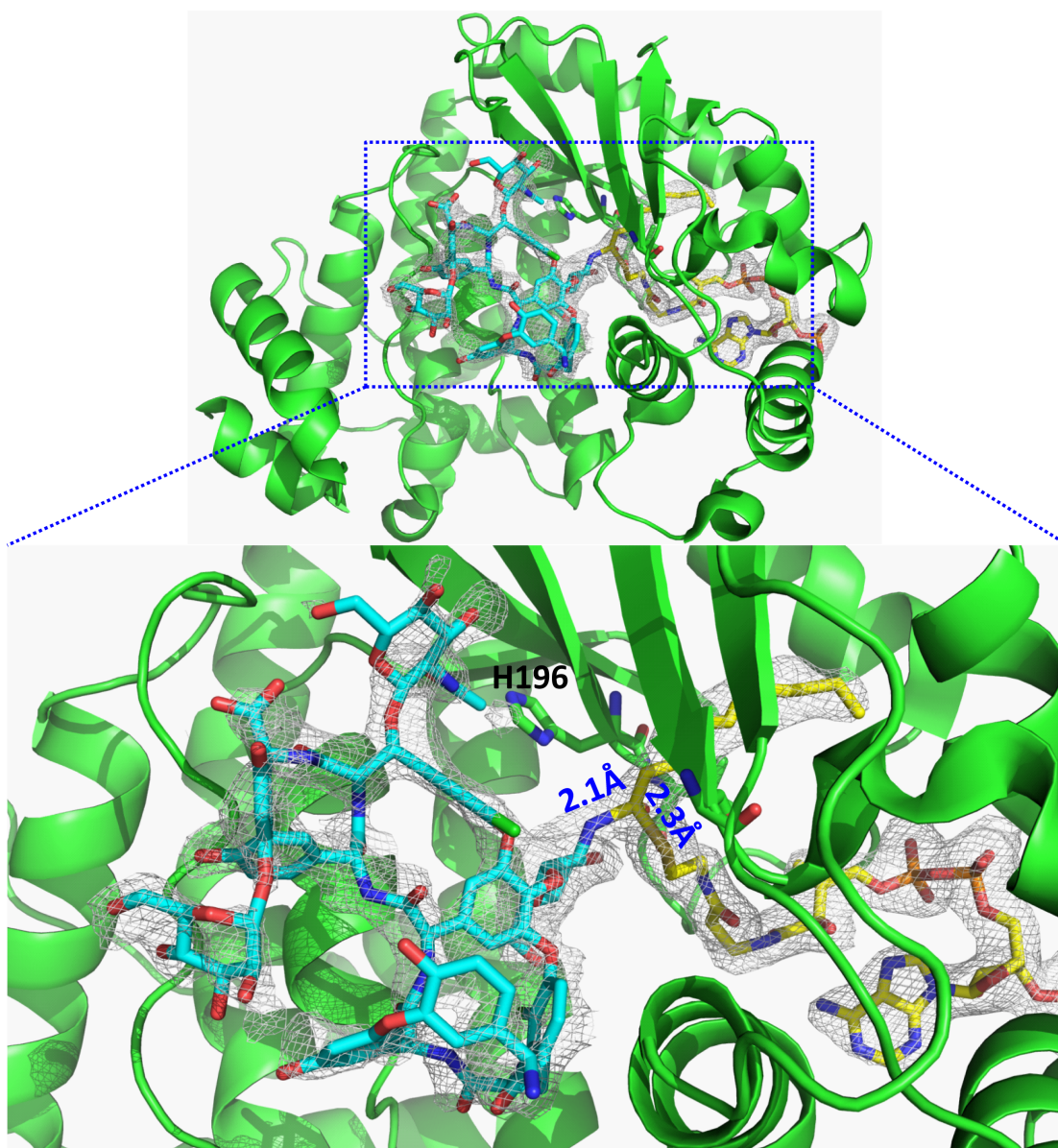
Figure S10. The active site of Orf11*H196A/decanoyl-CoA-Tei pseudoaglycone complex structure. The H196A is modeled back to His196 based on the corresponding geometry at the active site of the binary wild-type structure. The The difference electron density maps (F_o-F_c) are contoured at 2.0 σ.
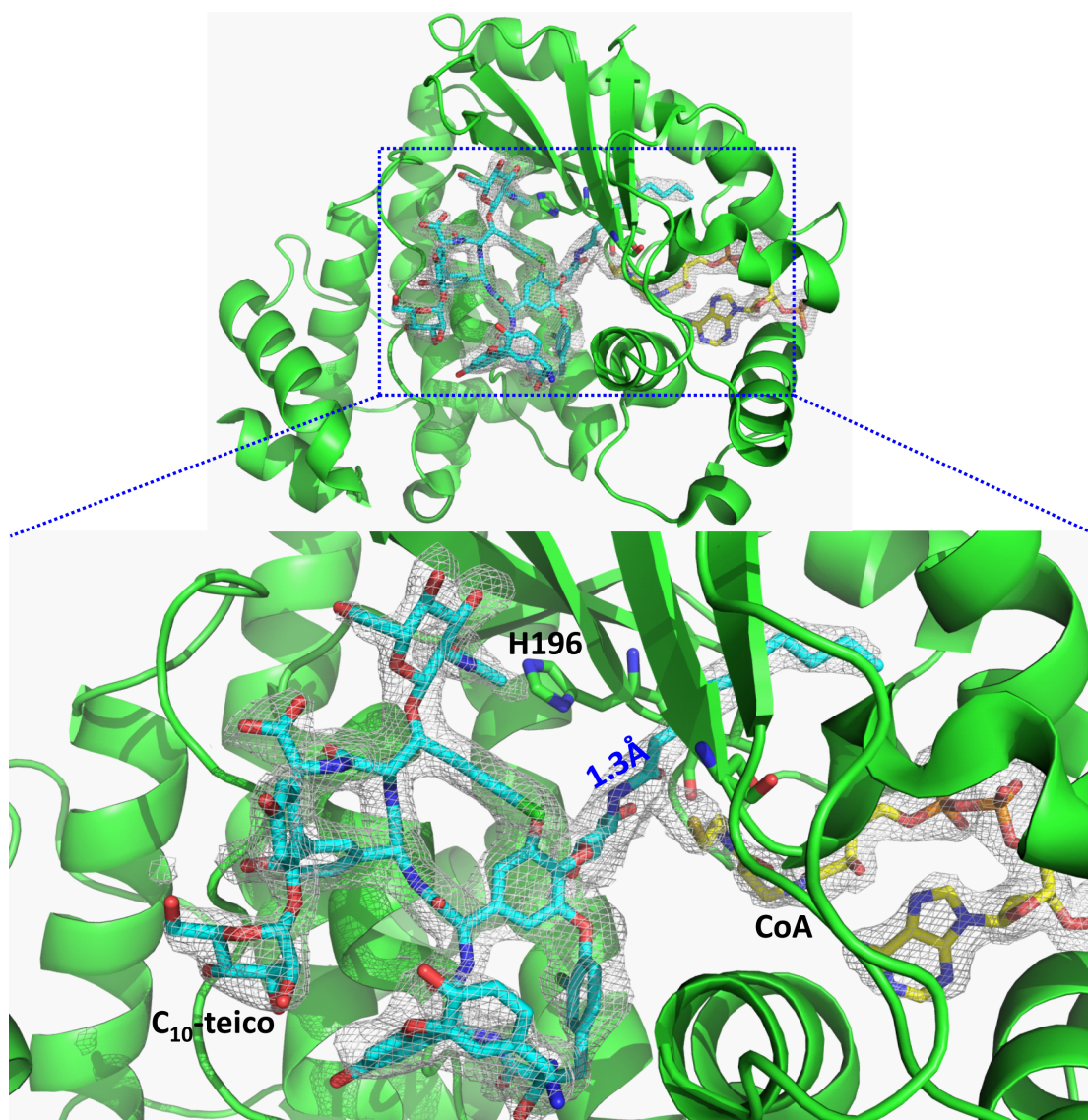
Figure S11. The active site of Orf11*H196A/CoA/10C-teicoplanin complex structure. The H196A is modeled back to His196 based on the corresponding geometry at the active site of the binary wild-type structure. The difference electron density maps (F_o-F_c) are contoured at 2.0 σ.

a

Chemical Formula: $C_{74}H_{89}Cl_2N_9O_{25}$
Exact Mass: 1573.53

Relative Abundance (y-axis): 0, 10, 20, 30, 40, 50, 60, 70, 80, 90, 100

m/z (x-axis): 1560, 1565, 1570, 1575, 1580, 1585, 1590

Peaks: 1574.44, 1575.41, 1576.43, 1577.45, 1578.40, 1579.42

b.

Chemical Formula: $C_{76}H_{93}Cl_2N_9O_{25}$
Exact Mass: 1601.57

Relative Abundance (y-axis): 0, 10, 20, 30, 40, 50, 60, 70, 80, 90, 100

m/z (x-axis): 1575, 1580, 1585, 1590, 1595, 1600, 1605, 1610, 1615, 1620, 1625, 1630

Peaks: 1602.72, 1603.74, 1604.71, 1605.70, 1606.70, 1607.71, 1608.75
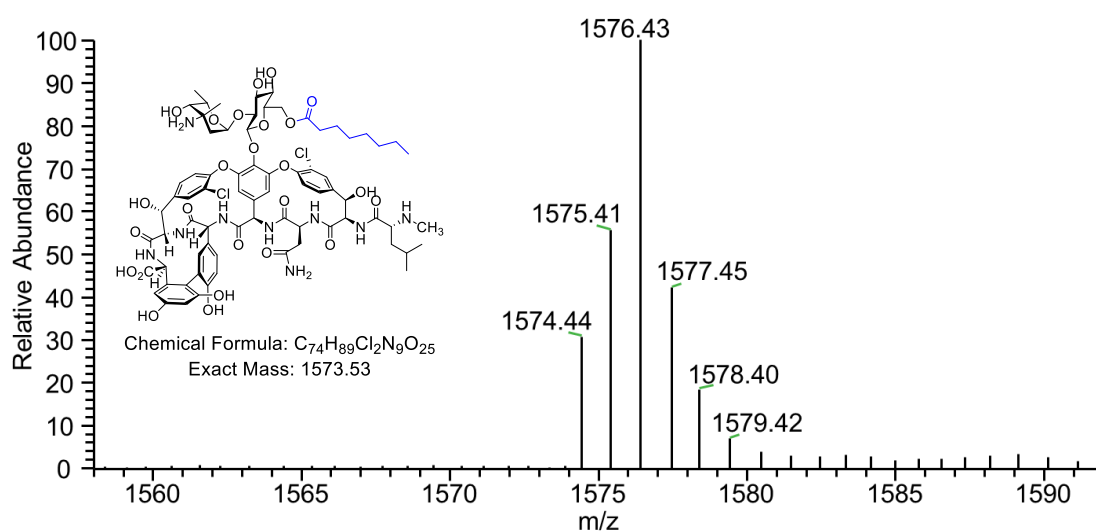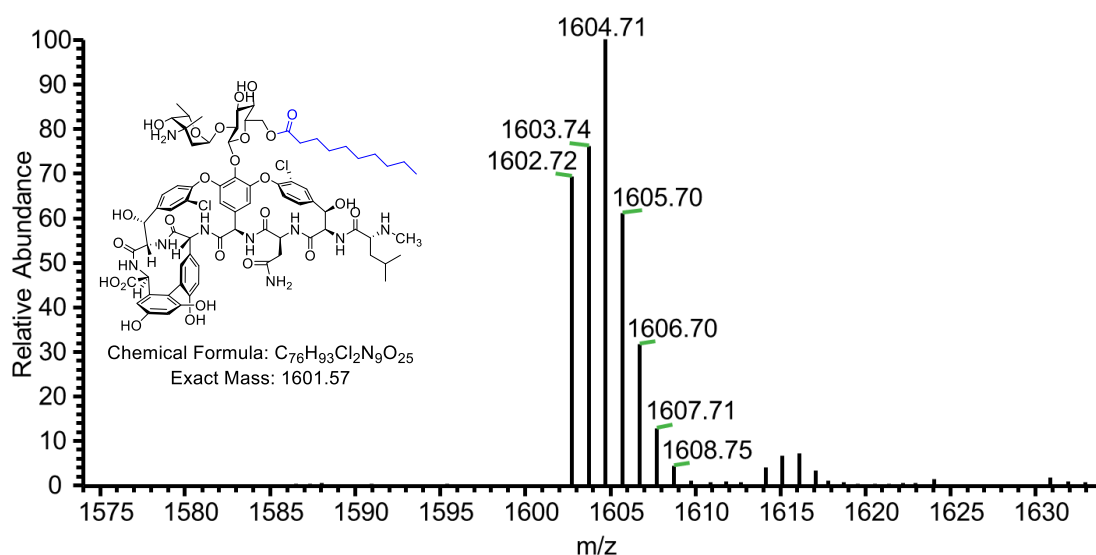
Figure S12. The structures and mass spectra of (a) C$_8$-vancomycin 7 and (b) C$_{10}$-vancomycin 8.

¹H NMR spectrum for compound 7

¹H NMR spectrum for compound 7

¹³C NMR spectrum for compound 7
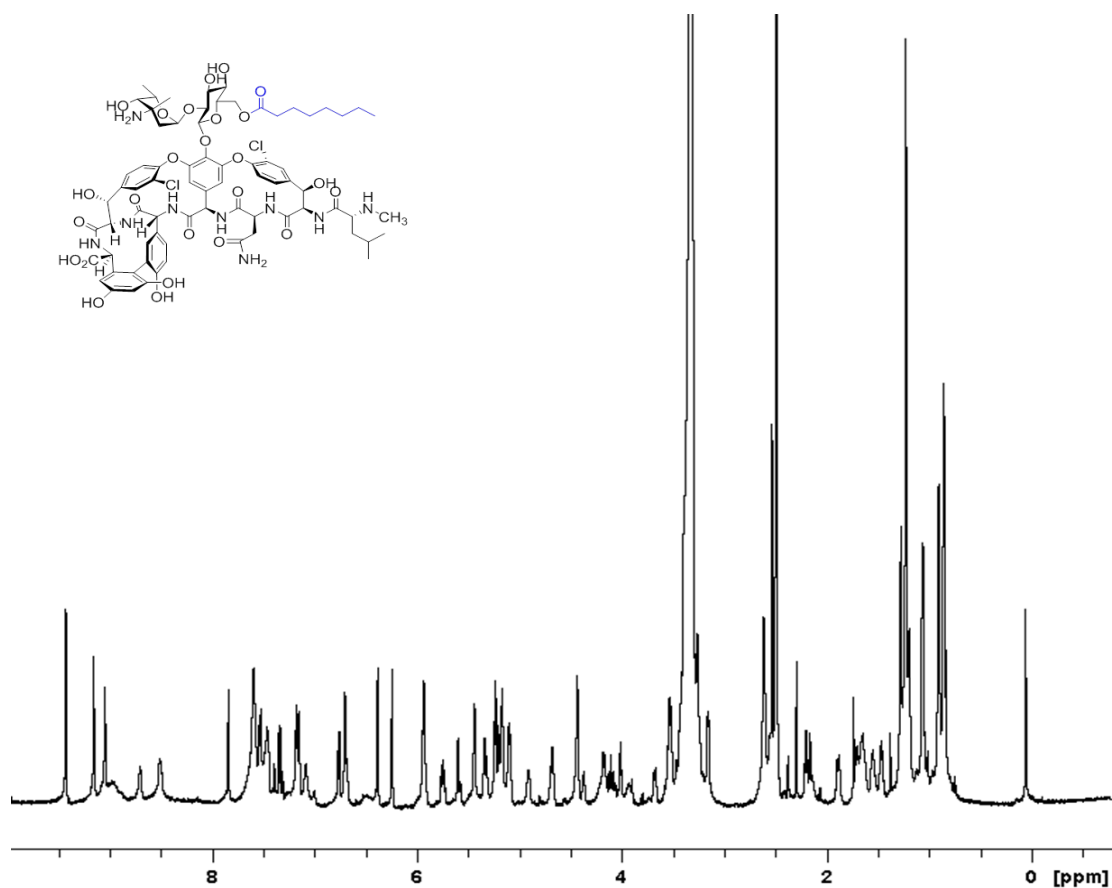
¹³C NMR spectrum for compound 7
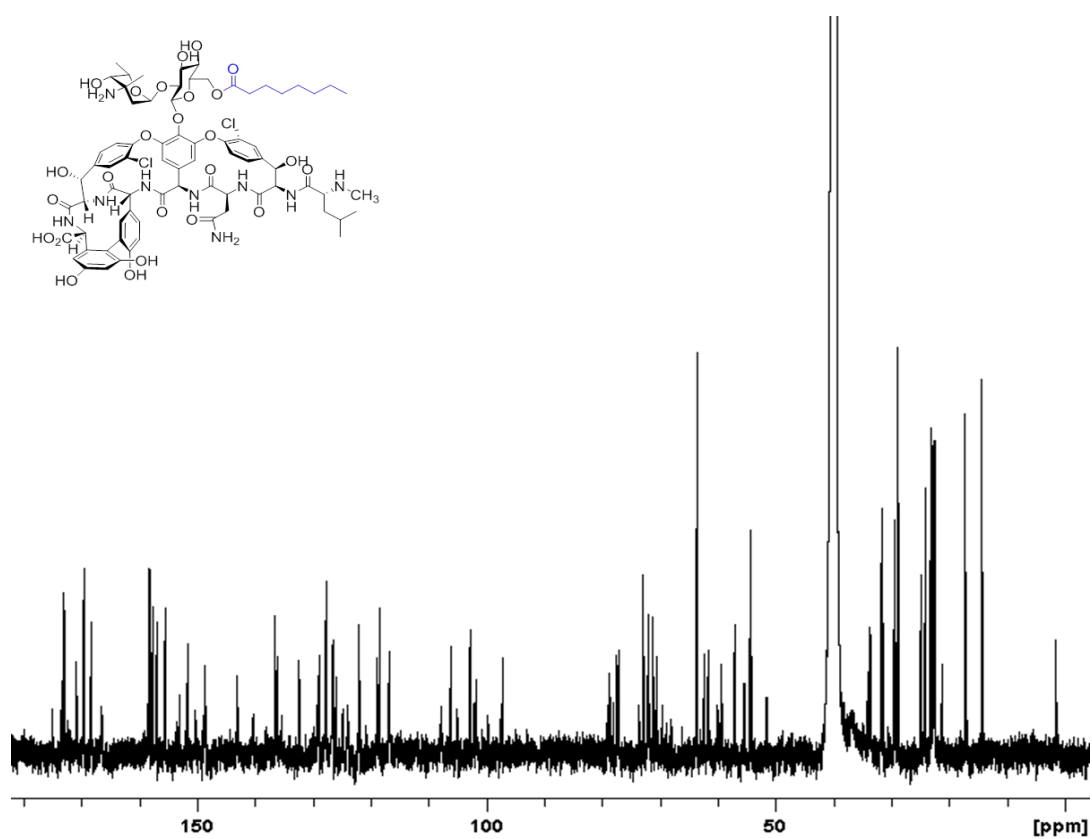
¹H COSY spectrum for compound 7
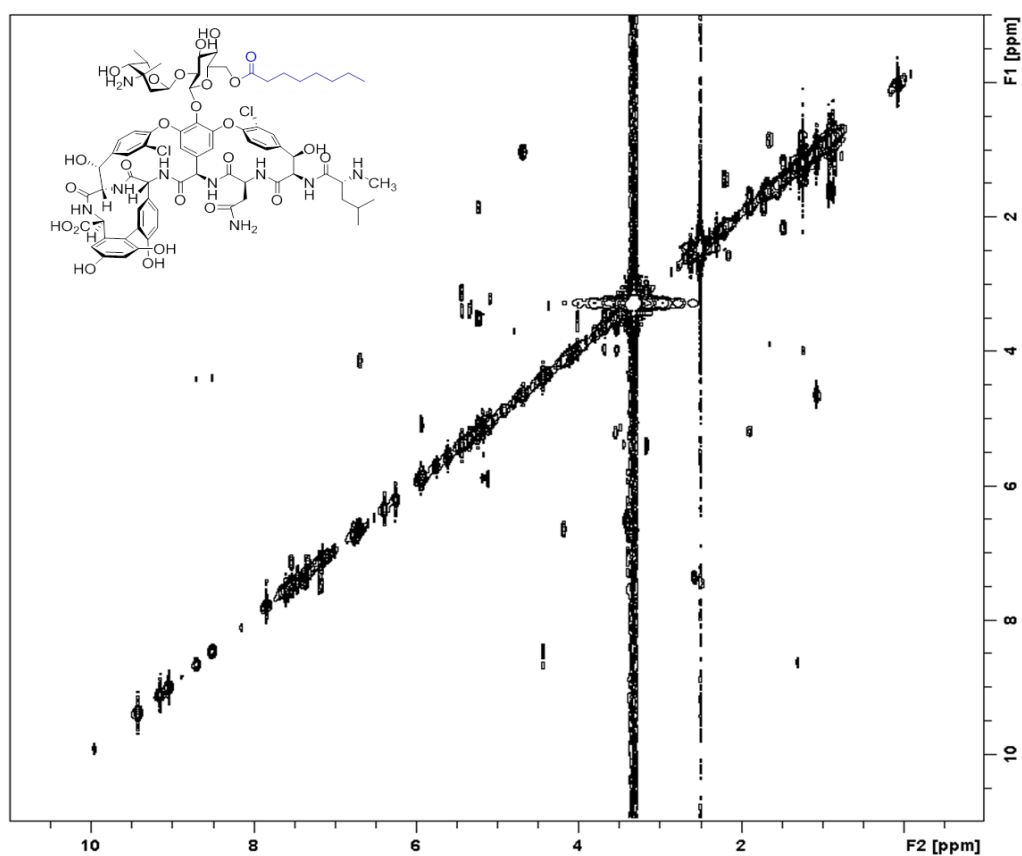
¹H¹³C HSQC spectrum for compound 7
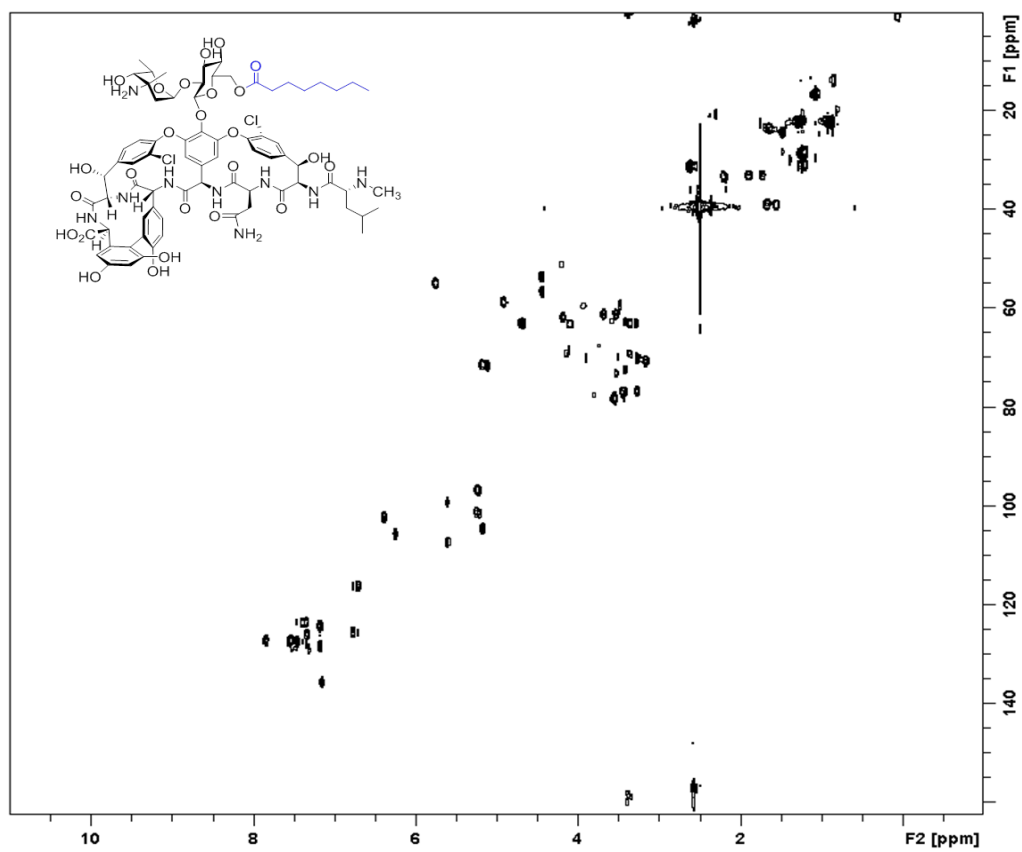
^{1}H^{13}C HMBC spectrum for compound 7
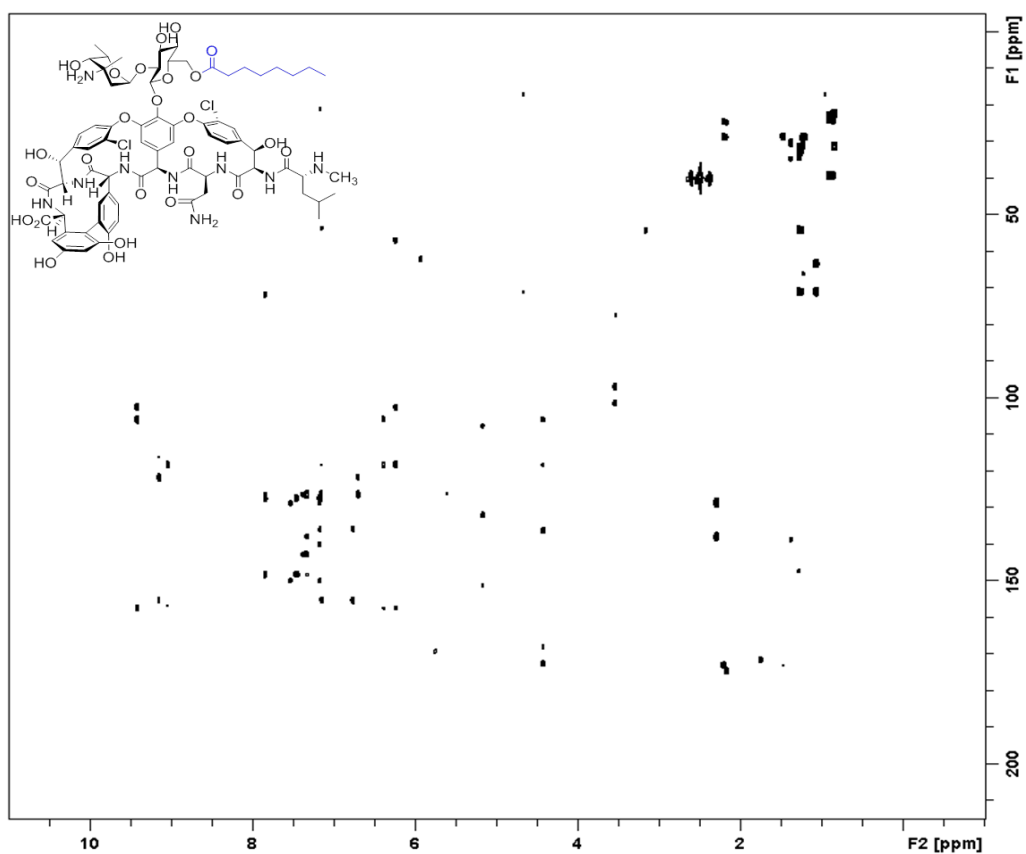
Figure S13. NMR information for compound 7. NMR spectra include ^{1}H, ^{13}C, COSY, HSQC, HMBC, and NOESY.
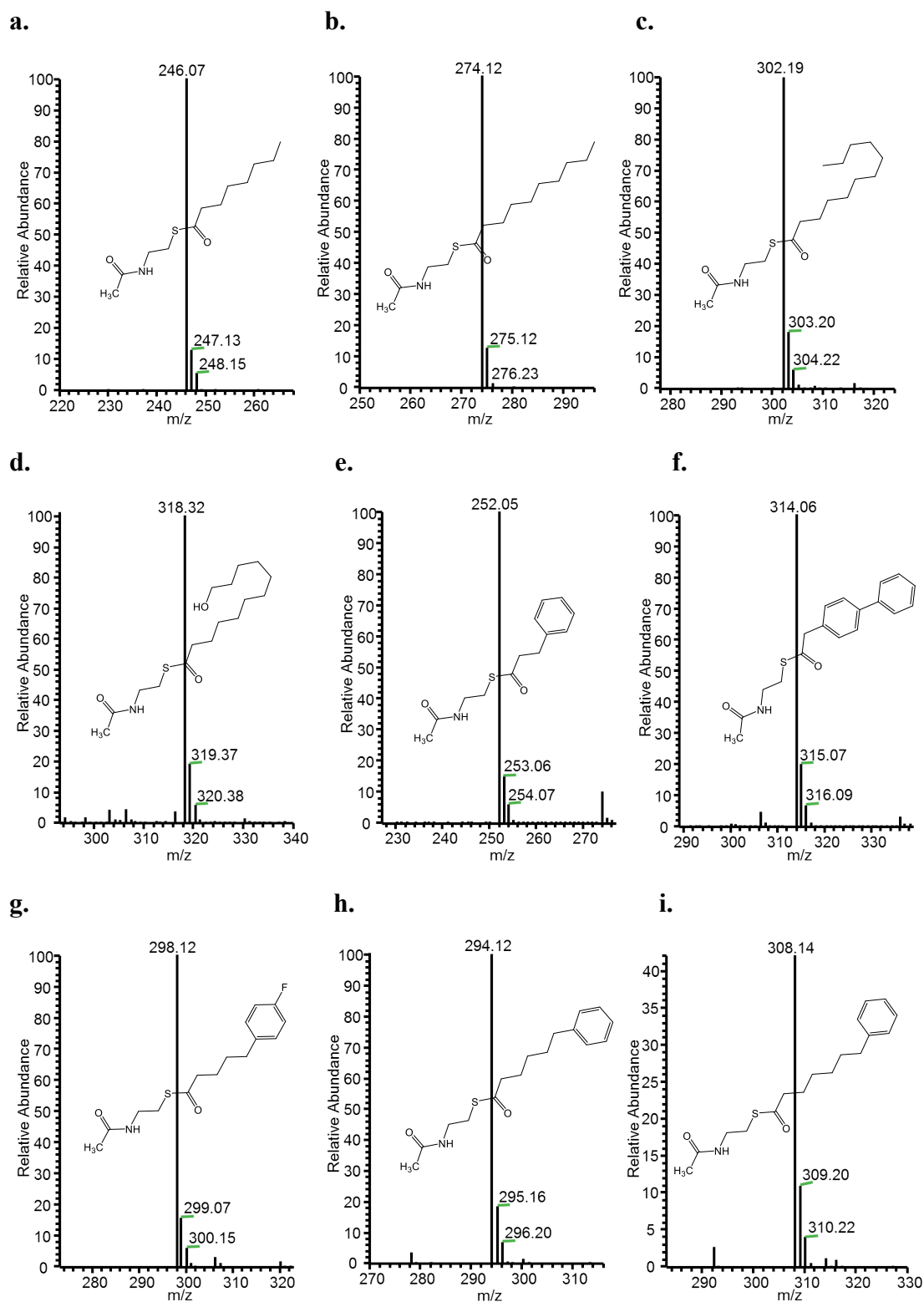
Figure S14. Structure and mass spectra of chemically synthesized acyl-NAC. (a) octanoyl-NAC (b) decanoyl-NAC (c) lauroyl-NAC (d) 12-hydroxydodecanoyl-NAC (e) dihydrocinnamoyl-NAC (f) 4-biphenylacetyl-NAC (g) 5-(4-fluoro-phenyl) valeryl-NAC (h) 6-phenyl hexanoyl-NAC (i) 7-phenyl heptanoyl-NAC.
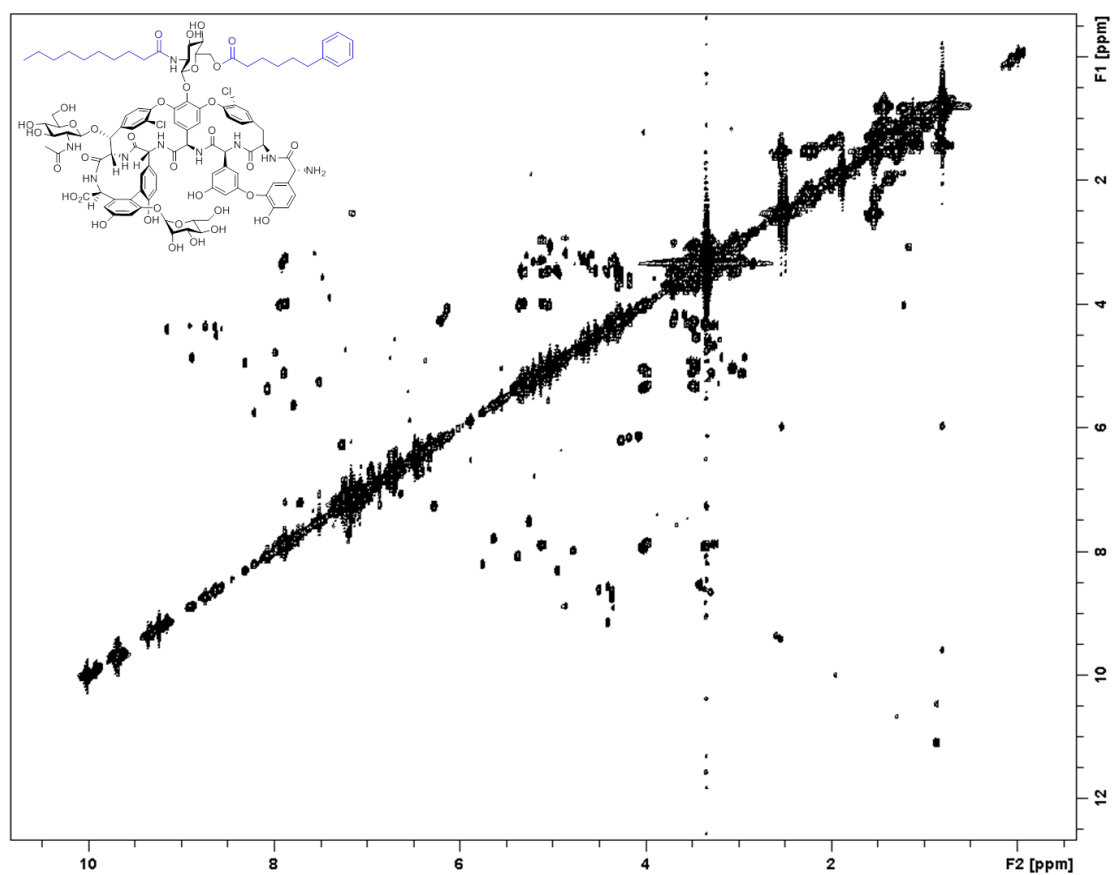
^{1}H NMR spectrum for compound 10
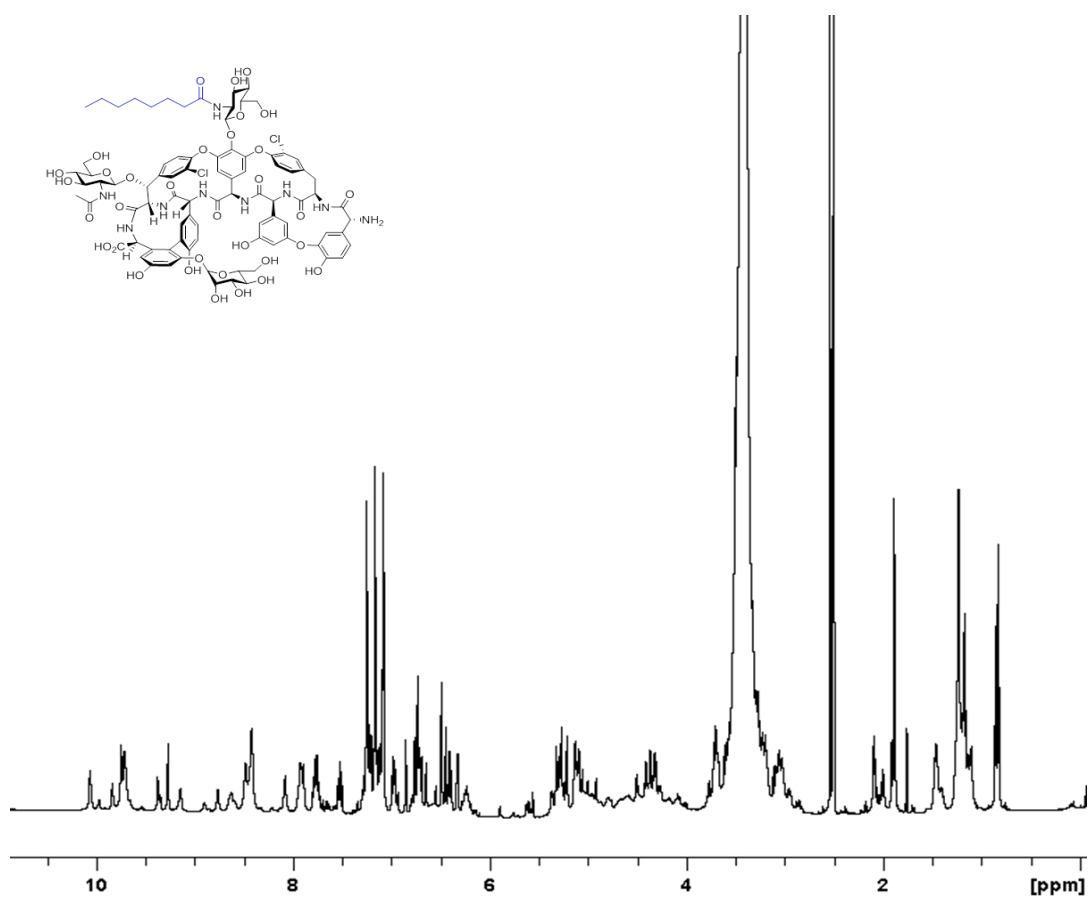
^{13}C NMR spectrum for compound 10
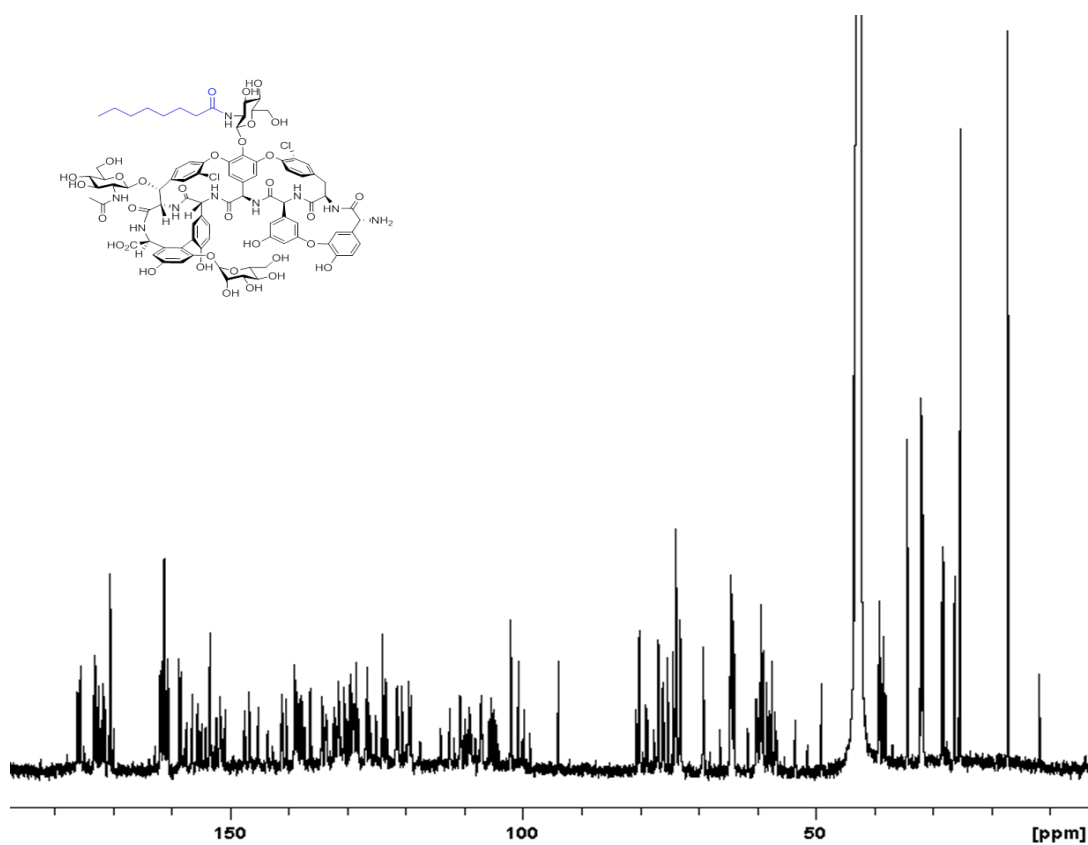
^{1}H COSY spectrum for compound 10
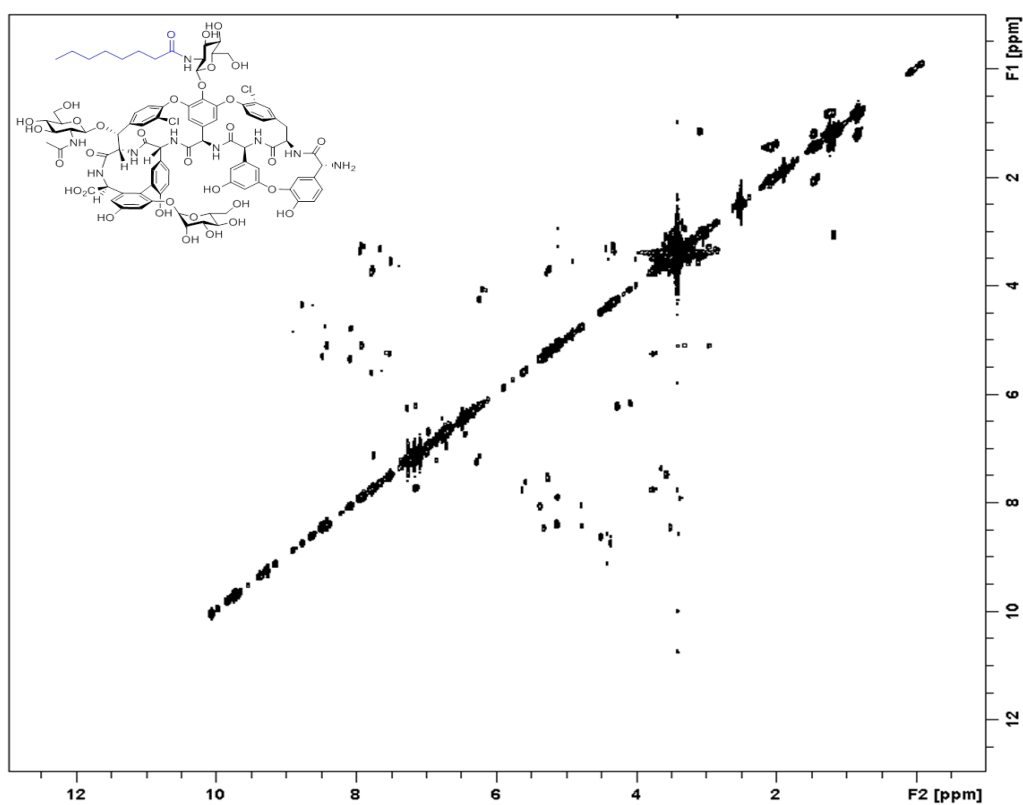
^{1}H^{13}C HSQC spectrum for compound 10
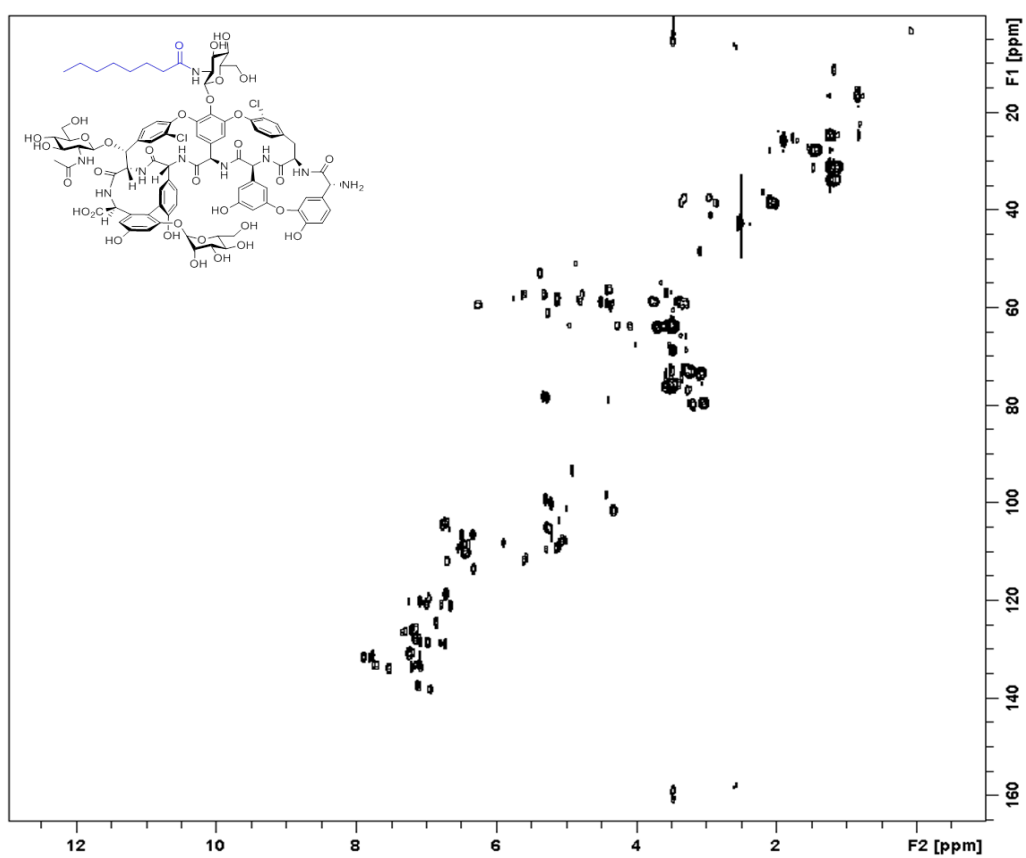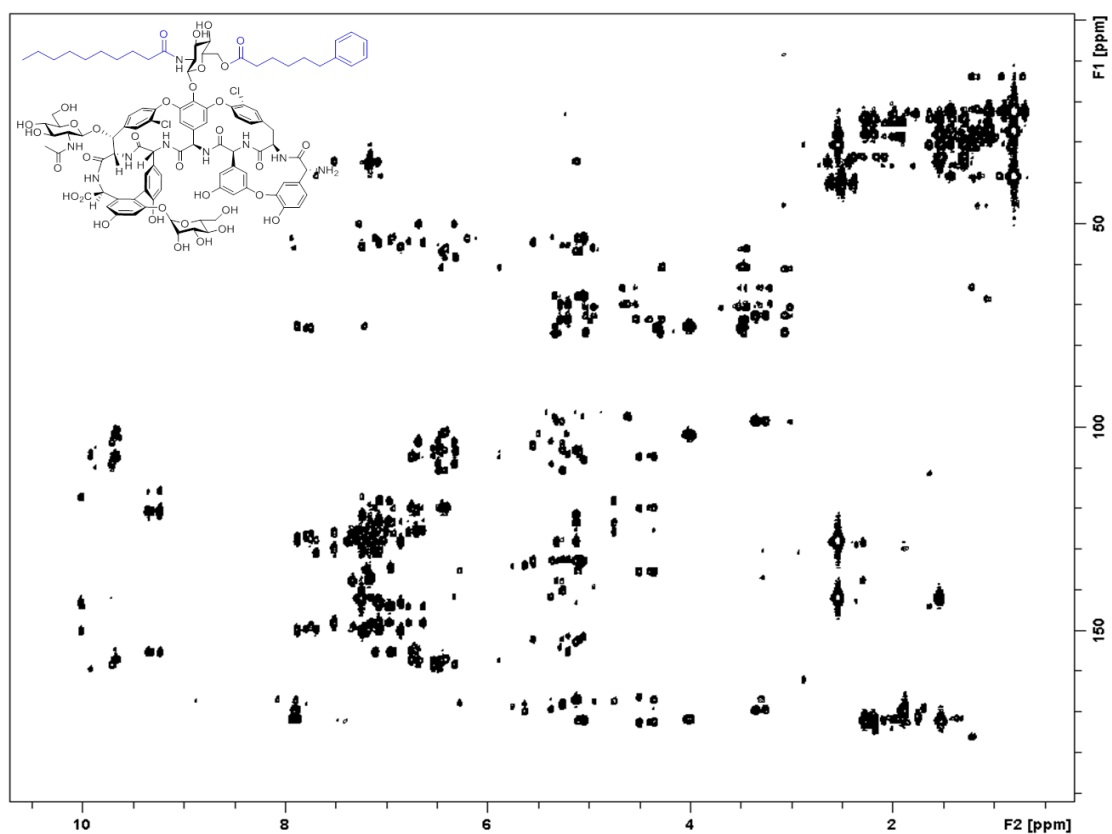
¹H¹³C HMBC spectrum for compound 10
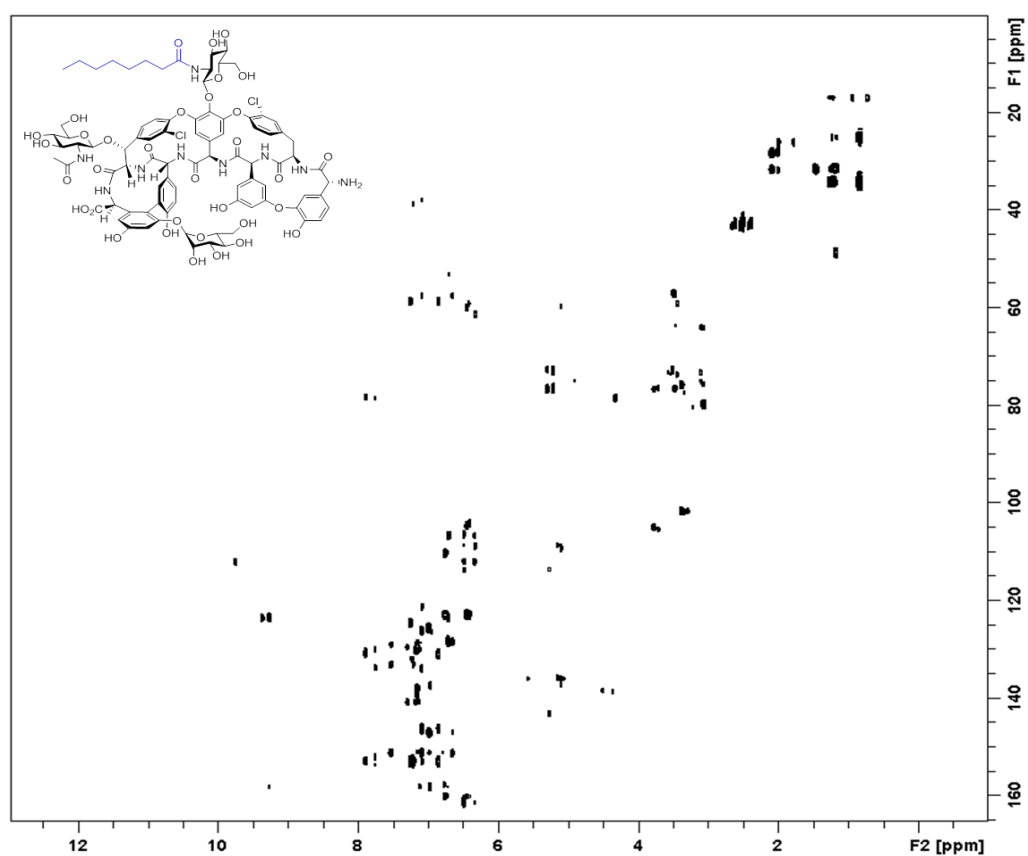
Figure S15. NMR information for compound 10. NMR spectra include ¹H, ¹³C, COSY, HSQC, HMBC, and NOESY.

¹H NMR spectrum for compound 11
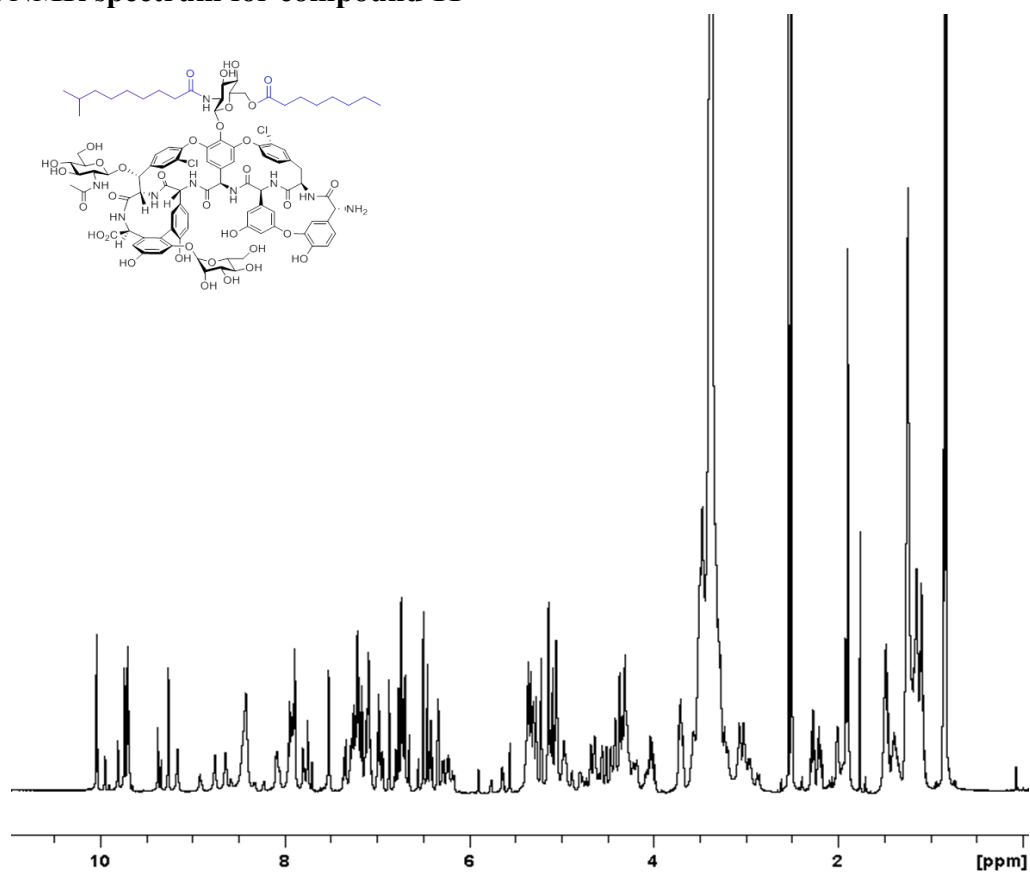
¹³C NMR spectrum for compound 11
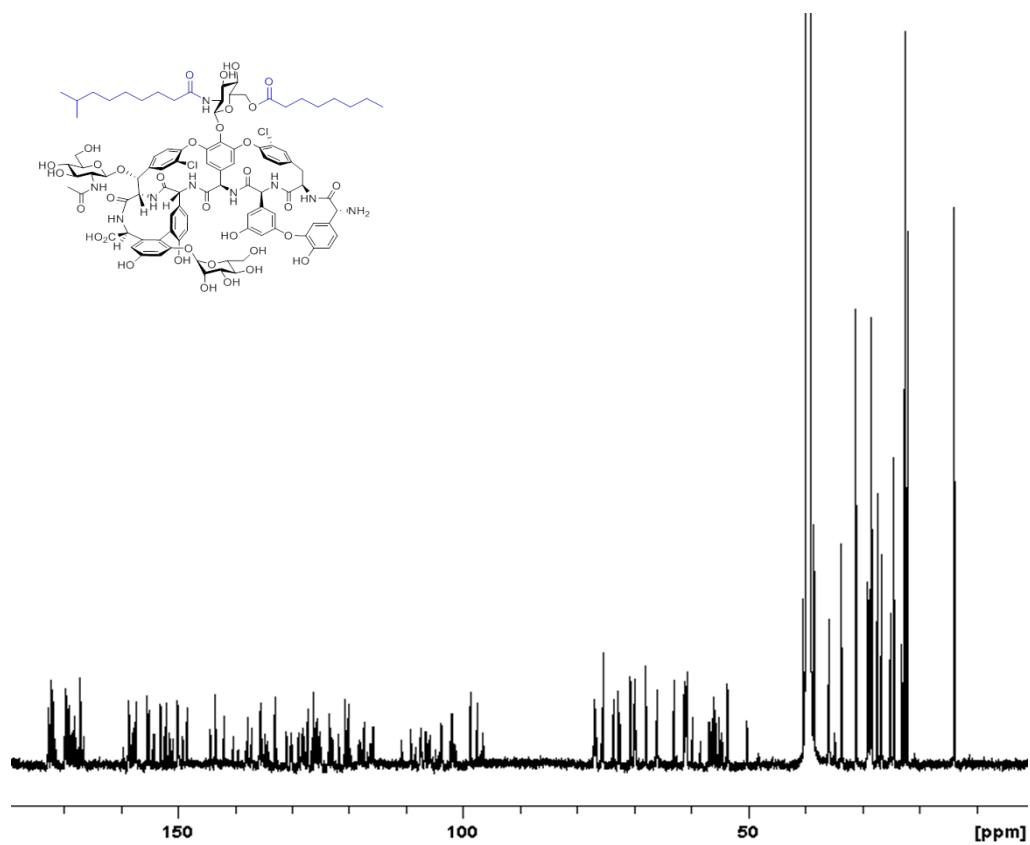
¹H COSY spectrum for compound 11
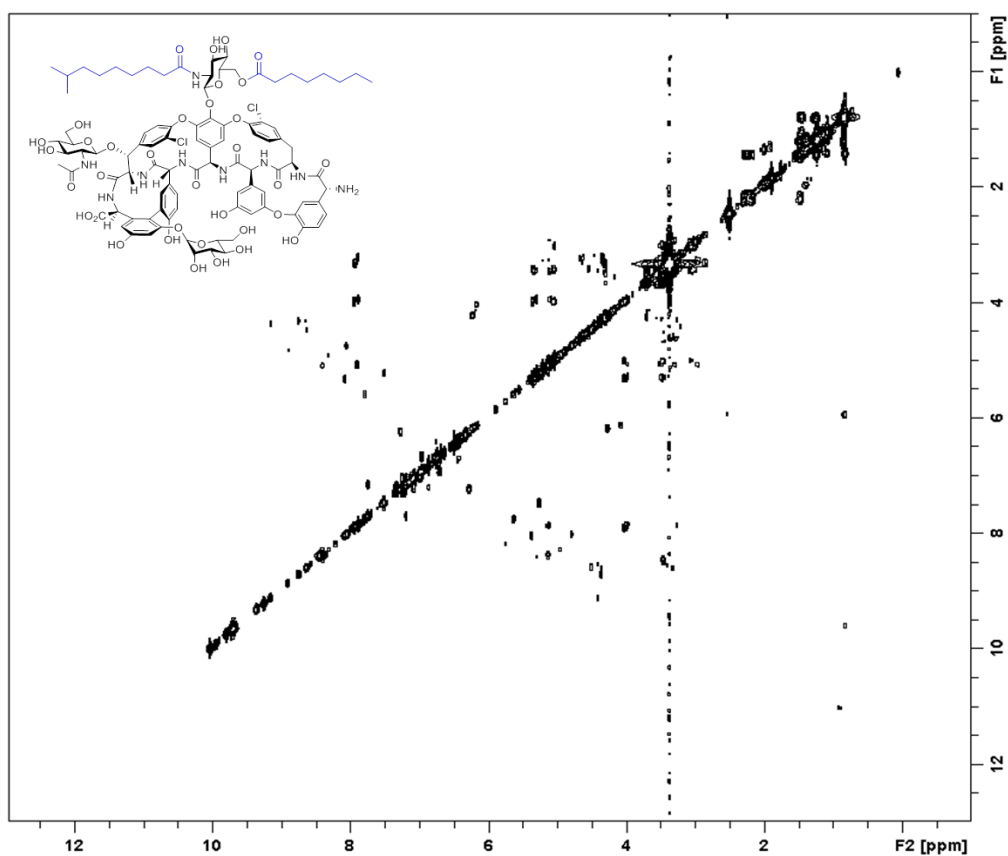
¹H¹³C HSQC spectrum for compound 11
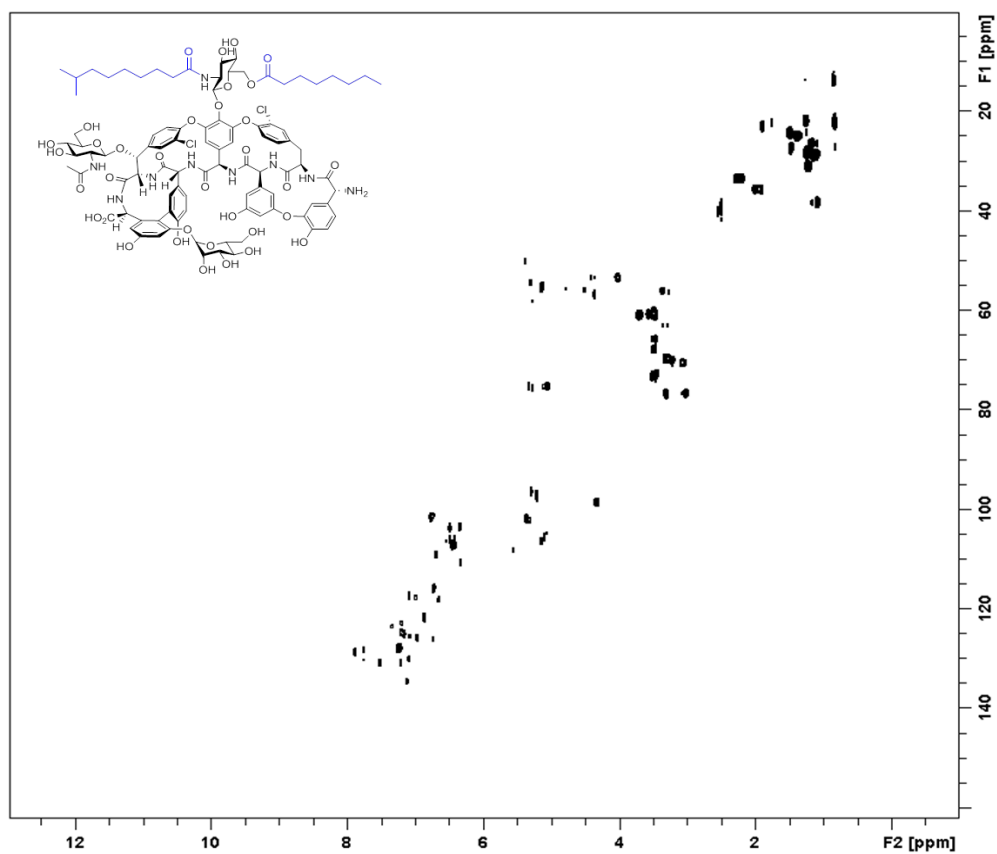
# $^1H^{13}C$ HMBC spectrum for compound 11
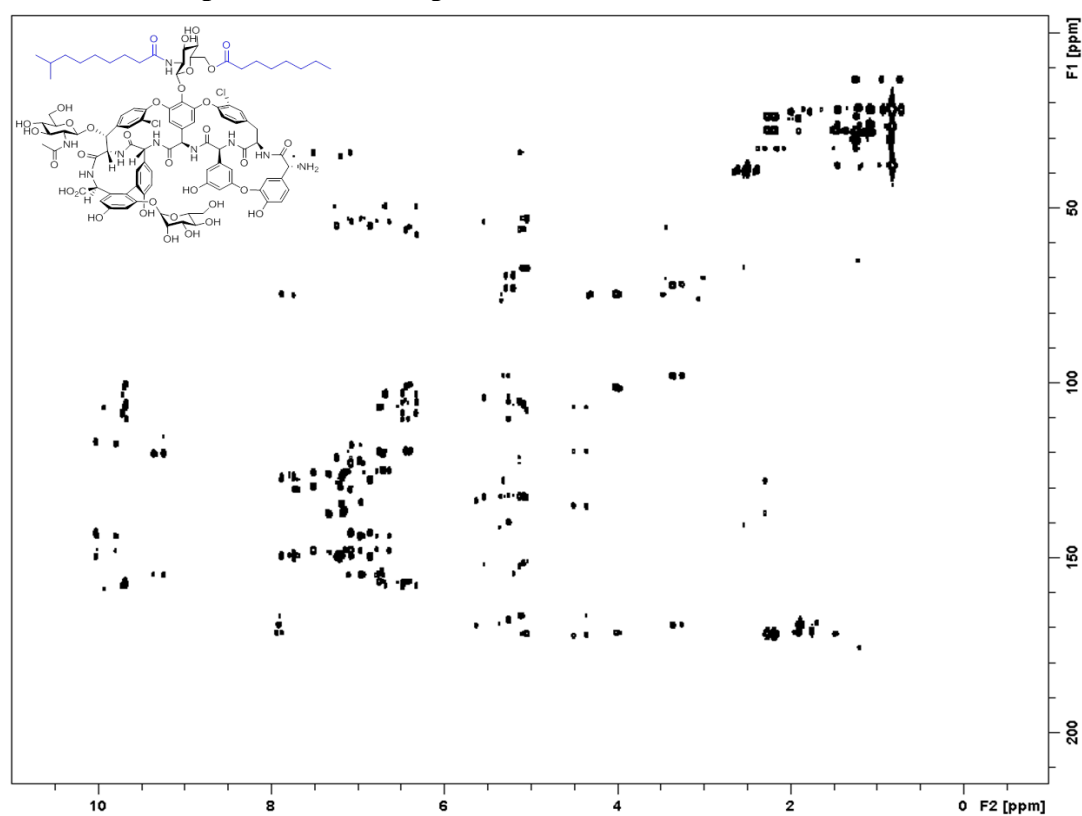
**Figure S16. NMR information for compound 11.** NMR spectra include ^1H, ^{13}C, COSY, HSQC, HMBC, and NOESY.
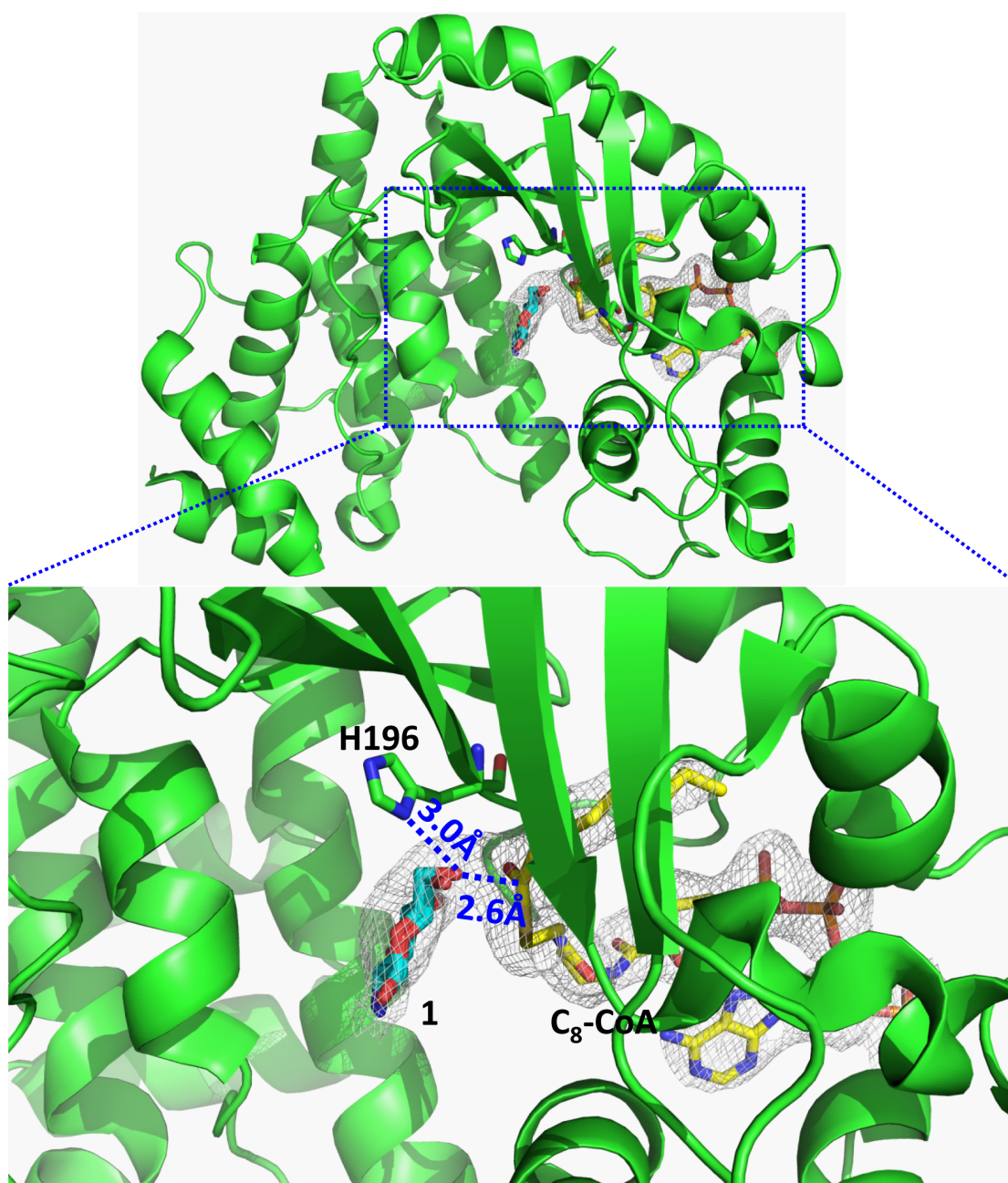
Figure S17. The active site of Orf11*/octanoyl-CoA/teicoplanin complex structure. The glucosamine moiety with its C6-OH points to the acyl-CoA carbonyl carbon. The difference electron density maps (F_o-F_c) are contoured at 2.0 σ.
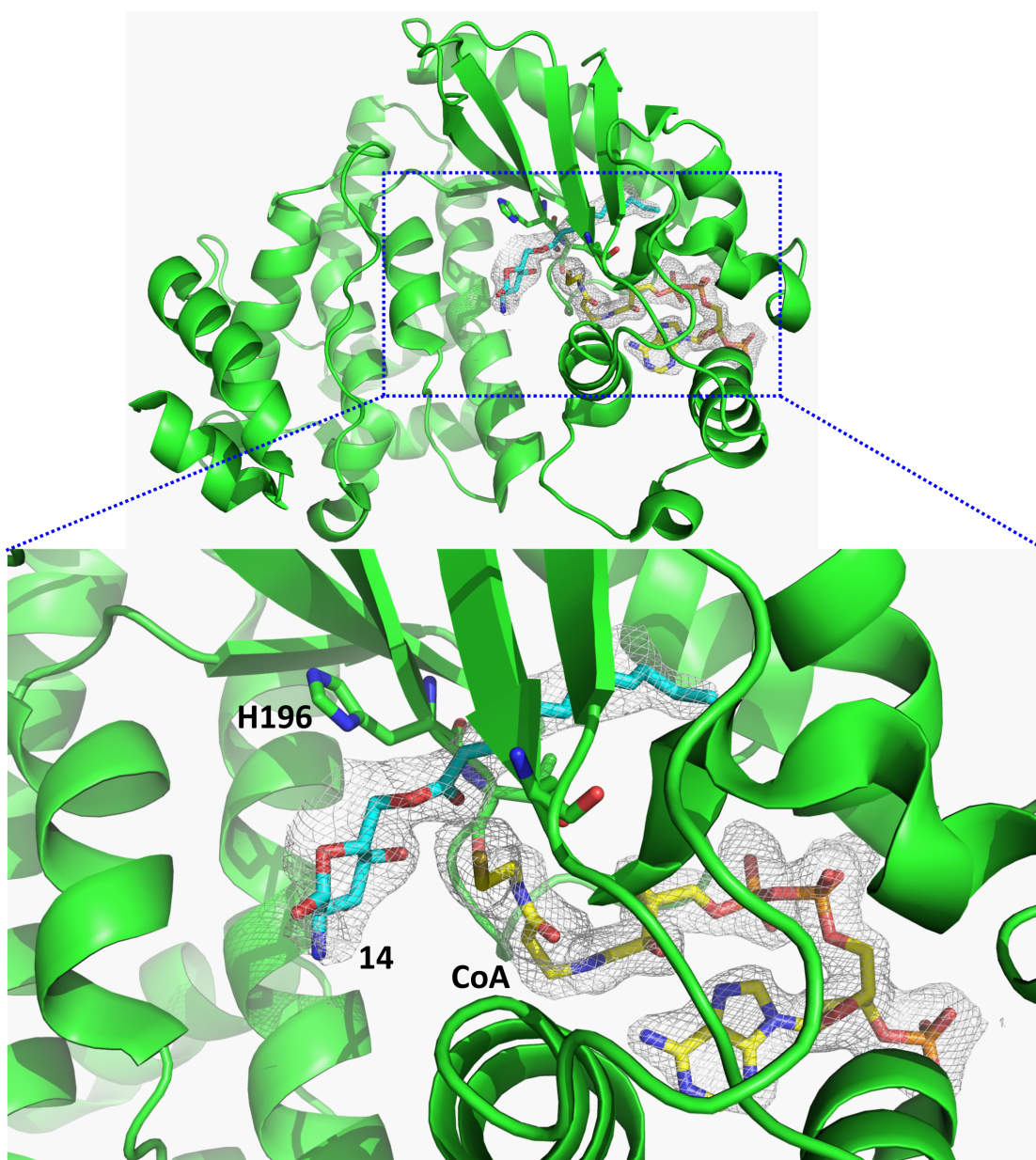
Figure S18. The active site of Orf11*/CoA/O6-decanoyl-teicoplanin complex structure. The glucosamine moiety has its amine group covalently linked to the acyl group. The difference electron density maps (F_o-F_c) are contoured at 2.0 σ.

^{1}H NMR spectrum for compound 20

^{13}C NMR spectrum for compound 20

S33
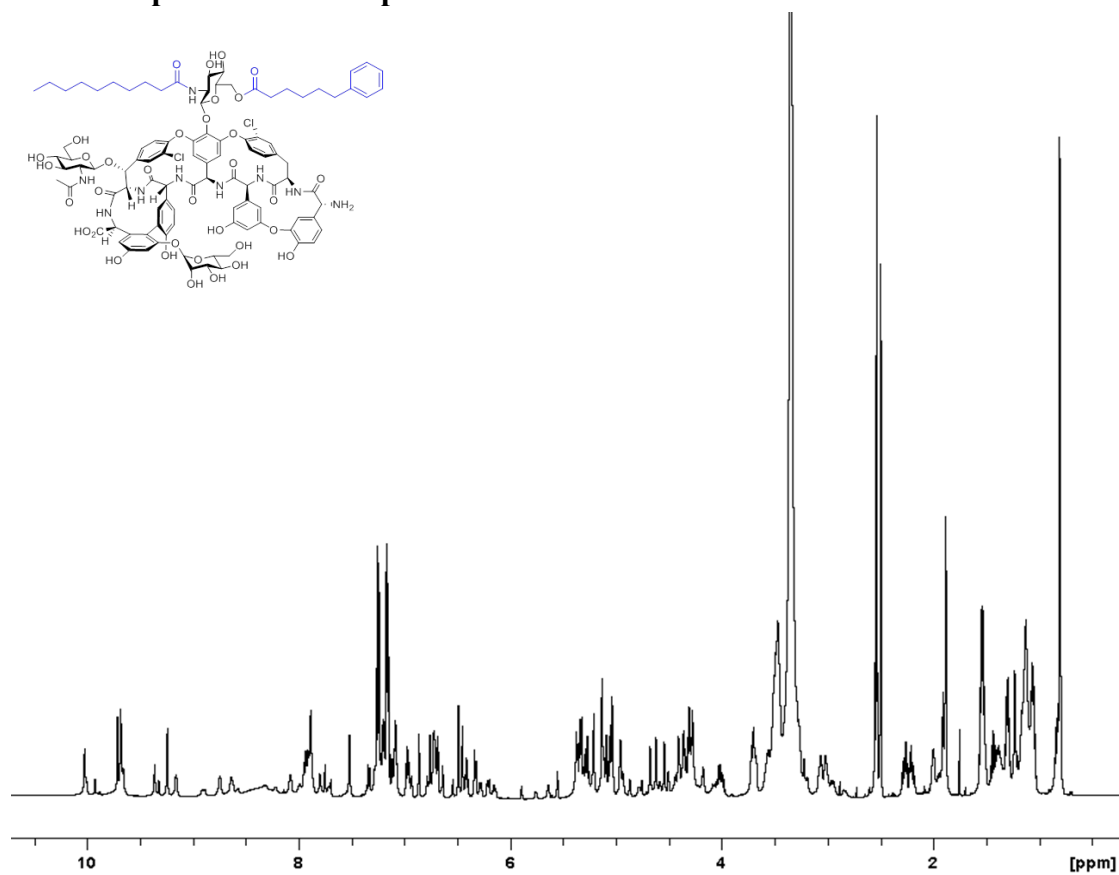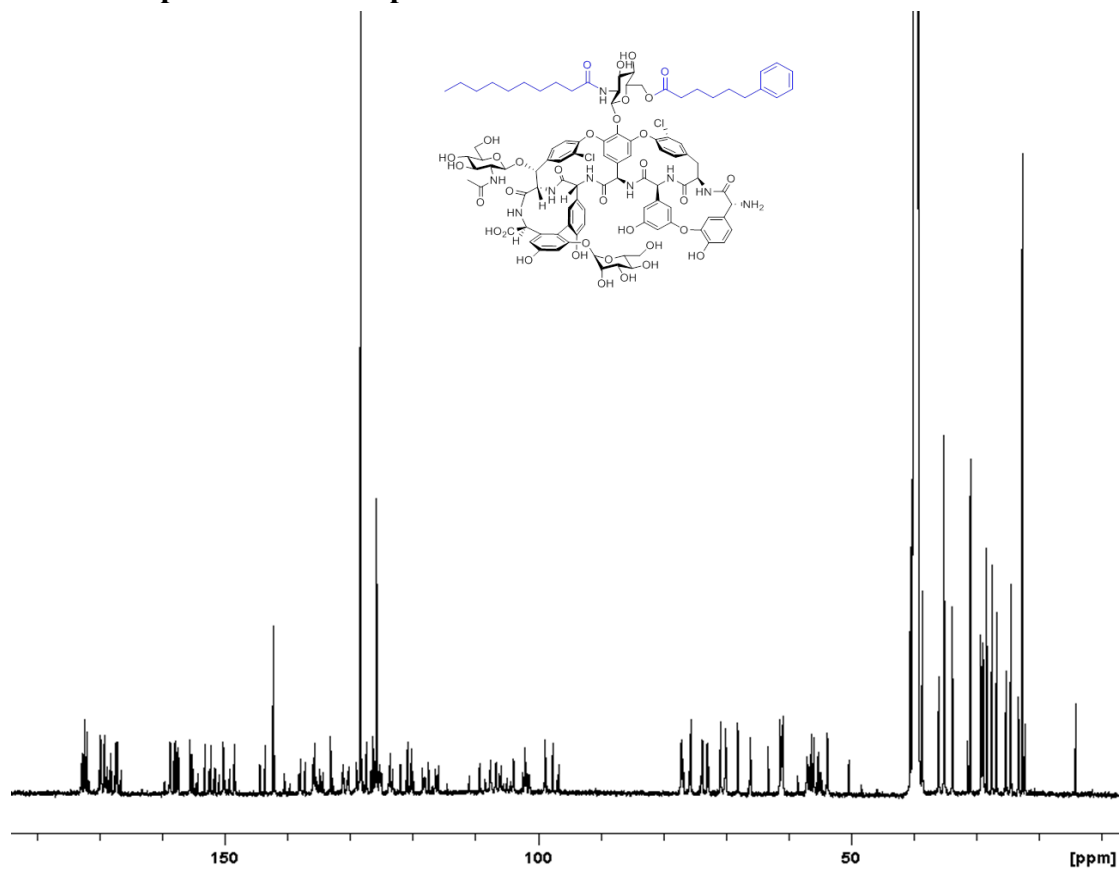
¹H COSY spectrum for compound 20

¹H¹³C HSQC spectrum for compound 20
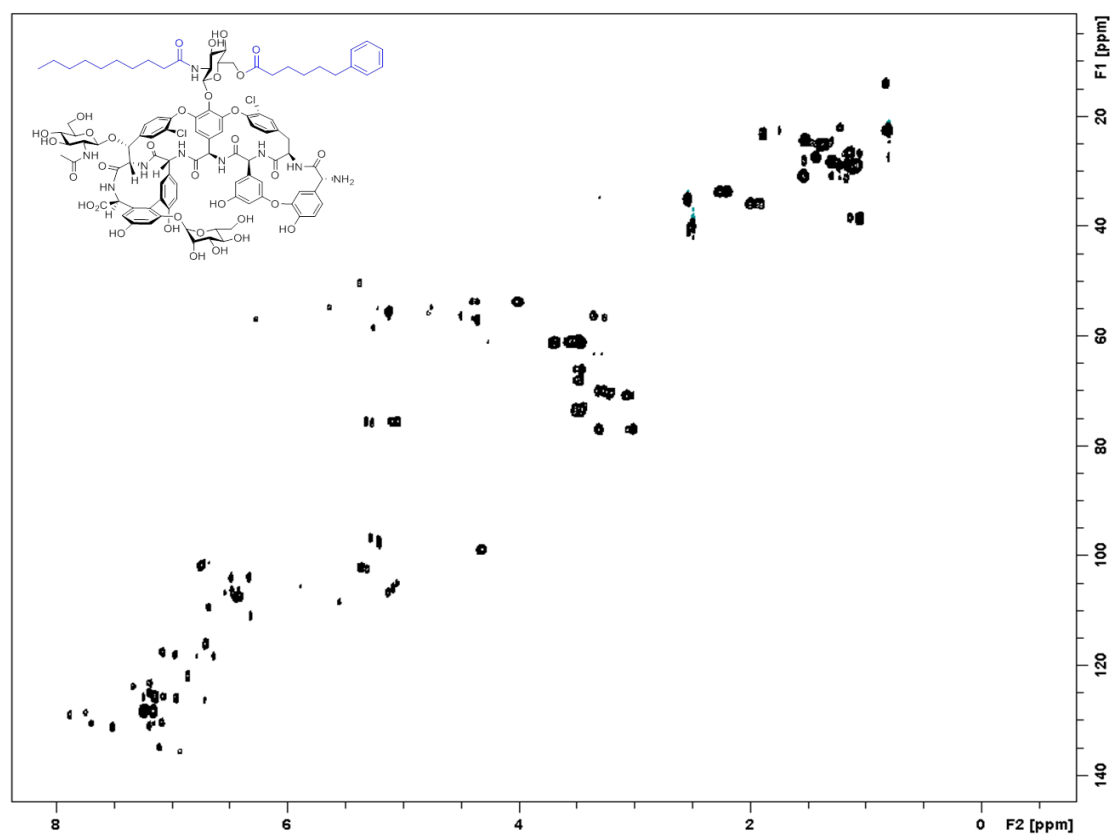
^{1}H^{13}C HMBC spectrum for compound 20

Figure S19. NMR information for compound 20. NMR spectra include ^{1}H, ^{13}C, COSY, HSQC, HMBC, and NOESY.
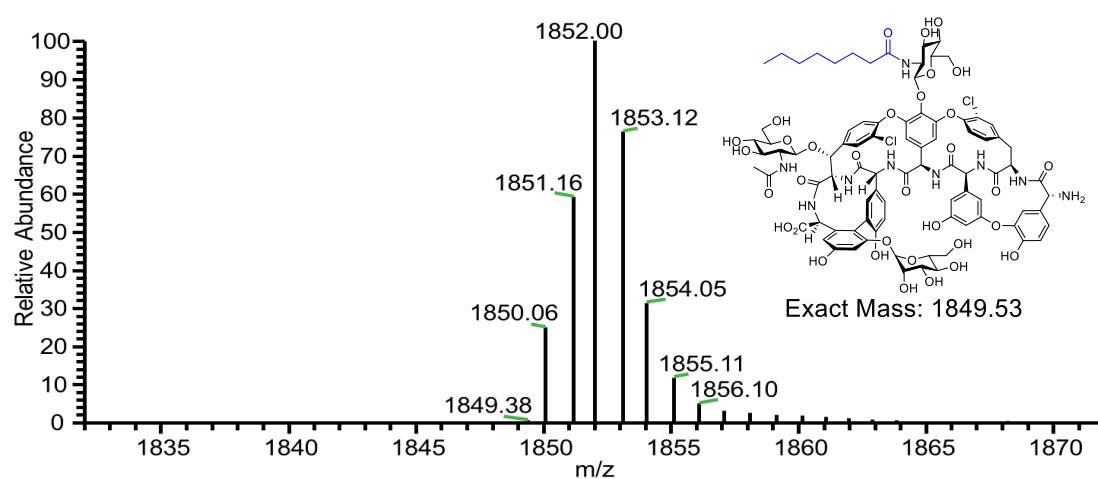
a.

b. compound 23 (C$_2$-Tei)

Exact Mass: 1765.43
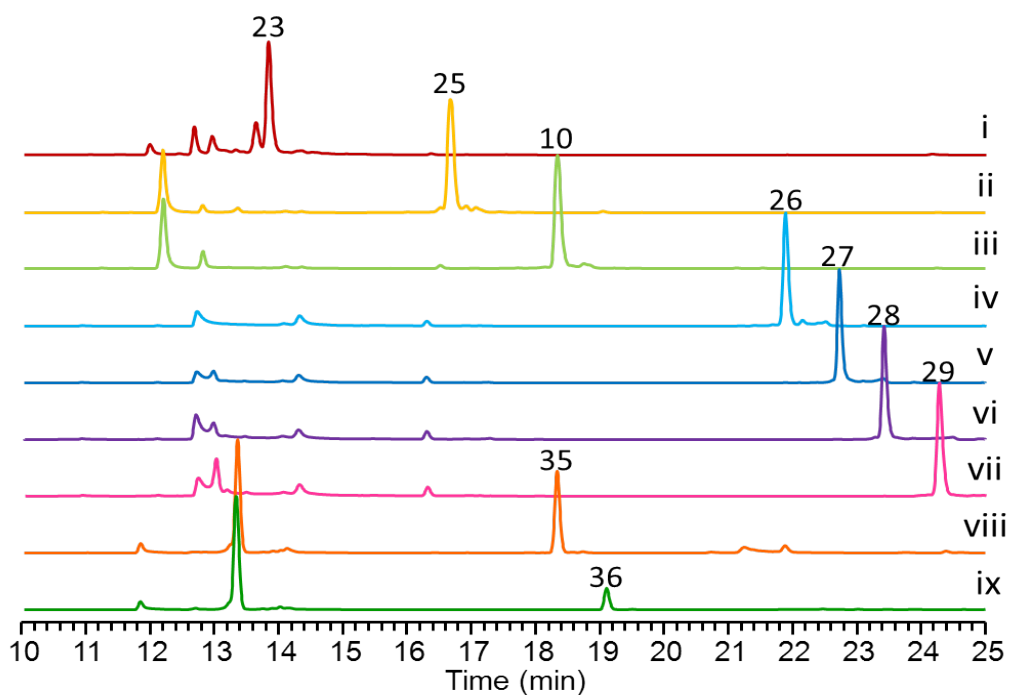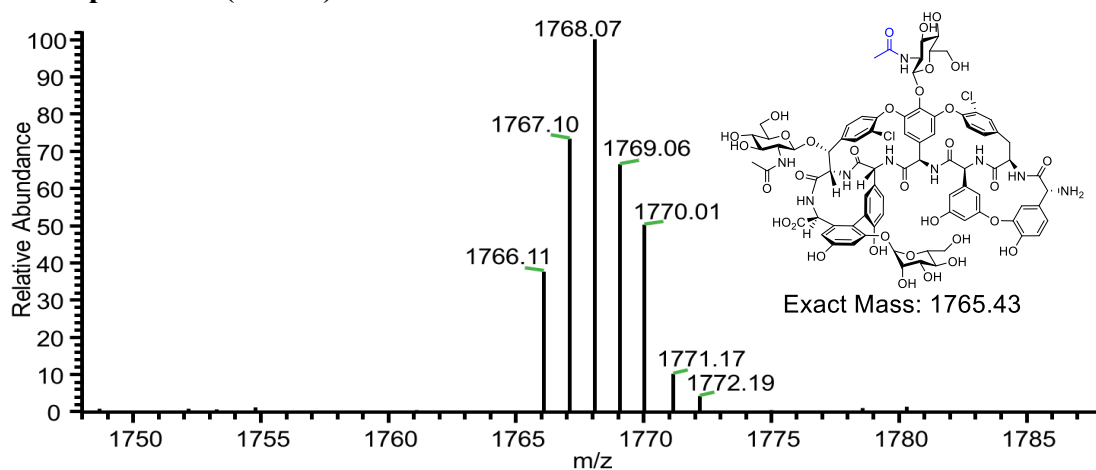
c. compound 24 (C$_4$-Tei)

Exact Mass: 1793.46
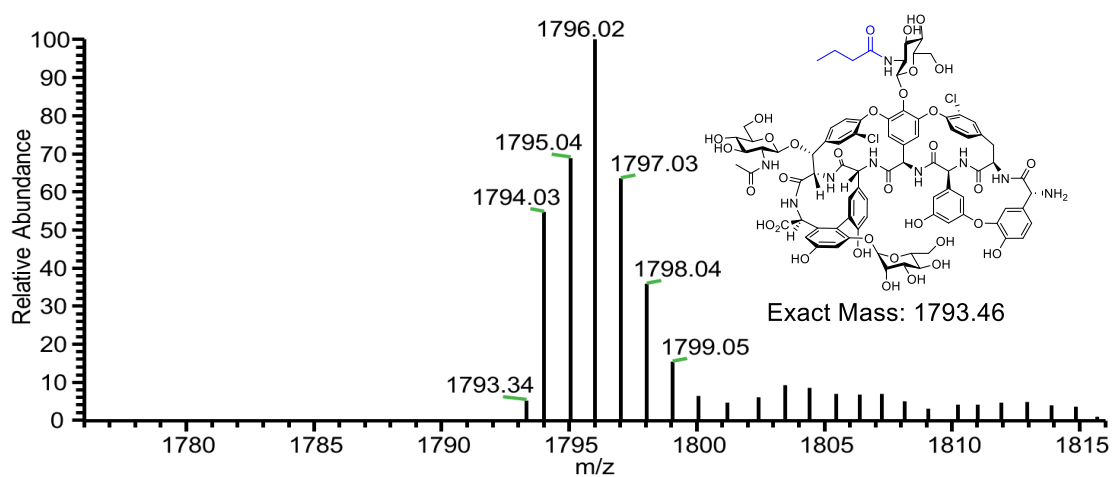
d. compound 25 (C$_6$-Tei)
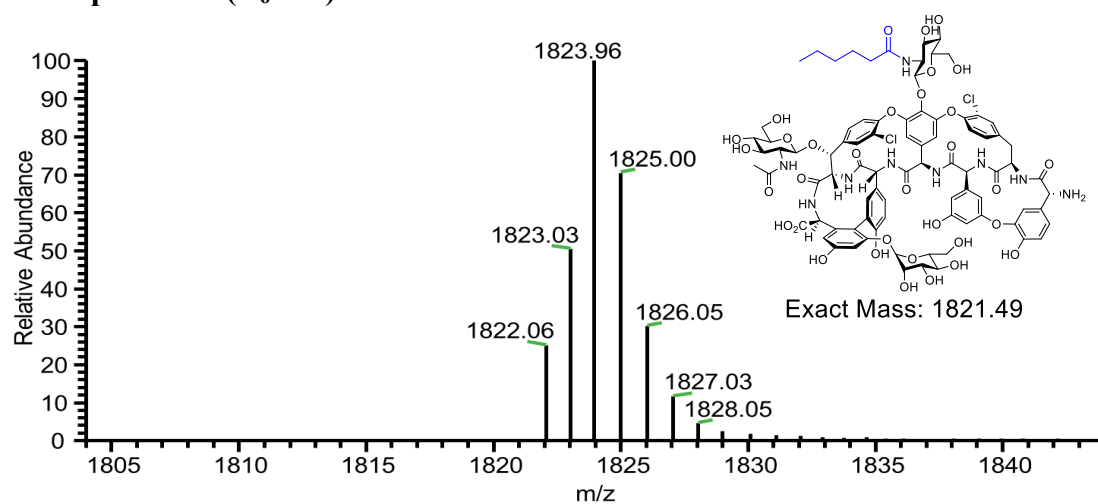
e. compound 10 (C$_8$-Tei)

f. compound 26 (C$_{12}$-Tei)

g. compound 27 (C$_{14}$-Tei)

Exact Mass: 1933.62
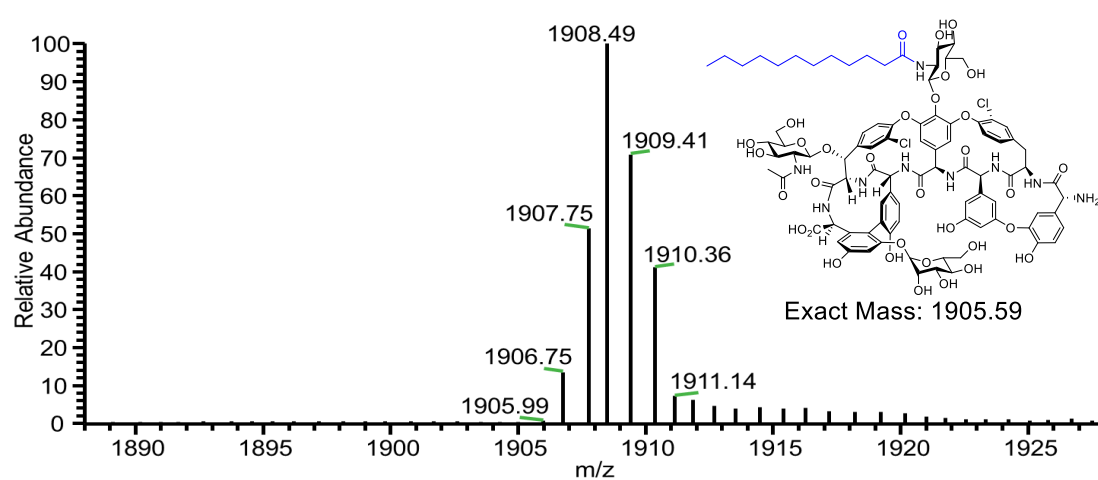
h. compound 28 (C$_{16}$-Tei)

Exact Mass: 1961.65
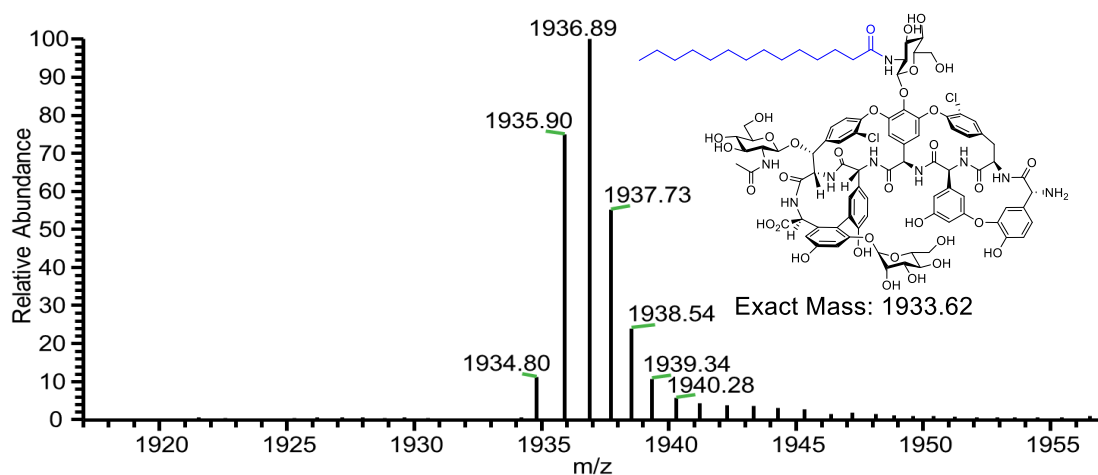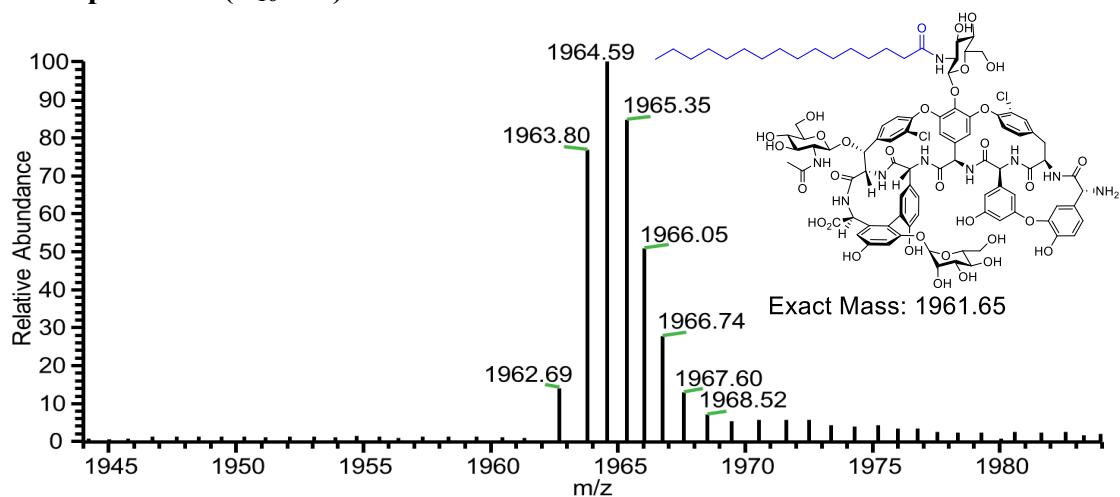
i. compound 29 (C$_{18}$-Tei)
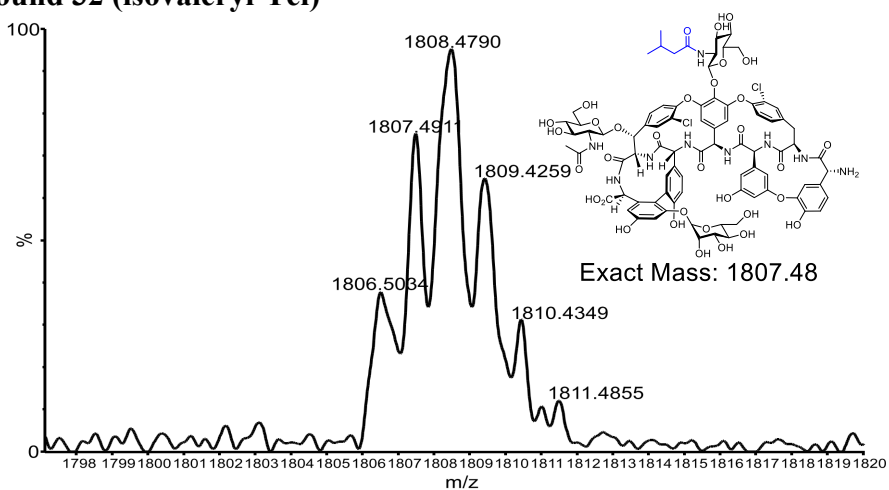

Exact Mass: 1989.68
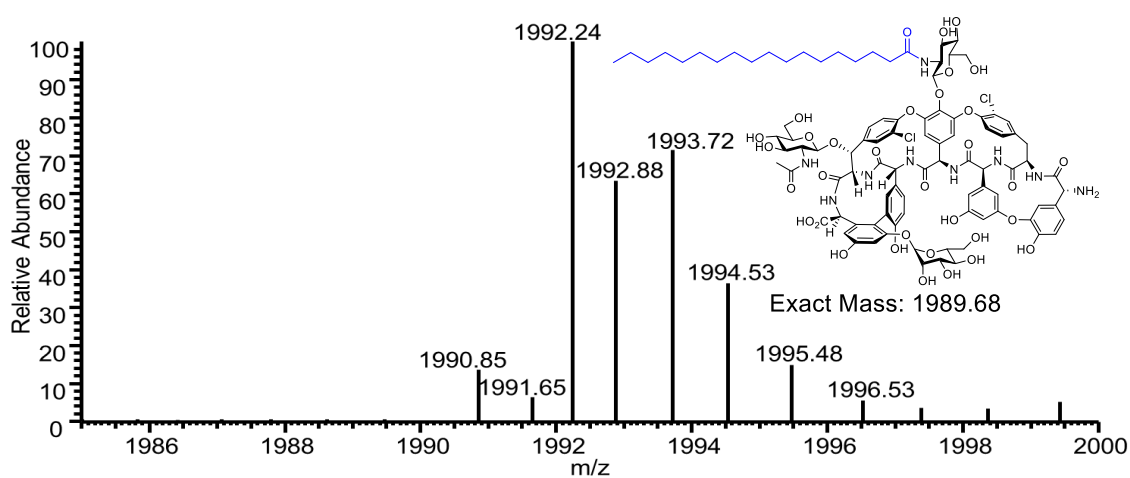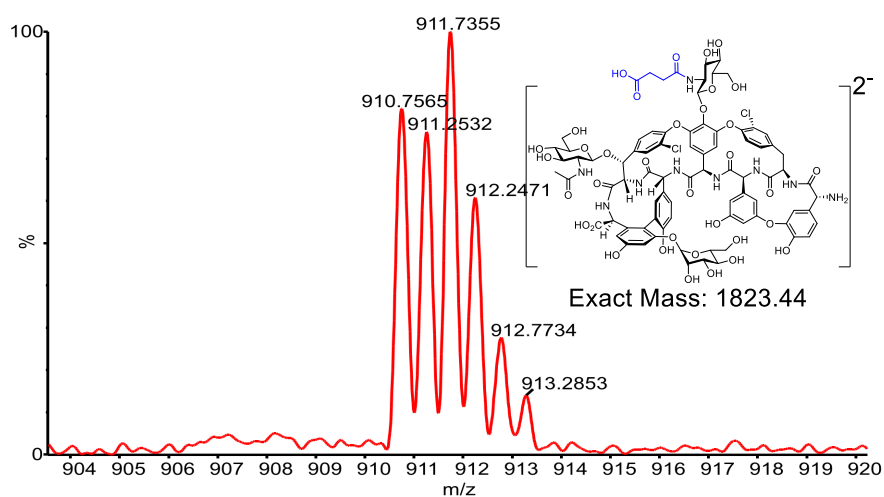
j. compound 30 (acetoacetyl-Tei)
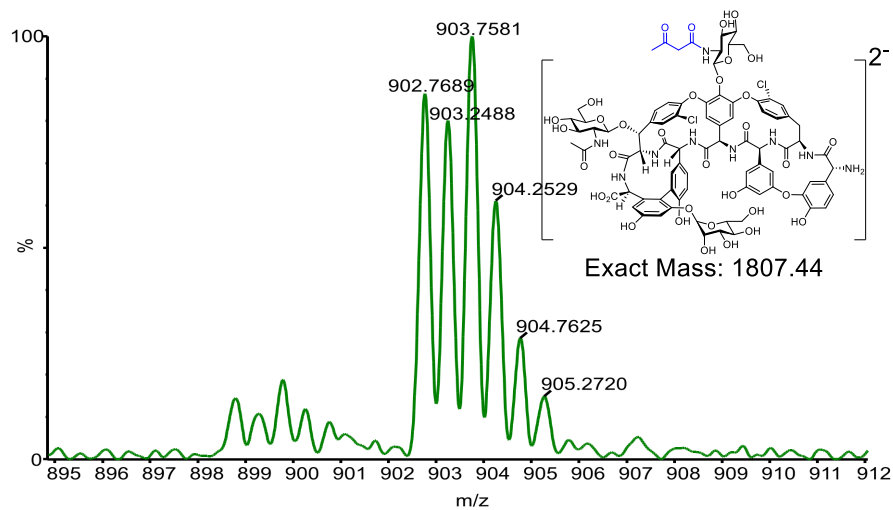
k. compound 31 (β-hydroxybutyryl-Tei)
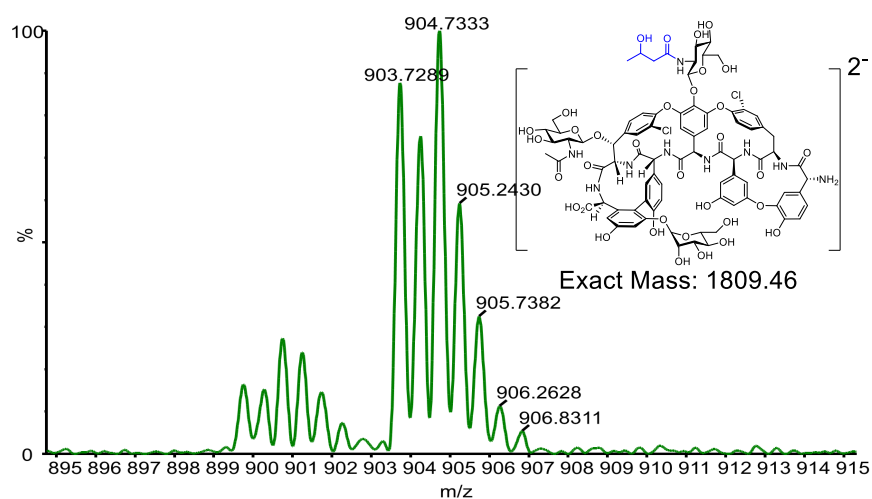
l. compound 32 (isovaleryl-Tei)
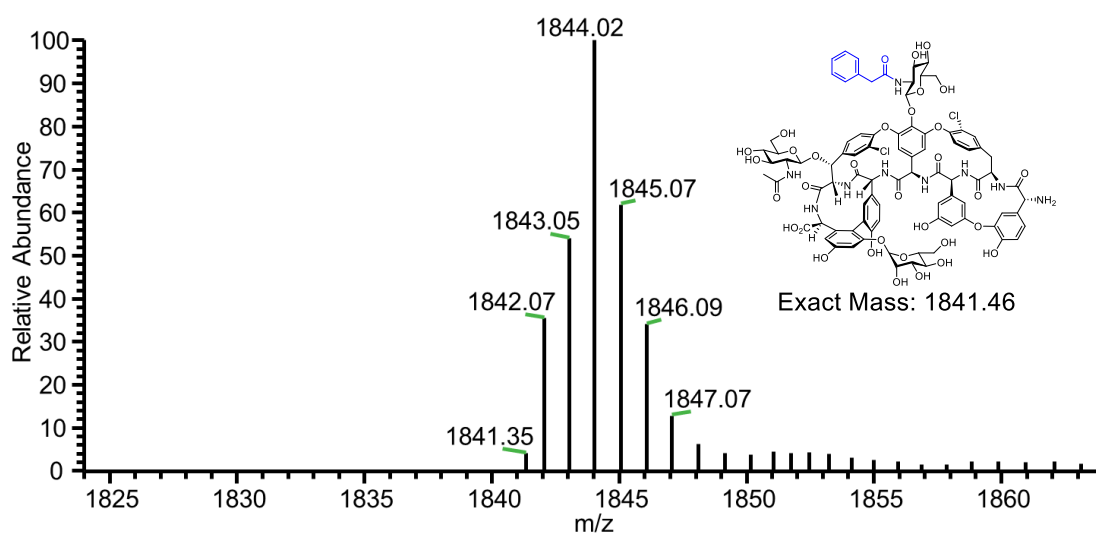

S39

m. compound 33 (succinyl-Tei)

Exact Mass: 1823.44

n. compound 34 (glutaryl-Tei)

Exact Mass: 1837.45
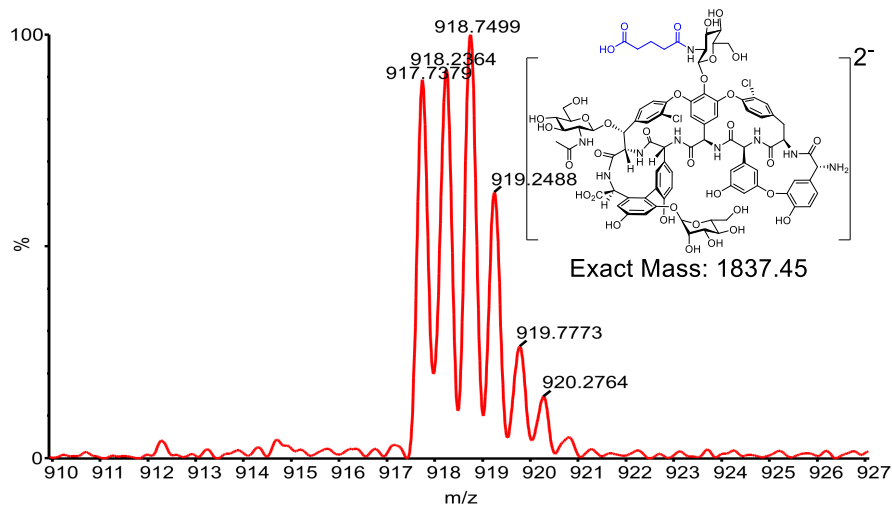
o. compound 35 (phenyl acetyl-Tei)

Exact Mass: 1841.46

p. compound 36 (4-biphenthyl acetyl-Tei)

Exact Mass: 1917.49
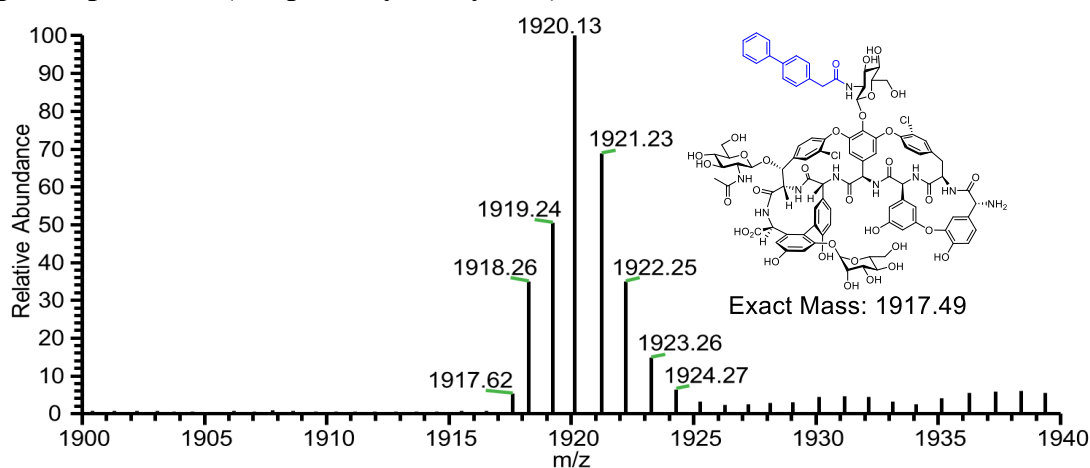
q. compound 37 (3-naphthlen propionyl-Tei)

Exact Mass: 1905.49
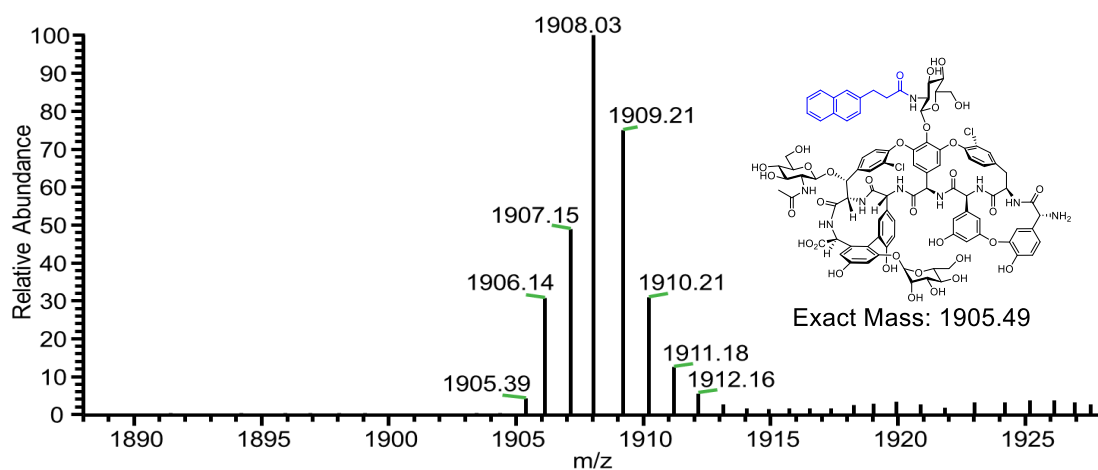
r. compound 38 (4-pentynoyl-Tei)

Exact Mass: 1803.45
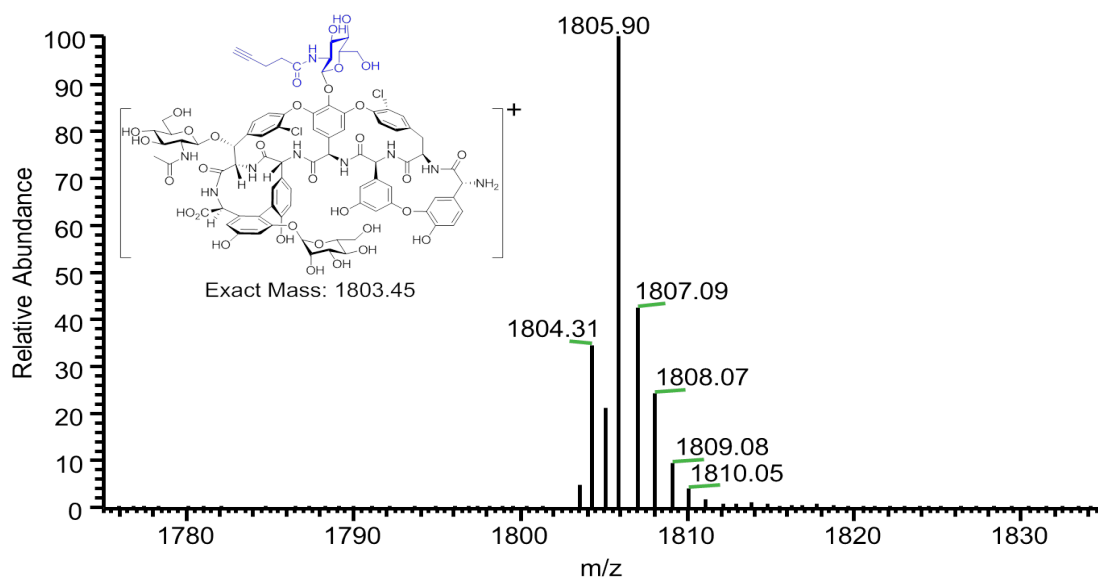
s. compound 39 (12-hydroxydodecanoyl-Tei)

Exact Mass: 1921.58
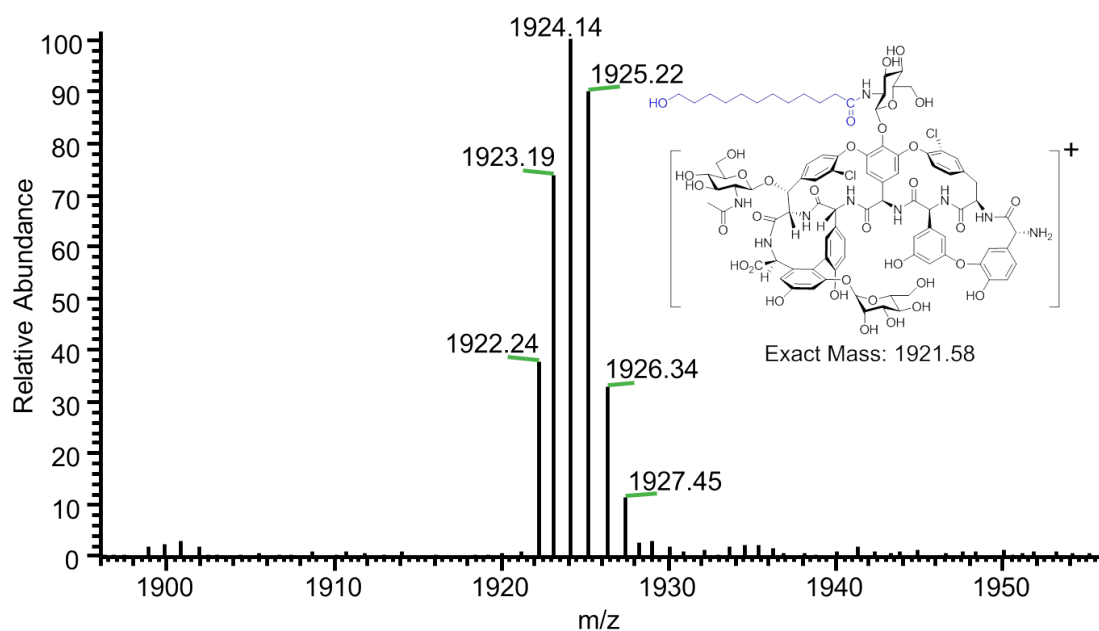
t. compound 40 (7-phenyl heptanoyl-Tei)

Exact Mass: 1911.54
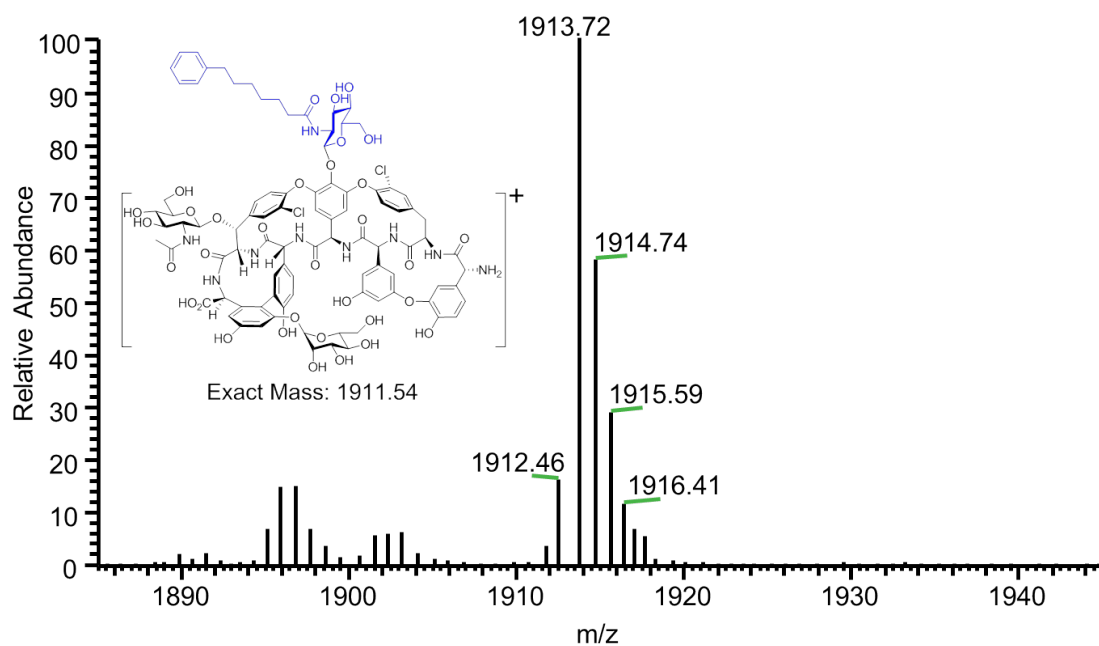
Figure S20. LC traces (a) and mass spectra (b-t) for major acylated Tei derivatives generated in the Orf11* catalysed reactions. (i) LC trace of C_2-Tei **23**. (ii) LC trace of C_6-Tei **25**. (iii) LC trace of C_8-Tei **10**. (iv) LC trace of C_{12}-Tei **26**. (v) LC trace of C_{14}-Tei **27**. (vi) LC trace of C_{16}-Tei **28**. (vii) LC trace of C_{18}-Tei **29**. (viii) LC trace of phenyl acetyl-Tei **35**. (ix) LC trace of 4-biphenthyl acetyl-Tei **36**.

a.
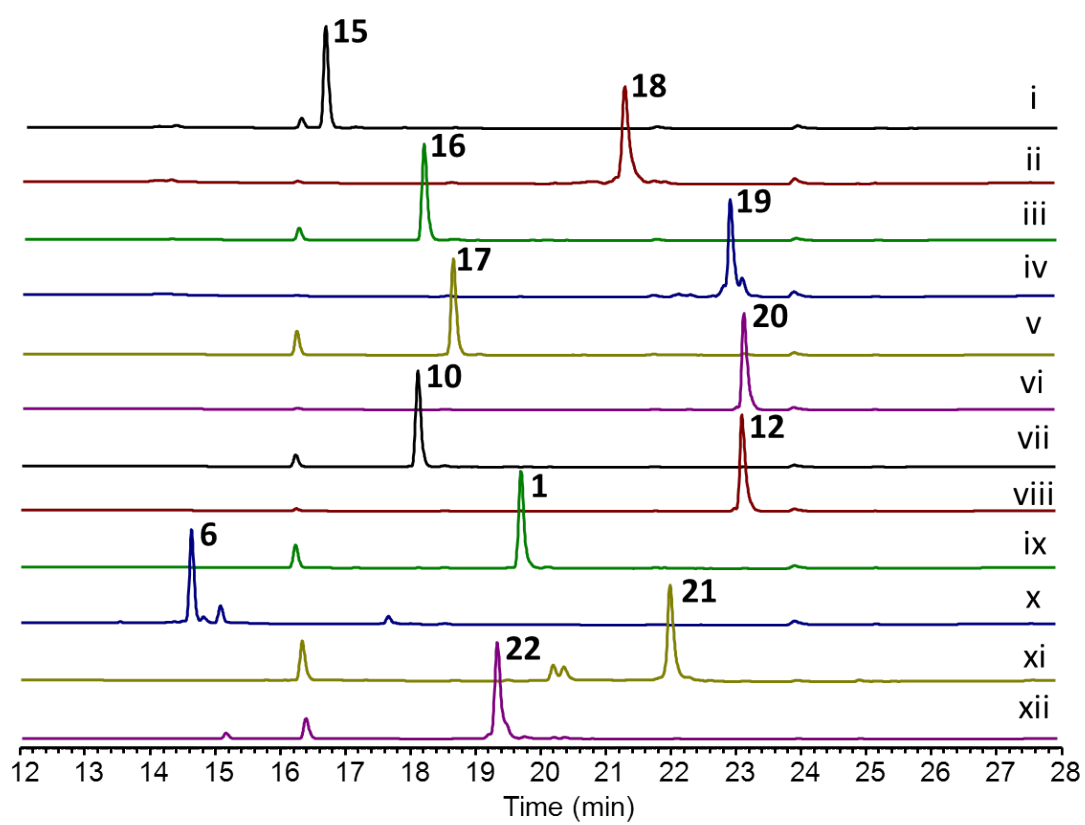
b. compound 15 (dihydrocinnamoyl-Tei)
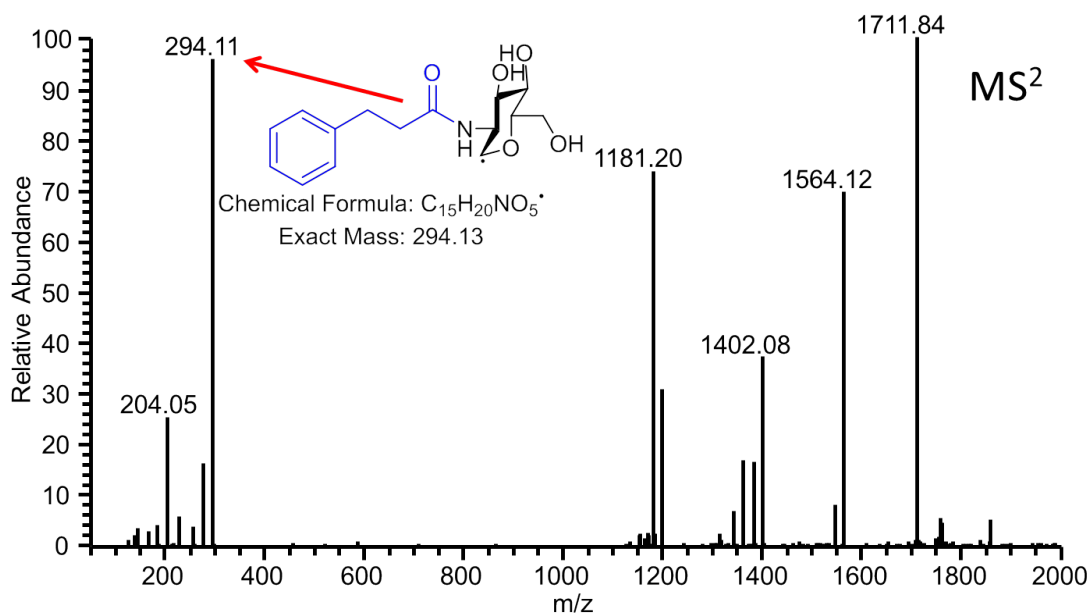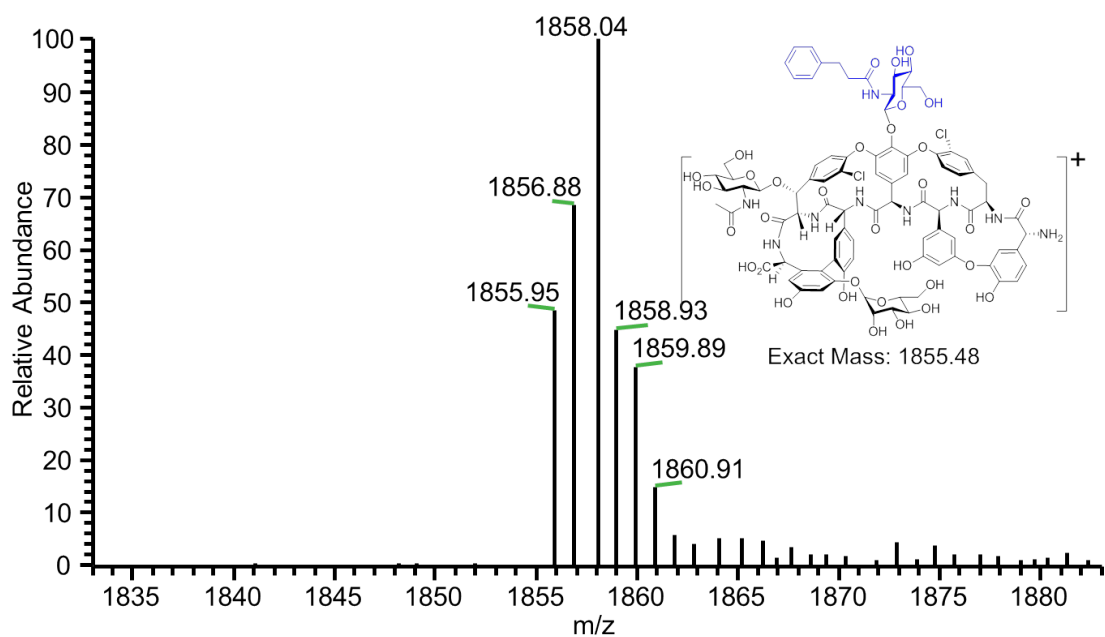
c. compound 18 (2N-decanoyl, 6O-dihydrocinnamoyl-Tei)

Exact Mass: 2009.61

Chemical Formula: $C_{25}H_{38}NO_6$
Exact Mass: 448.27

MS^2
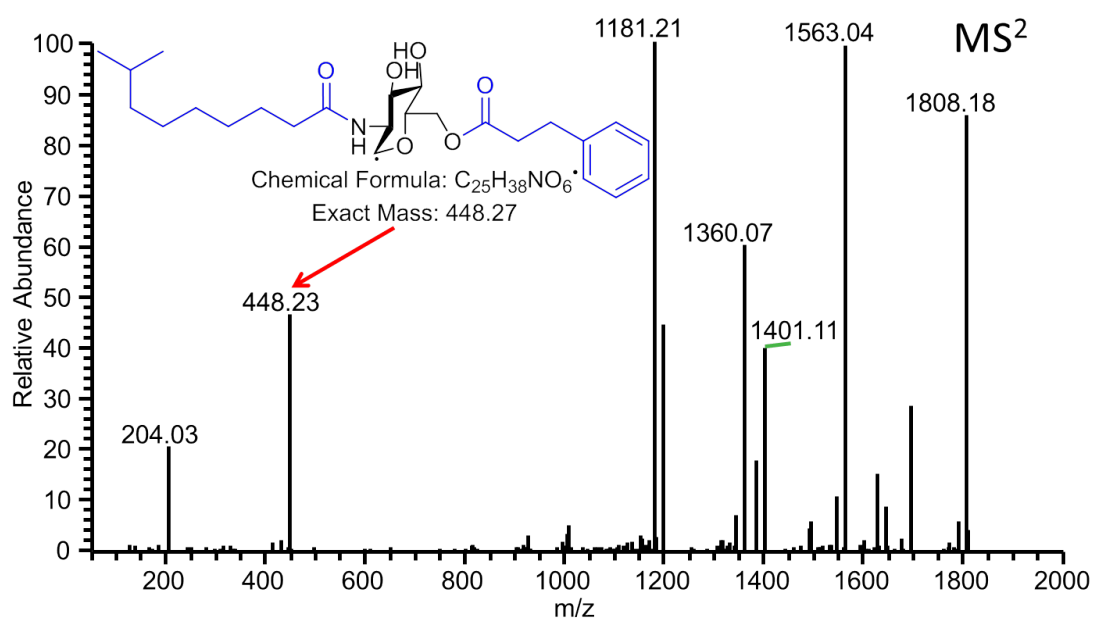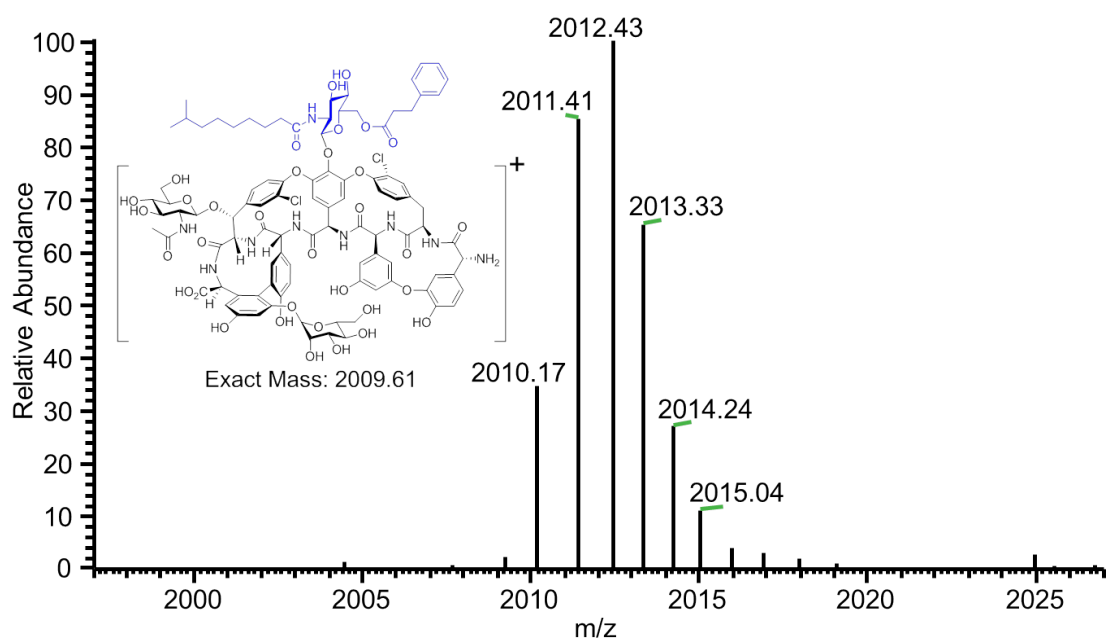
d. compound 16 (5-(4-fluoro-phenyl) valeryl-Tei)
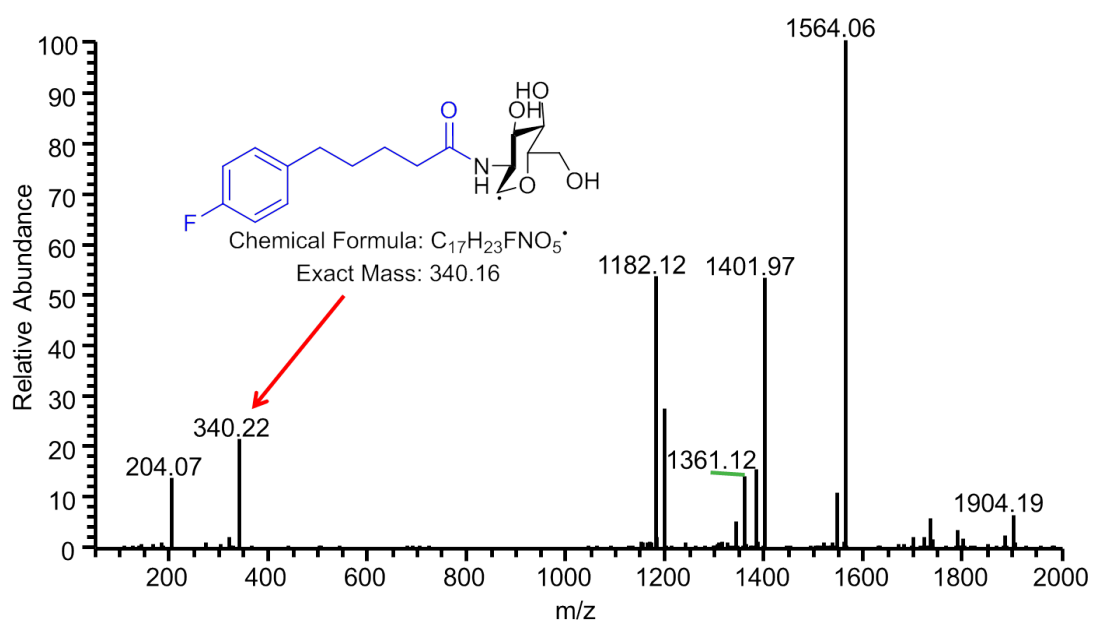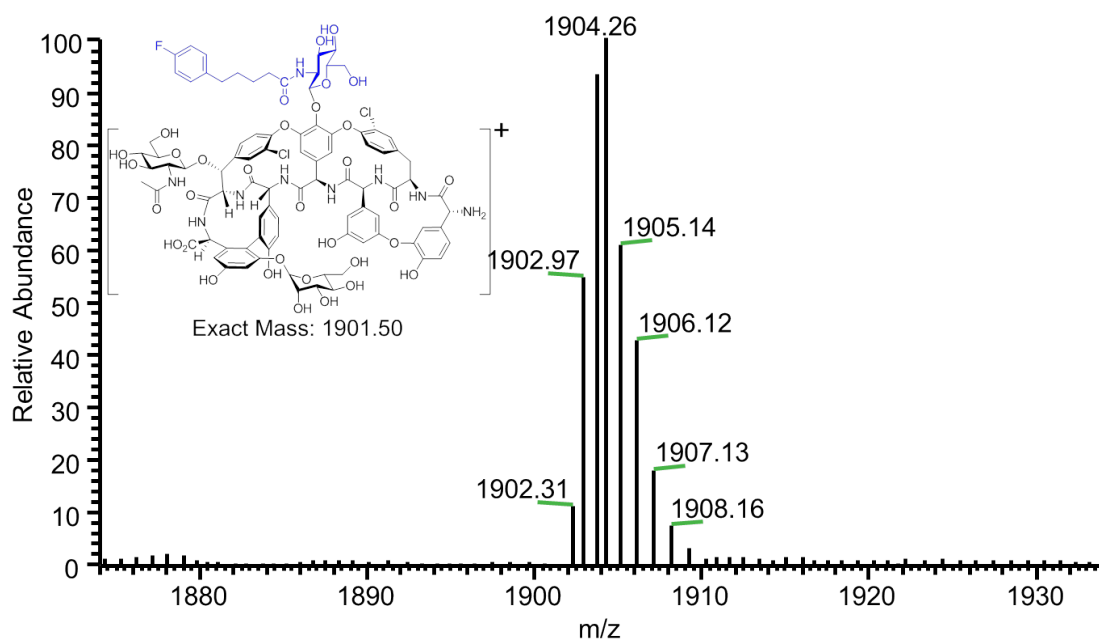
e. compound 19 (2N-decanoyl, 6O-5-(4-fluoro-phenyl) valeryl-Tei)
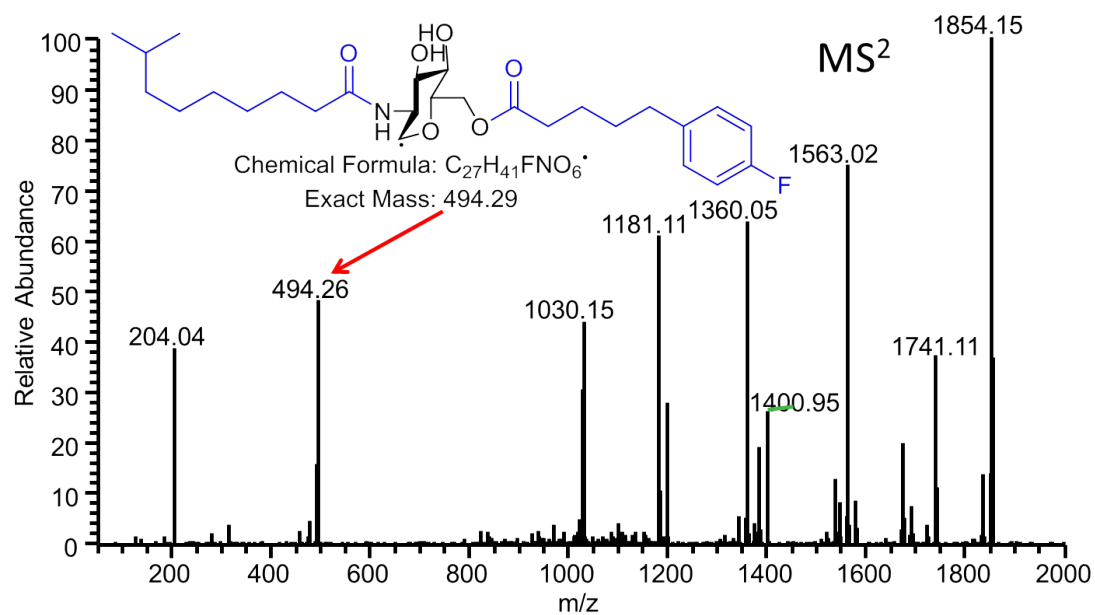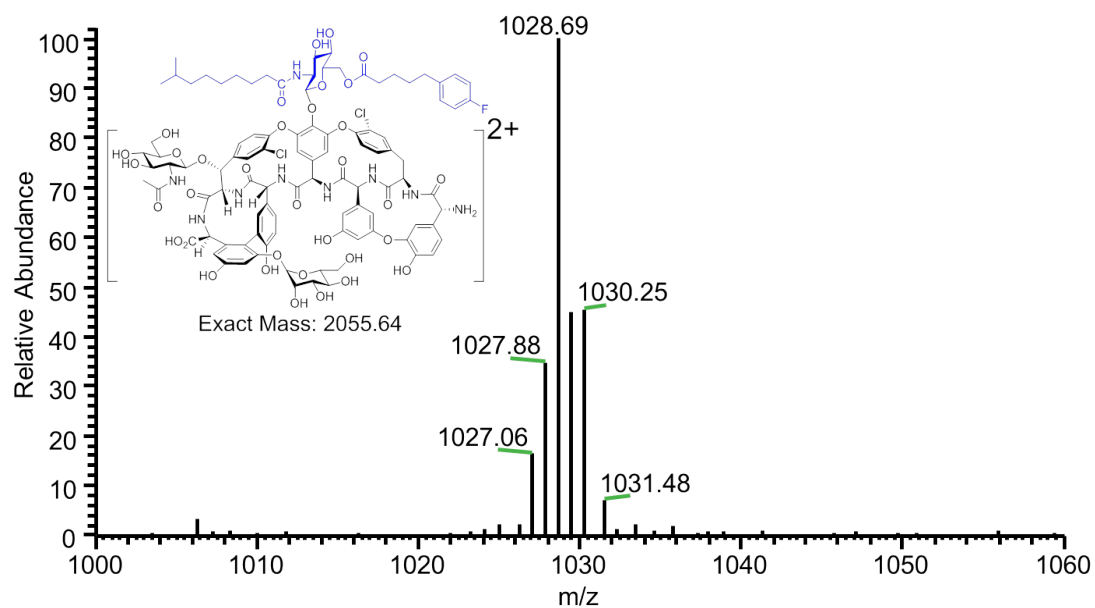
f. compound 17 (6-phenyl hexanoyl-Tei)

Exact Mass: 1897.53

Chemical Formula: $C_{18}H_{26}NO_5{}^\bullet$
Exact Mass: 336.18

MS^2
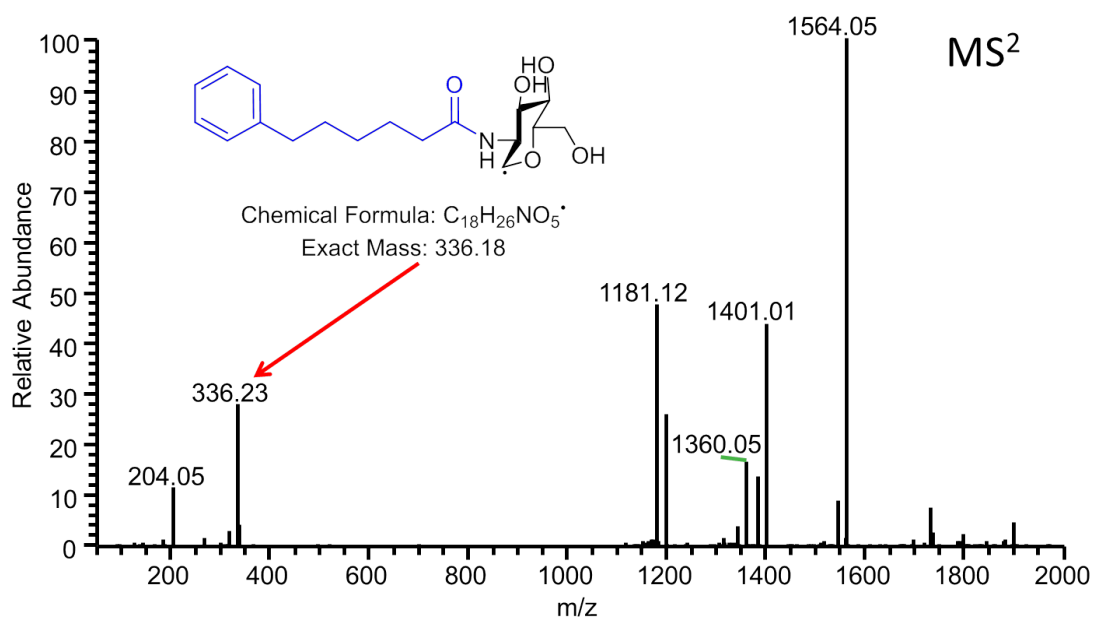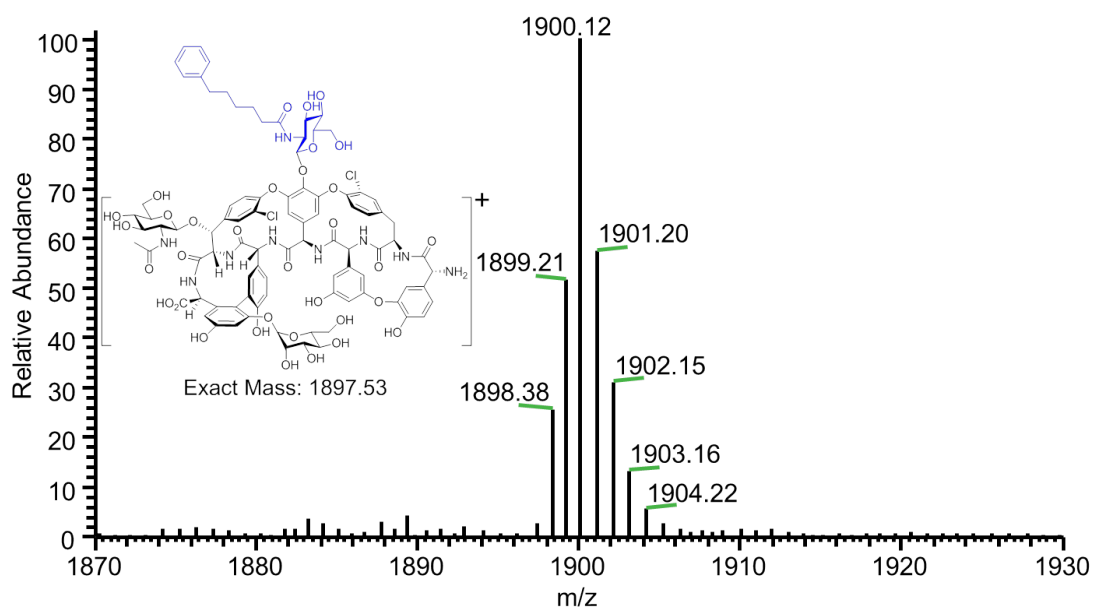
g. compound 20 (2N-decanoyl, 6O-6-phenyl hexanoyl-Tei)
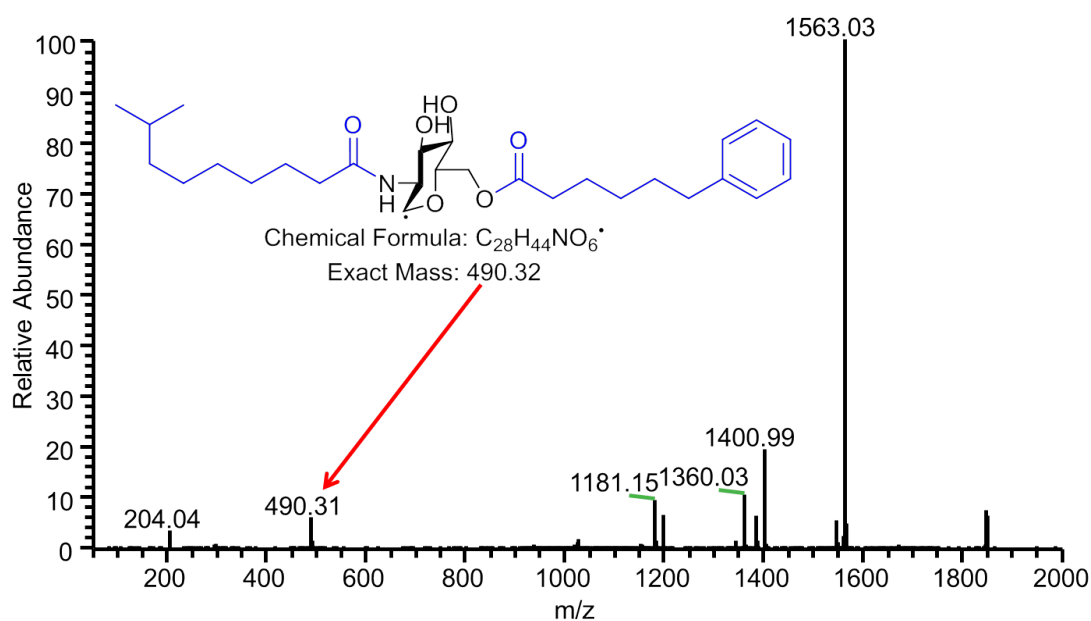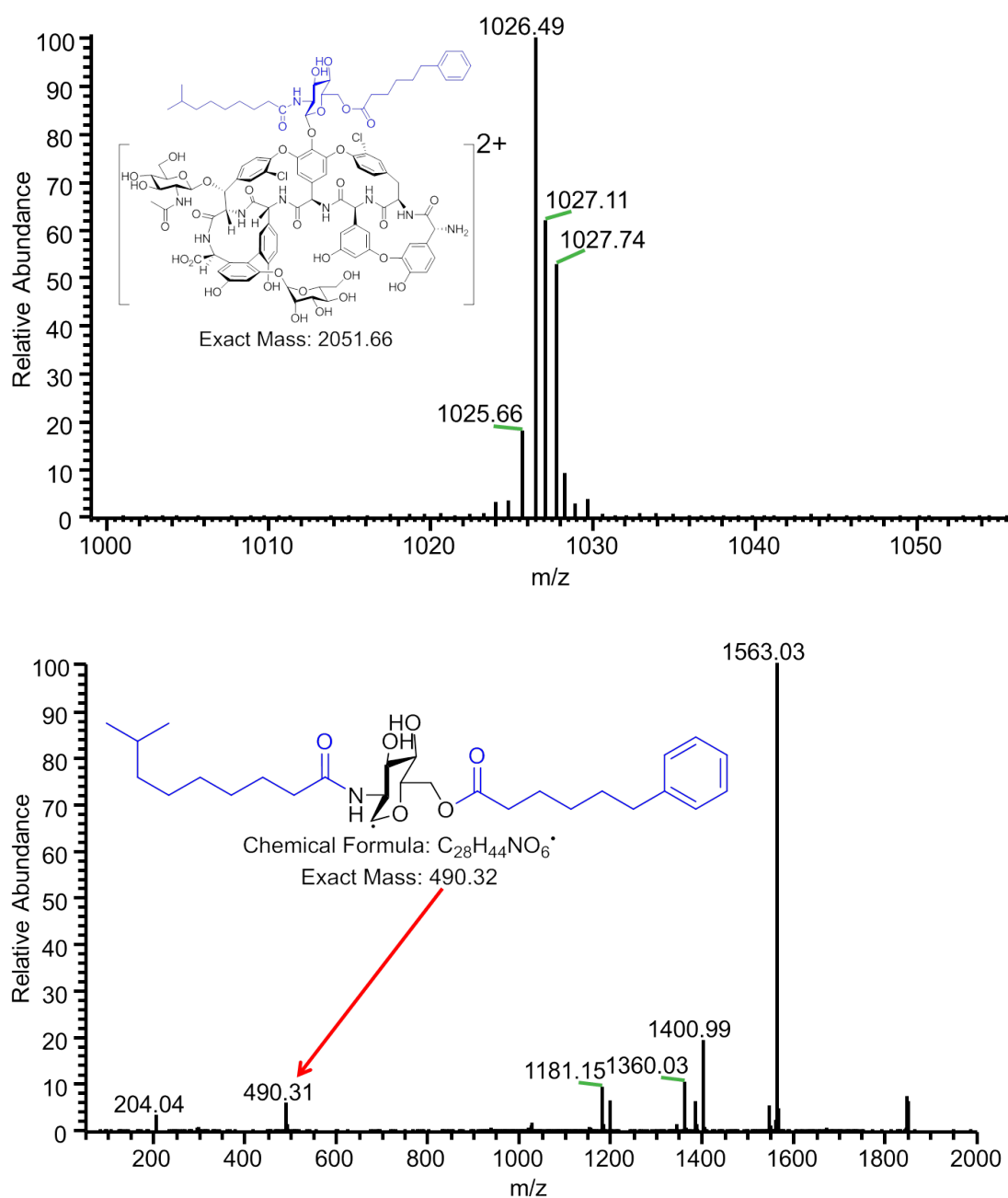
Figure S21. LC traces (a) and mass spectra (b-g) for the Tei analogs used in the MIC assays. (i) LC trace of dihydrocinnamoyl-Tei **15**. (ii) LC trace of 2*N*-decanoyl, 6*O*-dihydrocinnamoyl-Tei **18**. (iii) LC trace of 5-(4-fluoro-phenyl) valeryl-Tei **16**. (iv) LC trace of 2*N*-decanoyl, 6*O*-5-(4-fluoro-phenyl) valeryl-Tei **19**. (v) LC trace of 6-phenyl hexanoyl-Tei **17**. (vi) LC trace of 2*N*-decanoyl, 6*O*-6-phenyl hexanoyl-Tei **20**. (vii) LC trace of C$_8$-Tei **10**. (viii) LC trace of 2*N*-decanoyl, 6*O*-octanoyl-Tei **12**. (ix) LC trace of teicoplanin **1**. (x) LC trace of vancomycin **6**. (xi) LC trace of *C*6-decylaminated Tei **21**. (xii) LC trace of *C*6-benzylamine-Tei **22**.

```
Orf11*       MDPETVRIALGLEERTAAWLTELDELGPPAEPVRLPRGEEARDLLRRLEVPELDAEEIVA 60
Dbv8         MDAESVRRQLRLGENATAWLSRLEELGPPPEPVRLPQGDEARDLLHRLEVPAPDVEEIVA 60
             **.*:**    * * *.::***:.*:*****.******:*:******:*****   *.*****


Orf11*       AAPDPDRDPALWWLLERTHHAIVRHMGDHRAKPRGGPPLPYEGGAAARYFHVYVFLATVP 120
Dbv8         ATPGPDRDPALWWLLERAHHELVRHMGDYKVKVRGGPTLPYETGAAARYFHVYVFLATLP 120
             *:*.**************:**  :******::.* ****.**** ***************:*


Orf11*       AVRRFHAERGIPDEVGWETLSRLGELVAIHRRKYGQGGMNMQWWTTYHLRGILYRLGRLQ 180
Dbv8         ALRRFHATRDIPEATTWETLTQLGESVAIHRRKYGEGGTNMPWWLTLLVRGLVYRLGRLQ 180
             *:***** *.**:  . ****:.*** **********.** ** ** *   :**::*******


Orf11*       FSLATGKDGTPHLGLHVPEWGGPLLPKAYDESLHRARPFFDRHFPEHGARVAWGSSWMLD 240
Dbv8         YNLAVAKDGTPVLGLHIPEVGGPLIPDIYYDSLRRARPFFERHFPEHGARAATGTSWLLD 240
             :.**..***** ****:** ****:*. * :**:*****:********.* *:**:**


Orf11*       PQLEEYLTEDSNIIQLARFWTLTDSAPEPGNADGDSSILEFVFRYNGQPLDELPQRSSLE 300
Dbv8         PQLAEYLAEDSHILQLRRGWTLLDSEPQ----DGDDAILEFVFRYNGQPLEELPQRSTLE 296
             *** ***:***.*:** * *** ** *:    ***.:**************:******:**


Orf11*       RAVIAHLKAGRHWHMRTGFVKLP 323
Dbv8         KAVVTHLLAGRHWYQRSGRIELP 319
             :**:**.***** *:* ::.**
```

Figure S22. Sequence alignment results of Orf11* and Dbv8. The sequence identity and similarity are 71% (228/323) and 82% (265/323), respectively.

Table S1. Data collection, phasing and refinement statistics for structures of Dbv8, Orf11* and mutants thereof.

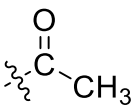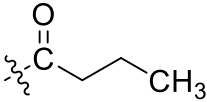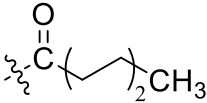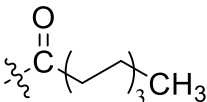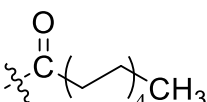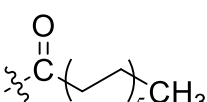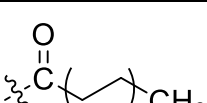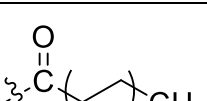|	Se-Orf11*	Orf11*H196A/ decanoyl-CoA	Dbv8/ decanoyl-CoA	Orf11*H196A/ decanoyl-CoA/ Tei pseudoaglycone	Orf11*H196A/ decanoyl-CoA- Tei pseudoaglycone
Data collection					
Space group	$P6_2$	$P6_5$	$P2_12_12_1$	$P6_5$	$P6_5$
Cell dimensions					
a, b, c (Å)	105.5, 105.5, 133.9	133.4, 133.4, 49.5	53.7, 68.5, 95.1	133.6, 133.6, 49.3	133.7, 133.7, 49.4
α, β, γ (°)	90.0, 90.0, 120.0	90.0, 90.0, 120.0	90.0, 90.0, 90.0	90.0, 90.0, 120.0	90.0, 90.0, 120.0
Wavelength	0.97893	0.97622	0.97622	1.00000	1.00000
Resolution (Å)	30.0-2.90(3.00-2.90)	30.0-1.90(1.97-1.90)	30.0-2.10(2.18-2.10)	30.0-1.90(1.97-1.90)	30.0-2.15(2.23-2.15)
R_{sym} or R_{merge} (%)	8.6(69.0)	9.3(54.8)	14.2(57.2)	5.1(56.8)	7.8(58.2)
$I/\sigma I$	33.3(5.1)	16.3(3.5)	13.5(2.3)	38.7(3.9)	25.5(5.3)
Completeness (%)	98.8(99.6)	100.0(100.0)	99.6(97.2)	100.0(100.0)	99.9(100.0)
Redundancy	12.6(12.4)	5.9(6.0)	7.4(5.6)	5.9(6.0)	7.0(7.4)
Refinement					
Resolution (Å)	2.9	1.90	2.10	1.90	2.15
No. reflections	17598	37919	19900	37841	26394
R_{work}/ R_{free} (%)	18.0/22.9	16.4/20.2	18.9/25.7	17.4/21.1	17.7/21.7
No. atoms					
Protein	2643	2671	2586	2670	2699
Ligand/ion	-/-	59/0	59/0	180/0	180/0
Water	53	464	272	363	255
B-factors					
Protein	67.0	27.6	24.9	31.8	38.2
Ligand/ion	-/-	25.3/0	25.1/0	63.7/0	71.8/0
Water	50.9	40.5	31.9	42.8	47.4
R.m.s deviations					
Bond lengths (Å)	0.0087	0.0119	0.0118	0.0101	0.0122
Bond angles (°)	1.4367	1.3934	1.5415	1.302	1.555
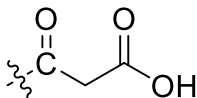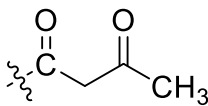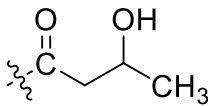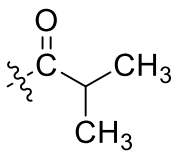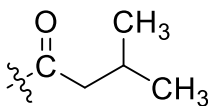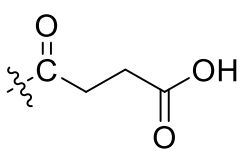
Highest resolution shell is shown in parenthesis.

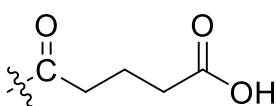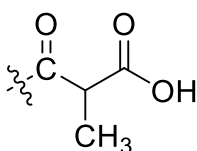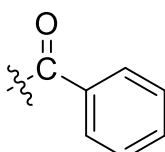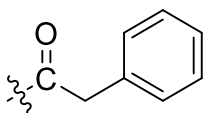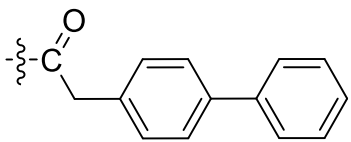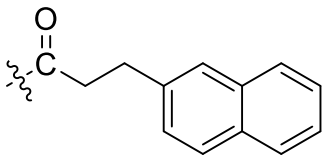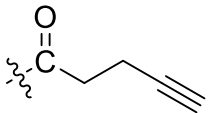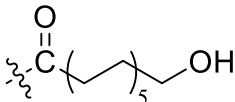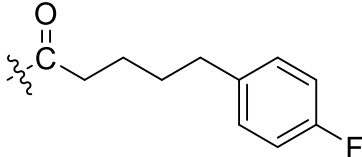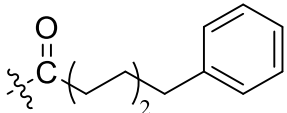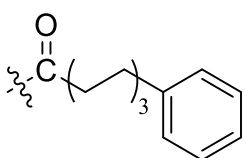|	Orf11*H196A/ CoA/ 10C-teicoplanin	Orf11*/ octanoyl-CoA/teicoplanin	Orf11*/CoA/ O6-decanoyl-teicoplanin
Data collection			
Space group	P6$_5$	P6$_5$	P6$_5$
Cell dimensions			
a, b, c (Å)	133.6, 133.6, 49.3	133.2, 133.2, 49.1	134.4, 134.4, 49.3
α, β, γ (°)	90.0, 90.0, 120.0	90.0, 90.0, 120.0	90.0, 90.0, 120.0
Wavelength	1.00000	1.00000	1.00000
Resolution (Å)	30.0-2.00(2.07-2.00)	30.0-2.35(2.43-2.35)	30.0-2.00(2.07-2.00)
R_{sym} or R_{merge} (%)	5.8(59.5)	6.6(51.6)	6.9(48.4)
$I/\sigma I$	34.4(3.6)	24.7(2.9)	5.8(4.1)
Completeness (%)	100.0(100.0)	99.9(99.9)	100.0(99.8)
Redundancy	7.5(7.5)	5.8(5.2)	6.6(7.0)
Refinement			
Resolution (Å)	2.00	2.35	2.00
No. reflections	32571	19955	32849
R_{work}/ R_{free} (%)	17.3/21.7	18.5/23.3	19.2/22.0
No. atoms			
Protein	2658	2632	2638
Ligand/ion	180/0	81/0	71/0
Water	311	107	299
B-factors			
Protein	35.3	48.9	33.5
Ligand/ion	45.5/0	59.3/0	37.4/0
Water	43.9	48.7	41.4
R.m.s deviations			
Bond lengths (Å)	0.0105	0.0098	0.0075
Bond angles (°)	1.456	1.3976	1.1807

Highest resolution shell is shown in parenthesis.

Table S2. Structures of acyl-CoAs and their availability in enzymatic reactions.

Acyl-CoA donor	Acyl group	Activity of Orf11*
acetyl-CoA (C_2), **23**		+
butyryl-CoA (C_4), **24**		+
hexanoyl-CoA (C_6), **25**		+
octanoyl-CoA (C_8), **10**		+
decanoyl-CoA (C_{10}), **13**		+
lauroyl-CoA (C_{12}), **26**		+
myristoyl-CoA (C_{14}), **27**		+
palmitoyl-CoA (C_{16}), **28**		+
stearoyl-CoA (C_{18}), **29**		+

Acyl-CoA donor	Acyl group	Activity of Orf11*
malonyl-CoA		-
acetoacetyl-CoA, **30**		+
β-hydroxybutyryl-CoA, **31**		+
isobutyryl-CoA		-
isovaleryl-CoA, **32**		+
succinyl-CoA, **33**		+
glutaryl-CoA, **34**		+
methylmalonyl-CoA		-
benzoyl-CoA		-
phenylacetyl-CoA, **35**		+

4-biphenyl acetyl-CoA, **36**		+
3-naphthlen propionyl-CoA, **37**		+
4-pentynoyl-CoA, **38**		+
12-hydroxydodecanoyl-CoA, **39**		+
5-(4-fluoro-phenyl) valeryl-CoA, **16**		+
6-phenyl hexanoyl-CoA, **17**		+
7-phenyl heptanoyl-CoA, **40**		+

The enzymatic activities were determined by LC/MS. "+" represents the given acyl-CoA can be utilized by Orf11* to generate corresponding acyl Tei derivatives. Malonyl-, isobutyryl-, methylmalonyl- and benzoyl-CoA cannot be utilized by Orf11* due to steric hindrance. Major LC traces and mass spectra for positive reactions are shown in **Figure S20**.

Table S3. Relative enzymatic activities of mutants and proposed functions for the selected residues.

Mutant	Relative activity[a] (%)	Expected functions
H196A	5	an active site residue (general base)
S236A	10	an active site residue (general acid)
H196A/S236A	0	active site residues
W163S	38	a sugar binding site residue (r4-glucosamine of pseudoaglycone)
W164S	46	a sugar binding site residue (r4-glucosamine of pseudoaglycone)
E145A	79	a residue for salt bridge formation
W237A	8	an acyl-CoA binding site residue (decanoyl-CoA)
F281S	2	a sugar binding site residue (r4-glucosamine of pseudoaglycone)

a. The activities of mutants were determined by HPLC. The reaction rates were calculated using the linear regression equation on the basis of averaged peak areas in triplicate. The relative activities were determined by dividing individual reaction rates with that of WT, where the relative activity of WT is 100%.

Table S4. NMR assignments for compound 7.
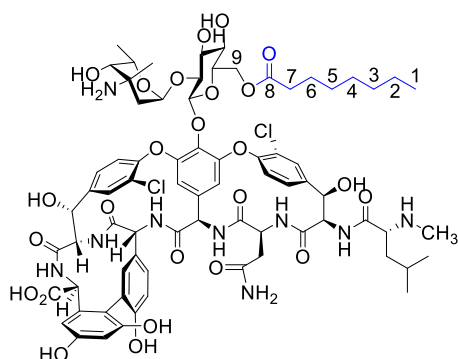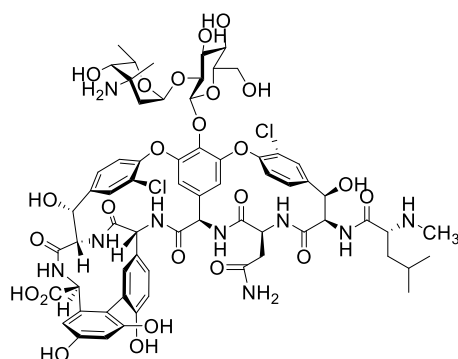
7	**reference: 6 (vancomycin)**

Position	^{13}C-NMR (δ ppm)	^{1}H-NMR (δ ppm)
C-1	14.4	0.85 m
C-2	22.5	1.28 m
C-3	31.6	1.20 m
C-4	29.5	1.23 m
C-5	28.8	1.21 m
C-6	24.8	1.47 m
C-7	33.9	2.20 m
C-8	173.4	—
C-9	63.6	3.28 m

The assignment is based on the spectra shown in **Figure S13**.

Table S5. NMR assignments for compound 10.

10		**reference: 1 (teicoplanin A2-2)**
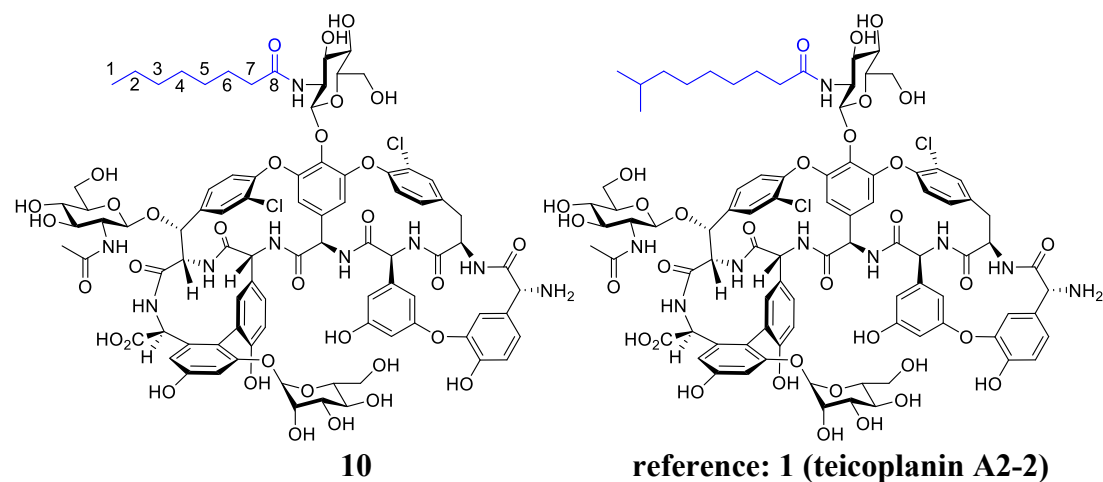
Position	^{13}C-NMR (δ ppm)	^{1}H-NMR (δ ppm)
C-1	17.2	0.83 m
C-2	25.3	1.22 m
C-3	34.4	1.20 m
C-4	31.7	1.10 m
C-5	32.0	1.23 m
C-6	28.2	1.46 m
C-7	39.07	2.08 m
C-8	175.4	—

The assignment is based on the spectra shown in **Figure S15**.

Table S6. NMR assignments for compound 11.

| 11 | reference: 1 (teicoplanin A2-2) |
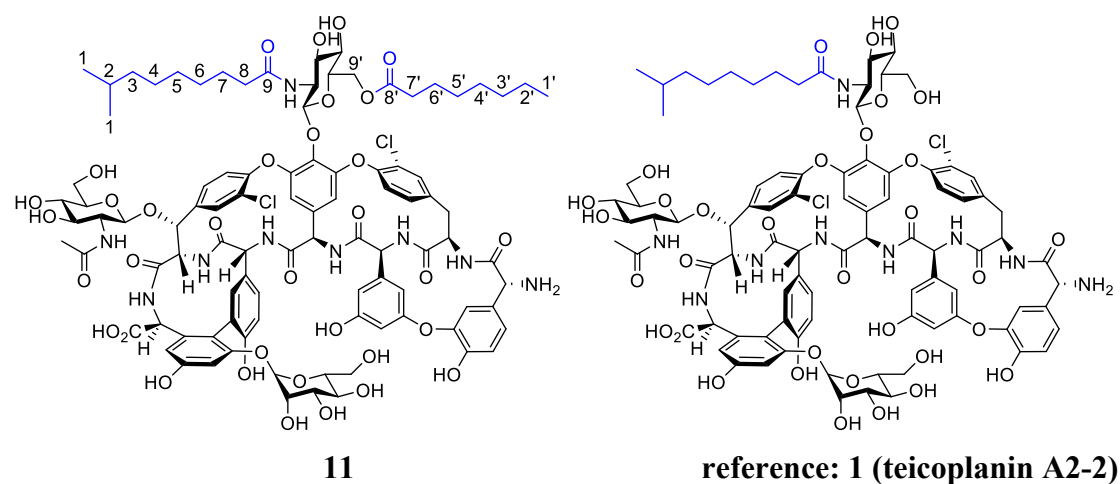
Position	^{13}C-NMR (δ ppm)	^{1}H-NMR (δ ppm)
C-1	22.5	0.82 d (J 6.6)
C-2	27.4	1.46 m
C-3	38.5	1.07 m
C-4	26.6	1.16 m
C-5	29.2	1.13 m
C-6	28.5	1.23 m
C-7	24.5	1.47 m
C-8	35.8	2.0 m
C-9	172.33	—
C-1'	13.9	0.85 m
C-2'	22.1	1.25 m
C-3'	31.2	1.22 m
C-4'	26.7	1.08 m
C-5'	28.9	1.10 m
C-6'	25.2	1.38 m
C-7'	33.7	2.22 m
C-8'	169.61	—
C-9'	63.12	3.35 m

The assignment is based on the spectra shown in **Figure S16**.

Table S7. NMR assignments for compound 20.

20	**reference: 1 (teicoplanin A2-2)**
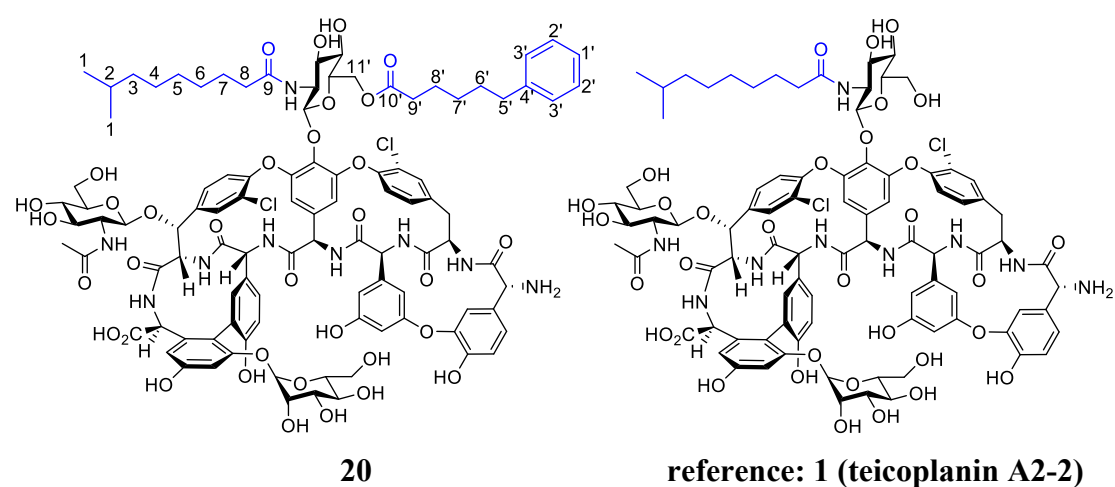
Position	^{13}C-NMR (δ ppm)	^{1}H-NMR (δ ppm)
C-1	22.4	0.81 d (J 6.8)
C-2	27.2	1.43 m
C-3	38.5	1.05 m
C-4	26.6	1.14 m
C-5	28.8	1.12 m
C-6	28.7	1.23 m
C-7	24.4	1.52 m
C-8	35.8	1.99 m
C-9	172.33	—
C-1'	115.8	6.7 m
C-2'	125.6	7.15 m
C-3'	128.26	7.24 m
C-4'	142.17	—
C-5'	35.02	2.54 m
C-6'	28.24	1.29 m
C-7'	30.8	1.54 m
C-8'	24.17	1.526 m
C-9'	33.54	2.276 m
C-10'	169.59	—
C-11'	63.09	3.352 m

The assignment is based on the spectra shown in **Figure S19**.

Supporting References

(1) Otwinowski, Z.; Minor, W. In *Methods in Enzymology*; Charles W. Carter, Jr., Ed.; Academic Press: 1997; Vol. Volume 276, p 307.

(2) Kantardjieff, K. A.; Rupp, B. *Protein Science* **2003**, *12*, 1865.

(3) Ness, S. R.; de Graaff, R. A. G.; Abrahams, J. P.; Pannu, N. S. *Structure* **2004**, *12*, 1753.

(4) De Graaff, R. A. G.; Hilge, M.; Van Der Plas, J. L.; Abrahams, J. P. *Acta Crystallographica Section D* **2001**, *57*, 1857.

(5) Pannu, N. S.; Read, R. J. *Acta Crystallographica Section D* **2004**, *60*, 22.

(6) Abrahams, J. P.; Leslie, A. G. W. *Acta Crystallographica Section D* **1996**, *52*, 30.

(7) Cowtan, K. *Acta Crystallographica Section D* **2006**, *62*, 1002.

(8) Cowtan, K. *Acta Crystallographica Section D* **2008**, *64*, 83.

(9) Emsley, P.; Cowtan, K. *Acta Crystallographica Section D* **2004**, *60*, 2126.

(10) Emsley, P.; Lohkamp, B.; Scott, W. G.; Cowtan, K. *Acta Crystallographica Section D* **2010**, *66*, 486.

(11) Murshudov, G. N.; Vagin, A. A.; Dodson, E. J. *Acta Crystallographica Section D* **1997**, *53*, 240.

(12) National Committee for Clinical Laboratory Standards. **2006**, Methods for Dilution Antimicrobial Susceptibility Tests for Bacteria That Grow Aerobically. Approved standard, 7th ed. NCCLS document M7-A7. Clinical and Laboratory Standards Institute, Villanova, Pa.